A Collection of Various Research Projects in Astronomy

by

Daniel J. Majaess

A Thesis Submitted to Saint Mary's University, Halifax, Nova Scotia in Partial Fulfillment of the Requirements for the Degree of

MASTER OF SCIENCE

in

Astronomy

(Department of Physics and Astronomy)

SAINT MARY'S UNIVERSITY

August 2008, Halifax, Nova Scotia

© Daniel J. Majaess, 2008

Library and
Archives Canada

Published Heritage
Branch

395 Wellington Street
Ottawa ON K1A 0N4
Canada

Bibliothèque et
Archives Canada

Direction du
Patrimoine de l'édition

395, rue Wellington
Ottawa ON K1A 0N4
Canada

Canada

CONTENTS

LIST OF FIGURES

LIST OF TABLES

CHAPTER 1

FOREWARD

Presented here is a collection of various studies inspired from a list of end of term projects[1] given in the graduate course Galactic Astronomy (5500.2) taught by Turner. The posed questions included: *Do open clusters provide realistic limits on the progenitor masses of planetary nebulae? How reliable are the open cluster and Cepheid distance scales? Does the motion of the Sun through the Galactic plane cause mass extinction episodes?* Additional questions from the course concerned *the distance to the Galactic Center, the initial mass function, and what is the best current delineation of the Galaxy's spiral arms, is a four armed spiral Milky Way realistic?* are currently being addressed, aided by techniques developed during the initial foundation work. Indeed, such studies are in the advanced stages of preparation.

The first research project dealt, ultimately, with the search for planetary nebulae in open clusters. Incidentally, it comes as a surprise to most astronomers to learn that not a single case has been established based on a trifecta correlation of distance estimates, reddenings, and radial velocities between a planetary nebula and an open cluster. Reasons are put forth, mainly from an empirical perspective, to explain why that is an expected observation. Although a null result was obtained *vis à vis* the primary objective, the study provided a valuable platform to facilitate subsequent investigations by the broader community (e.g., Bonatto et al., 2008). More importantly, the necessity to improve upon the parameters of several poorly studied open clusters pertinent to the search resulted in an effective use of data from the 2MASS all-sky infrared survey that allowed for: the determination of distances and mean reddenings to open clusters (within the accuracy limits of the survey and to an acceptable precision), establishing membership probabilities for stellar constituents

---

[1] see http://www.ap.smu.ca/ turner/a5602proj.pdf

of a given cluster, constructing comprehensive star counts to guage the cluster's true angular size (Turner et al., 2008b), the creation of an empirical color-color relation that has been used with great success—previous color-color relations derived from models yielded less accurate fits by contrast— which permits the assessment of field reddenings (Turner et al., 2008a,b), and the latter development inevitably enabled constraints to be placed on the reddenings of individual Cepheid variables (Turner et al., 2008c). Lastly, it was noted that most established cluster Cepheids (Turner & Burke, 2002) are short-period variables that exhibit lower masses (Turner et al., 2006) and are thus consistent with predictions for the progenitors of planetary nebulae, meaning that the bulk of cluster Cepheids may inevitably become planetary nebulae. Therefore, these stars offer a unique opportunity from which evolutionary and abundance constraints can be inferred for planetary nebulae, since the distances to such evolved supergiants are well established (cluster membership).

The project to investigate Cepheids is primarly tied to establishing period changes for their pulsation, which provides a direct means of probing predictions from stellar evolutionary models (Turner et al., 2006). Previously, the project had been operating successfully from the Burke-Gaffney Observatory (Turner, 1998; Turner et al., 1999, 2005), yet the newly minted Abbey-Ridge Observatory offered a site with darker skies. The work to transform the Abbey-Ridge Observatory into a facility that could engage in precision photometry was led by Lane, with casual support from Turner and Majaess. Many novel techniques were developed and implemented which are far too numerous to elaborate upon (Lane, 2007), however, the diversity of the projects highlighted here, along with the collaborations forged (e,g,. Turner et al., 2007, 2008a), undoubtedly attest to the Observatory's success. A brief discussion of the facility and pipeline to process and acquire the data are highlighted in the attached study detailing the serendipitous discoveries of several variable stars found in the same field of view as the Cepheid targets. This latter study included the interesting discovery of a member of the Vul OB1 association (Turner, 1986), a famous, albeit poorly constrained association whose most evolved member is the long period Cepheid SV Vul (Turner & Berdnikov,

2004). SV Vul is an absolutely critical calibrator of the period-luminosity relation, offering a clamp to the vastly undersampled long-period end of the relation. The discovery provides further confirmation of the association's existence, and estimates for the Cepheid's distance determined from relations developed below also reaffirm the distance implied by membership in the association. The study also included a section on the remarkable open cluster Berkeley 87 (Turner & Forbes, 1982; Turner et al., 2006b), which has been identified as the primary source of Northern Hemisphere γ and cosmic rays, and hosts an abundance of astronomical phenomena (compact H II regions, molecular clouds, masers, and radio sources) and exotic stellar constituents. Radial velocity studies and deep CCD photometry envisioned for this fall would secure efforts to gain insights into the effects of initial mass and mass loss on the end states of evolution for O-type stars, and may allow us to place new constraints on the initial progenitor masses for WO stars and red supergiants—a very exciting and important prospect. Lastly, the study demonstrated the viability of all-sky photometry from Nova Scotia, where variable atmospheric conditions severely undermine such an effort and require the deduction of extinction and transformation coefficients on an hourly basis. All-sky photometry permits the data to be standardized directly to the Johnson system.

The project to continue the search for calibrators of the period-luminosity relation via Cepheids in open clusters included addressing the implied broader topics concerning: refining equations to determine the distances and color excesses to Cepheid variables, assessing the universality of the PL relation, etc. It is perhaps the most relevant research of the collection issued here, allowing for a direct segway into the assessment of Galactic spiral structure and other Galactic parameters (e.g., the scale height of the Galactic plane). One of the future objectives not highlighted within the text *may* be to experiment with PHOENIX models to determine exactly how the distance to a particular Cepheid is affected as a function of metallicity.

The last projects concern asteroids and resulted in part from a continuation of research started at the undergraduate level. The main intent of the paper on 349 Dembowska was to provide experience

in dealing with the observational analysis of asteroids. Of particular interest here, although clearly unorthodox, was the use of photometric data from surveys such as 2MASS, SDSS, and IRAS, to detail the asteroid's spectral energy distribution and to infer its surface composition via noted absorption features. The second study arose from a paper investigated in Journal Club. 298 Baptistina is alleged to be a family member of the K/T impactor, the asteroid which ended the reign of the dinosaurs 65 Myr ago. The study mobilized a team of international observatories (a consensus-seeking task far more complicated than imagined!) and put forth new constraints on the asteroid 298 Baptistina, while highlighting many areas of concern regarding its reputed status. The study was specifically tailored for the JRASC audience (and non-interdisciplinary astronomers) seeking to be introduced to the topic, with an emphasis on context. More broadly, the correlation between mass extinctions and impactors is of great interest to this student, motivated again by one of the topics highlighted in Galactic astronomy, coupled with the student's undergraduate thesis which dealt with the transport of comets from the Kuiper Belt into planet crossing orbits. The student's real intentions regarding treating the question of mass extinctions is far more ambitious and would demand a return to n-body simulations. However, such an effort would require an enormous allotment of time which is probably too much to undertake.

REFERENCES

Bonatto, C., Bica, E., & Santos, J. F. C. 2008, MNRAS, 386, 324

Lane D. J., 2007, 96th Spring Meeting of the AAVSO

Turner, D. G., & Forbes, D. 1982, PASP, 94, 789

Turner, D. G. 1986, A&A, 167, 157

Turner D. G., 1996, JRASC, 90, 82

Turner D. G., 1998, JAAVSO, 26, 101

Turner D. G., Horsford A. J., MacMillan J. D., 1999, JAAVSO, 27, 5

Turner D. G., Burke J. F., 2002, AJ, 124, 2931

Turner, D. G., & Berdnikov, L. N. 2004, A&A, 423, 335

Turner D. G., Savoy J., Derrah J., Abdel-Sabour Abdel-Latif M., Berdnikov L. N., 2005, PASP, 117, 207

Turner D. G., Abdel-Sabour Abdel-Latif M., Berdnikov L. N., 2006, PASP, 118, 410

Turner, D. G., Rohanizadegan, M., Berdnikov, L. N., & Pastukhova, E. N. 2006, PASP, 118, 1533

Turner, D. G., et al. 2007, PASP, 119, 1247

Turner, D. G., Panko, E. A., Sergienko, O., Lane, D. J., & Majaess, D. J. 2008, The Observatory, 128, 2

Turner, D. G., et al. 2008, MNRAS, 388, 444

Turner D. G., MacLellan R. F., Henden A. A., Berdnikov L. N., 2008, PASP, submitted

ABSTRACT

In Search of Possible Associations between Planetary Nebulae and

Open Clusters

by Daniel J. Majaess, David G. Turner, and David J. Lane.

Abstract: We consider the possibility of cluster membership for 13 planetary nebulae that are located in close proximity to open clusters lying in their lines of sight. The short lifetimes and low sample size of intermediate-mass planetary nebulae with respect to nearby open clusters conspire to reduce the probability of observing a true association. Not surprisingly, line of sight coincidences almost certainly exist for 7 of the 13 cases considered. Additional studies are advocated, however, for 6 planetary nebula/open cluster coincidences in which a physical association is not excluded by the available evidence, namely M 1-80/Berkeley 57, NGC 2438/NGC 2437, NGC 2452/NGC 2453, VBRC 2 & NGC 2899/IC 2488, and HeFa 1/NGC 6067. A number of additional potential associations between planetary nebulae and open clusters is tabulated for reference purposes. It is noteworthy that the strongest cases involve planetary nebulae lying in cluster coronae, a feature also found for short-period cluster Cepheids, which are themselves potential progenitors of planetary nebulae.

CHAPTER 2

PNe in Open Clusters

2.1 INTRODUCTION

For some time our knowledge of the intrinsic properties of the Galaxy's population of individual planetary nebulae has been restricted by large uncertainties in their derived distances. Zhang (1995) suggests that the *average* uncertainty in the distances cited to Galactic planetary nebulae is in the range 35-50%. Others are less optimistic. Such a large scatter may not be surprising, given that planetary nebulae exhibit various morphologies and span a large range in mass (Kwok, 2005).

In contrast, well-studied open clusters have distances and reddenings that are established to much greater precision, with distance uncertainties as small as 2.5% being possible (Turner & Burke, 2002). Planetary nebulae established as members of open clusters are therefore a potential alternative means of calibrating their fundamental properties. With an inferred distance from cluster membership in conjunction with a planetary's angular diameter and expansion velocity, its true dimensions and age can be deduced. Cluster membership has the potential for a more direct calibration of the core mass-nebular He, C, and N abundance relationship expected in planetary nebulae as a result of single star evolution with asymptotic giant branch dredge-up (Köppen & Acker, 2000; Cazetta & Maciel, 2000). Planetary nebulae confirmed as cluster members would enhance their importance as calibrators for the Shklovsky relation (Osterbrock & Ferland, 2006) or other similar methods used to establish their distances (Bensby & Lundström, 2001). On a cautionary note, significant improvement in such relationships may not be possible if the observed scatter is intrinsic.

Several factors conspire to reduce the probability of observing a planetary nebula associated with an open cluster. First, the effective sample of planetary nebulae includes a large number of objects

that appear to populate the Galactic bulge (Akhundova & Seidov, 1971; Ziznovsky, 1975), according to catalogue statistics (Kohoutek, 2001) on their distribution along the Galactic plane (Figure 1), as well as their observed radial velocities (Osterbrock & Ferland, 2006). Potential calibrators lying in nearby open clusters are greatly reduced in number when that population is excluded, although many spatial coincidences still exist (Ziznovsky, 1975). Associated open clusters with ages of less than $\sim 28 \times 10^6$ years ($\log(\tau) \leq 7.5$) are likely to be excluded, since stellar evolutionary models indicate that the end products of their evolved components are Type II supernovae explosions. Current knowledge of stellar evolution suggests that the immediate precursors of C/O white dwarfs were planetary nebulae central stars that did not undergo core carbon ignition.

In addition to a small sample size, the detection of an association between a planetary nebula and an open cluster is further hampered by the short lifetimes of planetary nebulae. Models indicate that their main-sequence progenitors were stars of $1 - 6.5$ $M_\odot$ (e.g., Weidemann, 2000), with an upper limit of ~ 8 $M_\odot$ being possible for production of Ne white dwarfs. The lifetime of the planetary nebula stage is very sensitive to initial progenitor mass and subsequent mass loss (e.g., Schoenberner & Bloecker, 1996), and varies significantly for main-sequence turnoff ages greater than $\sim 28 \times 10^6$ years, with estimates ranging from 10^3 to 10^5 years (Schoenberner & Bloecker, 1996; Köppen & Acker, 2000). The most common age for nearby Galactic open clusters is $\sim 100 \times 10^6$ years ($\log(\tau) \simeq 8$), according to the catalogue compilation of Dias et al. (2002) summarized in Figure 2. That corresponds to a main-sequence turnoff mass of $M_{TO} \simeq 4$ $M_\odot$. The lifetime of planetary nebulae associated with such progenitors is of order 10^3 years, essentially instantaneous on the Galactic stage.

It is of interest to note that many planetary nebulae with massive central stars are found in the field, which is populated by the remnants of dissolved open clusters. Such clusters exceed the number of bound open clusters by a sizeable order (Lada & Lada, 2003), which suggests that, despite the short lifetimes of planetary nebulae with massive central stars, increasing the statistical

sampling of possible spatial coincidences between planetaries and clusters may lead to successful detections. The usefulness of such surveys at extragalactic scales by Larsen & Richtler (2006) and Magrini (2006) is therefore obvious: larger statistics dominate and planetary nebulae are readily discernable, as demonstrated by their success as standard candles (Jacoby, 1989). The success of the Macquarie/AAO/Strasbourg Hα (MASH) survey (Parker et al., 2006) in detecting large numbers of additional Galactic planetary nebulae has also been extremely useful in revealing additional coincidences with Galactic clusters.

The discovery of planetary nebulae within globular clusters (Jacoby et al., 1997) raises a pertinent point that must be considered. If we consider $1 - 1.5$ $M_\odot$ as a strict lower mass limit for the progenitors of planetary nebulae (Kwok, 2005; Osterbrock & Ferland, 2006), then, for the ages assigned to globular clusters, corresponding to main sequence turnoffs of less than $1 M_\odot$, one must invoke binarity (mass transfer) to resolve the resulting discrepancy. That supports the scenario of De Marco (2006), Soker (2006), and Zijlstra (2007), who argue that a large fraction of observable planetaries may indeed stem from binary systems. Consequently, if a planetary nebula/open cluster association is established, we must be aware of the possibility that binarity might negate possible predictions for progenitor mass on the basis of the cluster's implied age from its main sequence turnoff.

In this paper we consider the possibility of cluster membership for a number of planetary nebulae that are located in close proximity to open clusters lying in their lines of sight. The often cited cases for planetary nebula/open cluster associations include the cluster and nebula designated as NGC 2818, as well as A9 in NGC 1912 (M38) and NGC 2438 in NGC 2437 (M46), but lesser known cases are also considered.

2.2   SUSPECTED PN/OPEN CLUSTER ASSOCIATIONS

Lubos Kohoutek has compiled an on-line list of suspected planetary nebula/open cluster associations, somewhat different from that given by Ziznovsky (1975), that is reproduced in Table 1. To that list we have appended a new case involving the planetary nebula M 1-80 and the open cluster Berkeley 57, and also consider two planetaries that may be outlying members of IC 2488 (Pedreros, 1987).

Table 1 includes, where available, a planetary nebula identifier tied to its Galactic co-ordinates, along with information on the dimensions of the spatially adjacent cluster and the angular separation of the planetary from the cluster center. Open clusters are generally larger than the obvious concentrations of stars comprising their core regions (Kholopov, 1969; Nilakshi et al., 2002), so we list in columns 4 and 5 estimates for the nuclear radius, r_n, and coronal radius, R_C, of each cluster, where the two dimensions are tied to the definitions of Kholopov (1969) based upon linear star counts. The cluster nucleus comprises the dense central region of a star cluster that is obvious to the eye, whereas the cluster corona is the much lower density outer region. Information on both parameters is not generally available for most clusters, although estimates of cluster angular diameter given by Dias et al. (2002) closely match the diameters of cluster nuclei defined by Kholopov (1969). Coronal radii can be 2.5 to 10 times larger (Kholopov, 1969), and the best means of estimating that parameter seems to be by scaling the large angular diameters for open clusters cited by Barkhatova (1950), as described in the table footnotes. The last values are crude approximations at best, but at least provide a sense of scale for establishing if a planetary nebula's angular separation from a cluster is consistent with a *bona fide* spatial coincidence.

Table 2 outlines the qualitative framework used to determine if the suspected associations are co-spatial. The primary criteria are the differences in radial velocity and color excess between the planetary nebula and cluster (ΔV_R, ΔE_{B-V}), and the ratio of the estimated distances (D_R). The following parameters are also considered: the apparent size of the objects, their angular separation,

and Galactic location. Because of the large number of planetary nebulae lying in the direction of the Galactic bulge noted earlier, there is a natural bias towards purely line of sight coincidences with open clusters for planetaries lying in that direction (recall Figure 1).

The interstellar reddenings of planetary nebulae cited throughout this study were usually derived from the standard constant of extinction, c, via the following generic approximation:

$$E_{B-V} \simeq 0.77 \times c$$

from Osterbrock & Ferland (2006), where c is related to the logarithmic extinction at Hβ. The resulting reddenings may be systematically higher than those for stars in the surrounding fields if there is inherent self-absorption by dust within the planetary nebulae themselves.

Reddening is not necessarily a strong criterion for a spatial coincidence. The spatial distribution of interstellar extinction near the Sun (Neckel & Klare, 1980) is clearly defined, and indicates that the dust is concentrated in distinct clouds rather than more or less uniformly distributed along the Galactic plane. Between the dust clouds along some lines of sight are large gaps, of a kiloparsec or more, within which all stars share similar reddenings. Small spatial variations in reddening can be attributed to density variations within the clouds themselves.

2.2.1 M 3-20 AND TRUMPLER 31 ($\ell \simeq 2°$)

The open cluster Trumpler 31 was studied photographically on the RGU system by Svolopoulos (1966). Janes & Adler (1982) obtained a cluster distance of $d = 1.86$ kpc and a reddening of $E_{B-V} = 0.43$ after transforming the data to the UBV system. The cluster is not an obvious concentration of stars on POSS images of the field, and star counts are needed to assess its reality. A color excess of $E_{B-V} \simeq 1.10 \pm 0.08$ derived for the planetary nebula M 3-20 (Tylenda et al., 1992) places it beyond ~ 2 kpc according to the extinction maps of Neckel & Klare (1980). The estimated

distance is $d \simeq 5000 \pm 350$ pc (Zhang, 1995), which, in conjunction with the reddening, small angular

size, and Galactic location towards the Galactic bulge (Figure 2), confirm the planetary nebula as a

background object to the cluster Trumpler 31, which may not exist.

2.2.2 M 1-80 AND BERKELEY 57 ($\ell \simeq 108°$)

Berkeley 57 is an older cluster recently examined by Hasegawa et al. (2004), who derived a distance

of $d = 4150$ pc, a reddening of $E_{B-V} = 0.75$, and an age of 14×10^8 years ($\log(\tau) = 9.14$). The

planetary nebula M 1-80 is located $10'$ from the cluster, and is estimated to lie at a distance of

$d = 5250 \pm 500$ pc (Zhang, 1995) with a reddening of $E_{B-V} \simeq 0.54 \pm 0.11$ (Tylenda et al., 1992).

Reddening alone constrains the distance of both objects only to somewhere in the interval $2 - 6$ kpc

(Neckel & Klare, 1980), so the case rests mainly on the similarity of the distance estimates.

Star counts compiled from 2MASS data (Figure 3) lead to an estimated cluster nuclear radius of

$r_n = 5'$ (see Kholopov, 1969), which means that the planetary lies only $2 \times r_n$ from the cluster center.

It is therefore a potential member of the cluster corona, adding further interest to the study of its

potential association with Berkeley 57. The next step would be to use spectroscopic observations

of the many evolved cluster giants to establish the cluster's radial velocity, for comparison with the

value of $V_R = -58 \pm 10$ km s^{-1} derived for M 1-80 by Durand et al. (1998).

2.2.3 A9 AND NGC 1912 (M38) ($\ell \simeq 172°$)

Various literature studies of the parameters for NGC 1912 (M38) generated a wide range of distance

estimates for the open cluster, the likely reason being the 0.4-mag. spread in color excesses for

member stars. The cluster distance is $d \simeq 970 \pm 40$ pc (Turner, 1976) when that is taken into

account. An independent distance estimate was obtained using data from the *Two Micron All*

Sky Survey (2MASS, Cutri et al., 2003) to construct a J versus J–H color-magnitude diagram,

shown in Figure 4. Isochrones tailored specifically to the 2MASS system were obtained from the

Padova Database of Stellar Evolutionary Tracks and Isochrones (Bonatto et al., 2004). A sub-solar metallicity solution ($Z = 0.008$) provided the best visual fit, and is supported by the work of Jennens & Helfer (1975), who determined a cluster metallicity of [Fe/H]$\simeq$ -0.35, which corresponds to $Z \simeq 0.009$ according to the relationship found by Berdnikov (1994). The following relationships were adopted between extinction and color excess in the infrared and optical regions: $A_J = 0.276 \times A_V$, $E_{J-H} = 0.33 \times E_{B-V}$ (Bica & Bonatto, 2005; Dutra et al., 2002). The canonical distance modulus relation was reformulated and evaluated as:

$$\log(d) = 0.2[J - M_J - 0.84(E_{J-H} \times R_V) + 5]$$

The results, displayed in Figure 4, yield a distance of $d = 1050 \pm 150$ pc, a reddening of $E_{B-V} = 0.27 \pm 0.03$, and an age of 18×10^7 years ($\log(\tau) = 8.25 \pm 0.15$), essentially confirming previous estimates of a low reddening and a distance near 1 kpc.

With regard to the planetary nebula A9, a distance degeneracy has emerged, with both nearby, $d \simeq 4000$ pc, $E_{B-V} \simeq 1.05$ (Kaler et al., 1990), and $d = 5050$ pc (Phillips, 2004), and distant, $d = 8900 \pm 6100$ pc (Zhang, 1995), solutions being advocated. The planetary's large apparent diameter of $30''$, measured using the *Aladin* environment (Bonnarel et al., 2000), would seem to favor the nearer estimates. The extreme faintness of the central star (Kwitter et al., 1988) and the large reddening of the planetary nebula, which implies a distance in excess of ~ 4 kpc (Neckel & Klare, 1980) for A9, almost certainly place the planetary at a much greater distance than the cluster NGC 1912. A radial velocity of $V_R = -1.0 \pm 0.6$ km s^{-1} is available for a red giant member of the cluster (Glushkova & Rastorguev, 1991), but the radial velocity of A9 has not yet been measured. Presumably it would merely serve to confirm that the two are unrelated.

2.2.4 NGC 2438 AND NGC 2437 (M46) ($\ell \simeq 232°$)

The location of the planetary nebula NGC 2438 relative to the open cluster NGC 2437 (M46) is visually supportive of an association, given the planetary nebula's breadth, brightness, and proximity to the cluster core (Figure 5). Three estimates for the distance (Zhang, 1995) and reddening (Tylenda et al., 1992) to the planetary nebula yield mean values of $d \simeq 1775 \pm 630$ pc and $E_{B-V} \simeq 0.17 \pm 0.08$. Both are in general agreement with a zero-age main sequence (ZAMS) and isochrone fit to 2MASS photometry for M46 (Figure 6) that yields values of $d = 1700 \pm 250$ pc, $E_{B-V} = 0.13 \pm 0.05$, and an age of 22×10^7 years ($\log(\tau) = 8.35$). Color excesses increase along this line of sight from ~ 0.1 to ~ 0.3 at distances beyond ~ 1.5 kpc (Neckel & Klare, 1980), which confirms the distances estimated for both the cluster and the planetary nebula. The color excesses for both are also similar enough to confirm that they share the same space reddening. The case for a physical association therefore rests upon their space motions.

Early studies of the radial velocity of NGC 2438 and M46 by Cuffey (1941, citing measures by Struve) and O'Dell (1963) indicated a difference of $\Delta V_R \simeq 30$ km s^{-1} between the objects, which suggests that the pair constitutes a spatial coincidence only. A cluster red giant spectroscopic binary has an identical systemic velocity (Mermilliod et al., 1989) as that obtained for cluster dwarf members by Cuffey (see Table 3). However, Pauls & Kohoutek (1996) rekindled interest in a possible planetary nebula/open cluster association when they found similar radial velocities for both. While it is conceivable that the early radial velocity measures for cluster stars, which were made from spectrograms obtained from the northern hemisphere, might be affected by spectrograph flexure or by the presence of spectroscopic binaries in the sample, it is noteworthy that the radial velocity measured for the planetary nebula is similar to more recent measures (Table 3). If the radial velocity measurements of Pauls & Kohoutek (1996) are reliable, then there is a good case for a physical association of NGC 2438 with M46. But additional velocity measures are clearly needed to strengthen the case, given that proper motions may not provide a suitable test in this instance

(O'Dell, 1963).

2.2.5 NGC 2452 AND NGC 2453 ($\ell \simeq 243°$)

The derived distances to the open cluster NGC 2453 are unsatisfactorily varied, as Table 4 summarizes. Field star contamination may be important in this case, given that the cluster main sequence is dominated by B-type stars, which also populate the Puppis OB associations, and an extension of the Perseus arm behind them (Peton-Jonas, 1981), which lie along the same line of sight. The distances cited from two deep CCD studies by Massey et al. (1995) and Moitinho (2001) are favored because the main sequence morphology is well defined. The latter study of NGC 2453 implies a distance of $d = 5250$ pc, a reddening of $E_{B-V} = 0.50$, and an age of 40×10^6 years ($\log(\tau) = 7.6$). The parameters for the planetary nebula NGC 2452 generally agree with those of the cluster, although the cited distance of $d \simeq 2950 \pm 420$ pc (Zhang, 1995) and reddening of $E_{B-V} \simeq 0.36 \pm 0.12$ (Tylenda et al., 1992) might suggest that the planetary nebula lies foreground to the cluster. The reddening along this line of sight remains unchanged at $E_{B-V} \simeq 0.6$ for distances in excess of ~ 2 kpc (Neckel & Klare, 1980), so the small difference in color excesses is not useful for distance discrimination.

With reference to available radial velocities, Moffat & Fitzgerald (1974) obtained a value of $V_R = 67 \pm 14$ km/s for a cluster B5 star ideally positioned as an evolved main-sequence member in the cluster color-magnitude diagram. Despite the large uncertainty in the velocity and the fact that the spectrogram displayed double lines, the value is very similar to measures for the planetary nebula: $V_R = 62.0 \pm 2.8$ km s^{-1} (Meatheringham et al., 1988), and $V_R = 65 \pm 3$ km s^{-1} Durand et al. (1998). Additional radial velocity measurements for established cluster members are needed to assess the viability of the case further, although existing data do not rule out a possible spatial coincidence.

It is of interest to note that Cazetta & Maciel (2000) concluded that NGC 2452 was among the most massive planetary nebulae in their sample of ~ 100. Their argument was based on the

abundance ratio N/O, which is a tracer of mass for the progenitor star via the dredge-up scenario. Coincidentally, the cluster's young age also implies a massive progenitor of $M_{TO} \simeq 6.5 \; M_{\odot}$ (see Figure 2).

2.2.6 NGC 2818: Planetary Nebula and Cluster ($\ell \simeq 262°$)

The well known spatial coincidence of the planetary nebula NGC 2818 with its surrounding cluster is an example of a case that visually supports an association (Figure 7). Pedreros (1989) determined a distance of $d = 2300$ pc and a reddening of $E_{B-V} = 0.18$ for the cluster, consistent with the parameters derived for the planetary nebula: $d = 2660 \pm 830$ pc (Zhang, 1995), and $E_{B-V} \simeq 0.28 \pm 0.15$ (Tylenda et al., 1992). Equally encouraging are radial velocities from low dispersion spectra (230 Å mm^{-1}) by Tifft et al. (1972) for two A-type stars in the cluster that yielded $V_R = 3 \pm 20$ km s^{-1}, compared with $V_R = 8 \pm 13$ km s^{-1} obtained for the planetary nebula. Such evidence, in conjunction with the general agreement in distance and reddening, has been the basis for the conclusion that the two are associated.

More recent results suggest otherwise. A comprehensive radial velocity study of stars in the cluster field by Mermilliod et al. (2001) yields a cluster radial velocity from 15 red giant members of $V_R = 20.7 \pm 0.3$ km s^{-1}, while the radial velocity of the planetary nebula is established to be $V_R = -0.9 \pm 2.9$ km s^{-1} (Durand et al., 1998) and $V_R = -1 \pm 3$ km s^{-1} (Meatheringham et al., 1988), consistently smaller than the velocity of the cluster. The greater precision of recent estimates results in a velocity discrepancy of $\Delta V_R = 22$ km s^{-1} (Mermilliod et al., 2001), implying a spatial coincidence rather than a physical association, as concluded by Mermilliod et al. (2001).

2.2.7 VBRC 2 & NGC 2899 and IC 2488 ($\ell \simeq 277°$)

Perryman et al. (1997) conducted an extensive study of the planetary nebula VBRC 2 and derived a distance of $d = 1200 \pm 200$ pc and a reddening of $E_{B-V} = 0.38$. The values are consistent with

the parameters found for the cluster IC 2488 by Clariá et al. (2003), who derived a distance of $d = 1250 \pm 120$ pc, a reddening of $E_{B-V} = 0.24 \pm 0.04$, and a radial velocity of $V_R = -2.63 \pm 0.06$ km s^{-1}. Those values are smaller than the estimates of $d = 1445 \pm 120$ pc and $E_{B-V} = 0.26 \pm 0.02$ obtained for IC 2488 by Pedreros (1987).

There may be a tendency to dismiss an association between the cluster and planetary because of their large apparent separation ($\simeq 54'$), despite the consistent correlation among the parameters. Star counts of the field were therefore made using data available from the 2MASS survey (Figure 8). The data highlight IC 2488's broad extent ($r_n \simeq 17' - 18'$) and indicate that the planetary nebula VBRC 2 lies within $\simeq 3 - 4$ cluster nuclear radii. Since cluster coronae typically extend anywhere from 2.5 to 10 times beyond their nuclear radii (Kholopov, 1969), and the coronae of star clusters in the outer Galaxy are larger on average than those in the inner regions (Nilakshi et al., 2002), it may be premature to dismiss a possible association based solely on arguments of separation. It is of interest to note that a large fraction of short-period Cepheids, potential progenitors of planetary nebulae, fall within the coronae of their constituent clusters (Turner, 1985). A final decision on the case must therefore await a radial velocity for the planetary nebula, to assess its potential as a cluster member properly.

Published estimates for the parameters of the planetary nebula NGC 2899 imply a distance of $d \simeq 1560 \pm 570$ pc and a reddening of $E_{B-V} \simeq 0.32 \pm 0.24$ (Zhang, 1995; Tylenda et al., 1992), consistent with the parameters for IC 2488. Durand et al. (1998) measured the radial velocity of the planetary nebula to be $V_R = 3.4 \pm 2.8$ km s^{-1}, which differs slightly but only by slightly more than 2σ from the cluster value. NGC 2899 is in the same situation as VBRC 2, since it also lies nearly as far from the cluster center, yet possibly within the corona. Remeasuring the color excess and radial velocity of the planetary nebula with greater precision would help clarify the case for cluster membership. Thus, while not conclusive, both candidates offer encouraging evidence.

The reddening along this line of sight becomes larger than $E_{B-V} \simeq 0.3$ beyond ~ 1 kpc (Neckel

& Klare, 1980), so the observed color excesses for the cluster and planetary nebulae imply that they are reddened by foreground dust clouds. Reddening is therefore of little use for constraining the distances to the planetary nebulae. Presumably radial velocities would provide a stronger test for a physical association.

2.2.8 ESO 177-10 AND LYNGÅ 5 ($\ell \simeq 325°$)

The open cluster Lyngå 5 has not been studied since its discovery nearly forty-five years ago, so its parameters are essentially unknown. For this study we examined the field and estimated a peak in star density by eye at J2000.0 = 15:41:55, −56:38:38, and a corresponding nuclear radius measuring about $2'$. As a means of obtaining approximate values for its distance and reddening, data from the 2MASS survey (Cutri et al., 2003) for objects in the field of the putative cluster nucleus were used to construct *JHK* color-color and color-magnitude diagrams for cluster stars. The color-color diagram (Figure 9) suggests that there is a sizable group of reddened late B-type stars in the field, presumably associated with the cluster main sequence. The implied cluster reddening, $E_{J-H} = 0.33 \pm 0.03$, corresponds to $E_{B-V} = 1.18 \pm 0.11$. A simple ZAMS fit was used to estimate the distance (Figure 10), yielding $d = 1950 \pm 350$ pc. But the values cited are only preliminary, and still uncertain. A few cluster stars may be bright enough for spectroscopic follow-up, which might confirm the derived parameters. Interestingly enough, the cluster main-sequence turnoff appears to lie roughly at B5, implying an age of $\sim 50 \times 10^6$ years ($\log(\tau) = 7.7$), corresponding to masses of $\geq 6.5 M_\odot$ for cluster evolved components.

The cited distance of 2550 ± 670 pc (Zhang, 1995) to the planetary nebula ESO 177-10 is marginally consistent with the value obtained for the cluster, but the color excess of $E_{B-V} \simeq 2.46 \pm 0.07$ for the planetary derived from several radio measurements (Tylenda et al., 1992; Cahn et al., 1992) indicates that it suffers from much heavier extinction. Such a large reddening implies a distance in excess of ~ 2 kpc along this line of sight (Neckel & Klare, 1980), lending support to the

argument that the planetary nebula lies in the cluster background. Radial velocities would likely confirm that this pair represents a spatial coincidence only.

2.2.9 KoRe 1 and NGC 6087 ($\ell \simeq 328°$)

Koester & Reimers (1989) conclude that the planetary nebula KoRe 1 is in a highly excited state on the basis of nearly equal spectral intensities for He II $\lambda 4686$ and Hβ. According to the work of Gurzadian (1988), who formulated a relationship between the temperature of the central star and the various emission line ratios, KoRe 1 is among a small percentile of planetaries with *super-high* temperature central stars ($\simeq 300,000$ K). A correspondingly high intrinsic luminosity, faint apparent magnitude for the nebula and central star (near the Sky Survey limits), and a small apparent diameter ($14''$) for the associated planetary nebula suggest that it is probably much more distant than the cluster, which is nearby ($d = 902 \pm 10$ pc, Turner, 1986). The pair appears to represent another case of a spatial coincidence rather than a physical association.

2.2.10 HeFa 1 and NGC 6067 ($\ell \simeq 330°$)

Henize & Fairall (1983) concluded that the planetary nebula HeFa 1 is probably not associated with the open cluster NGC 6067, on the basis of an inferred reddening of $E_{B-V} = 0.66 \pm 0.04$ (Henize & Fairall, 1983; Tylenda et al., 1992), which is larger than that of the cluster. The large color excess implies a distance not much greater than ~1–2 kpc, according to the run of reddening with distance along this line of sight (Neckel & Klare, 1980). The cluster reddening is $E_{B-V} = 0.35 \pm 0.01$ according to Waelkens & Rufener (1985), and $E_{B-V} = 0.32$ from Meynet et al. (1993), which places a similar constraint on its distance. Meynet et al. (1993) find a distance of $d = 1665$ pc and an age of 17×10^7 years ($\log(\tau) = 8.22$) for the cluster, so the only difference in parameters between the cluster and planetary nebula is the reddening, which is not an ideal test of membership in this instance.

NGC 6067 is also statistically unique in that it hosts two Cepheid members (Eggen, 1983). There is consequently an *a priori* probability of detecting a planetary nebula associated with the cluster since short-period Cepheids are potential progenitors of stars that produce planetary nebulae. A radial velocity estimate for the planetary nebula would help resolve the question of its possible cluster membership, since a cluster velocity of $V_R = -39.3 \pm 1.6$ km s^{-1} has been measured (Mermilliod et al., 1987). The case for a potential physical association remains open.

2.2.11 SA 2-167 AND NGC 6281 ($\ell \simeq 348°$)

Feinstein & Forte (1974) established that the cluster NGC 6281 is nearby with a distance of $d = 560 \pm 30$ pc and a reddening of $E_{B-V} = 0.15 \pm 0.02$. The planetary nebula Sa 2-167, however, has a much larger color excess of $E_{B-V} \simeq 2.2$, according to Tylenda et al. (1992), which implies a distance in excess of ~ 2 kpc (Neckel & Klare, 1980). One can also note the location of the planetary towards the Galactic bulge. The reddening discrepancy alone indicates that the planetary nebula lies in the background of the open cluster NGC 6281.

2.2.12 M 3-45 AND BASEL 5 ($\ell \simeq 360°$)

A reanalysis by Janes & Adler (1982) of photographic *RGU* photometry for the cluster Basel 5 by Svolopoulos (1966) indicates that Basel 5 is relatively nearby with a distance of $d = 1360$ pc and a reddening of $E_{B-V} = 0.39$. Conversely, the planetary nebula M 3-45 may be a member of the Galactic bulge population (Mal'kov, 1998), given its galactic longitude and large reddening of $E_{B-V} \simeq 1.86 \pm 0.01$ (Tylenda et al., 1992; Cuisinier et al., 2000). As in the previous case, the large reddening discrepancy is sufficient to indicate that the planetary nebula cannot be associated with the cluster.

2.3 OTHER POSSIBLE COINCIDENCES

The list of potential spatial coincidences between planetary nebulae and open clusters presented in Table 1 is only a partial listing of the spatial coincidences that exist (e.g., Ziznovsky, 1975). A more exhaustive listing of potentially good cases is presented in Table 5, derived with the aid of on-line lists of planetary nebulae (and possible planetary nebulae) and open clusters, the latter including some rather sparse spatial groupings not yet confirmed as true clusters (such as the anonymous group lying near the planetary nebula A 69). The interesting case of AL 67−01 (Andrews & Lindsay, 1967) and PHR1315-6555 was highlighted by Parker et al. (2006), but there are a few other equally interesting coincidences, such as K4 4-41 near NGC 6846. Several dozen other spatial coincidences exist, but they consist mainly of planetary nebulae lying towards the region of the Galactic center (Jacoby & van de Steene, 2004) or bulge in purely spatial coincidence with foreground clusters. Most are extremely faint planetaries of small angular diameter that are almost certainly background to the relatively nearby clusters. Many of the objects in Table 5 are deserving of further study, however.

A noteworthy feature of both Table 1 and Table 5 is that there are very few planetary nebulae coincident with cluster nuclei, and even those cases may represent cluster coronal objects seen in projection against cluster nuclei. A sometimes overlooked property of Milky Way open clusters is that their dimensions and stellar content are invariably underestimated when gauged on the basis of stars populating their dense nuclear regions, which are oversampled in CCD studies. As noted in §2, Kholopov (1969) and Nilakshi et al. (2002) find that open clusters are surrounded by low density coronae that contain the bulk of their member stars. By inference, that should include the bulk of cluster members that evolve into planetary nebulae. Cluster coronae also contain a large proportion of each cluster's massive stars (Burki, 1978), and account for the majority of Cepheids that are associated with open clusters (Turner, 1985). Cluster Cepheids in the Large Magellanic Cloud exhibit an identical characteristic (Efremov, 2003).

There is no obvious explanation for the preference of massive stars and Cepheids, and presumably planetary nebulae progenitors, to cluster coronae. A dynamical origin for coronal Cepheids was proposed by Turner (1985), in which the greater frequency of stellar encounters in dense cluster nuclei (see Turner, 1996) results in a higher frequency of close binaries and merger products there, the former, because of Roche lobe overflow, being less likely to produce post-main-sequence stars capable of reaching supergiant dimensions. The same mechanism might explain the apparent shortage of planetary nebulae in cluster nuclei. An alternate explanation in terms of a radial dependence of Jeans mass M_J in proto-clusters was suggested by Burki (1978) to account for the discrepancy with respect to massive stars.

It is of interest to speculate on the future fate of cluster members with masses of $M \leq 8\ M_\odot$. Such objects eventually become Cepheids with pulsation periods $P \leq 10$ days (Turner, 1996) or planetary nebulae once they pass through intermediate stages as red supergiants and asymptotic giant branch stars. The duration of the Cepheid phase varies widely from $10^4 - 10^5$ years for first crossings of the instability strip to $10^6 - 10^7$ years for higher crossings, an order of magnitude (or more) longer than the planetary nebula stage. There are ~ 30 known cluster Cepheids with $P \leq 10$ days (e.g., Turner & Burke, 2002), so statistically one might expect only a few planetary nebulae to be members of open clusters, and a preference for cluster coronae would seem logical. The survey presented here appears to confirm such expectations.

2.4 DISCUSSION

We have yet to establish a single physical association between a planetary nebula and an open cluster based on a correlation between their radial velocities, reddenings, and distances. However, further follow-up is indicated for a number of cases where the evidence is suggestive, namely M 1-80/Berkeley 57, NGC 2438/NGC 2437, NGC 2452/NGC 2453, VBRC 2 & NGC 2899/IC 2488,

and HeFa 1/NGC 6067, six of the thirteen coincidences considered. Additional good cases may arise from closer examination of some of the other coincidences noted in Table 5, but most of the associated clusters are as yet unstudied, limiting further progress.

Almost all potential cluster planetary nebulae lie in cluster coronal regions, typically surrounding open clusters for which limited or no photometric data exist. The fact that very few Galactic open clusters have been studied to the extent that both their nuclear and coronal regions are examined (Turner, 1996) only compounds the situation. Further progress requires not only new studies of our Galaxy's many unstudied clusters, but studies of their coronal regions as well. Spectroscopic observations of potentially-associated planetary nebulae would also be of value.

ACKNOWLEDGEMENTS

Table 2.1. Possible Planetary Nebula/Open Cluster Associations.

Planetary Nebula	PN Identifier	Open Cluster	Cluster r_n (')[a]	Estimated R_C (')[b]	Separation (')
M 3-20	G002.1−02.2	Trumpler 31	3	24	7
M 1-80	G107.7−02.2	Berkeley 57	5	⋯	10
A9	PK172+00.1	NGC 1912 (M38)	10	31	13
NGC 2438	G231.8+04.1	NGC 2437 (M46)	10	35	5
NGC 2452	G243.3−01.0	NGC 2453	2	21	9
NGC 2818	G261.9+08.5	NGC 2818	5	24	1
NGC 2899	G277.1−03.8	IC 2488	17	⋯	54
VBRC 2	G277.7−03.5	IC 2488	17	⋯	53
ESO 177-10	G324.8−01.1	Lyngå 5	5	⋯	2
KoRe 1	G327.7−05.4	NGC 6087	7	31	4
HeFa 1	G329.5−02.2	NGC 6067	7	33	12
Sa 2-167	G347.7+02.0	NGC 6281	4	26	6
M 3-45	G359.7−01.8	Basel 5	3	⋯	5

[a]Estimated from the angular radius cited by Dias et al. (2002), except as noted in the text.

[b]From $R_C \simeq 35' +$ Angular Diameter (Barkhatova, 1950).

Table 2.2. Framework for Evaluating Possible Physical Associations.

Criterion	Likely Member	Potential Member	Nonmember
ΔV_R	≤ 5 km/s	$5 - 10$ km s^{-1}	≥ 10 km s^{-1}
ΔE_{B-V}	≤ 0.2	$0.2 - 0.6$	≥ 0.6
$d(\mathrm{PN})/d(\mathrm{cluster})$	$\simeq 1$	$1 - 2$	≥ 2

Table 2.3. Radial Velocities for NGC 2438 and NGC 2437 (M46).

Source	$V_R(\mathrm{PN})$ (km s^{-1})	$V_R(\mathrm{Cluster})$ (km s^{-1})	Stars
Struve (Cuffey, 1941)	77	45.1 ± 5.5	5
O'Dell (1963)	75 ± 5	48.1 ± 3.0	1
Meatheringham et al. (1988)	74 ± 4	⋯	⋯
Mermilliod et al. (1989)	⋯	48.1 ± 0.1	1 (orbit)
Durand et al. (1998)	75 ± 2.5	⋯	⋯
Pauls & Kohoutek (1996)	60.3 ± 3.6	60.8 ± 4.0	4

Table 2.4. Parameters for the Cluster NGC 2453.

Source	Distance (pc)	E_{B-V}
Moffat & Fitzgerald (1974)	2900	0.47
Glushkova et al. (1997)	2400	⋯
Massey et al. (1995)	5900 ± 200	⋯
Dambis (1999)	2400	0.48
Mottini (2006)	5250	0.50

Table 2.5. Additional Planetary Nebula/Open Cluster Coincidences ($r < 15'$).

Planetary Nebula	PN Identifier	Open Cluster	Cluster r_n $(')^c$	Estimated R_C $(')^d$	Separation $(')$
NGC 6741	G033.8−02.6	Berkeley 81	3	$\cdots$	13
K4 4-41	G068.7+01.9	NGC 6846	1	$\cdots$	1
KLW 6	G070.9+02.4	Berkeley 49	2	$\cdots$	11
K 3-57	G072.1+00.1	Berkeley 51	1	$\cdots$	12
A 69	G076.3+01.1	Anon (Turner)	3	$\cdots$	4
Bl 2-1	G104.1+01.0	NGC 7261	3	22	7
FP0739-2709	G242.3−02.4	ESO 493−03	4	$\cdots$	8
PHR0840-3801	G258.4+02.3	Ruprecht 66	1	$\cdots$	2
PHR0905-5548	G274.8−05.7	ESO 165−09	8	$\cdots$	9
Pe 2-4	G275.5−01.3	van den Bergh-Hagen 72	1	$\cdots$	9
$\cdots$	$\cdots$	NGC 2910	2	24	14
NeVe 3-1	G275.9−01.0	NGC 2925	5	26	12
Hf 4	G283.9−01.8	van den Bergh-Hagen 91	3	$\cdots$	14
He 2-86	G300.7−02.0	NGC 4463	2	22	3
PHR1315-6555	G305.3−03.1	AL 67−01	2	$\cdots$	1
PHR1429-6043	G314.6−00.1	NGC 5617	5	25	1
vBe 3	G326.1−01.9	NGC 5999	2	25	5

^{c}Estimated from the angular radius cited by Dias et al. (2002), except as noted in the text.

^{d}From $R_C \simeq 35'+$ Angular Diameter (Barkhatova, 1950).
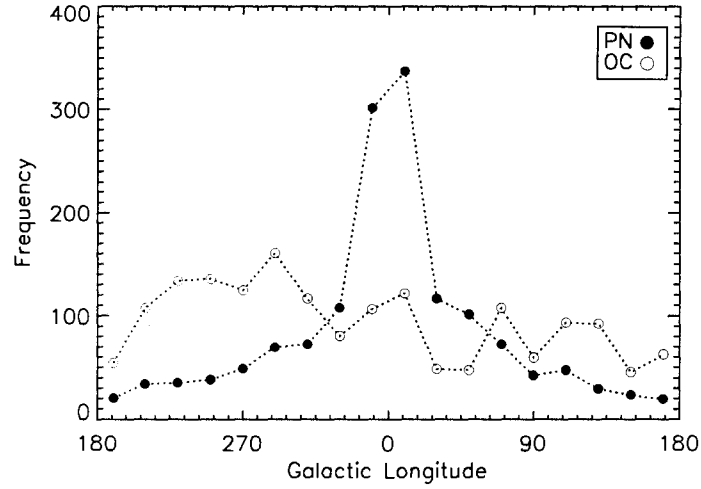
Figure 2.1 The distribution of planetary nebulae and open clusters with galactic longitude, from data tabulated in the catalogs of Kohoutek (2001) and Dias et al. (2002). Open clusters appear to be randomly distributed along the Galactic plane, whereas planetary nebulae are concentrated towards the Galactic bulge.
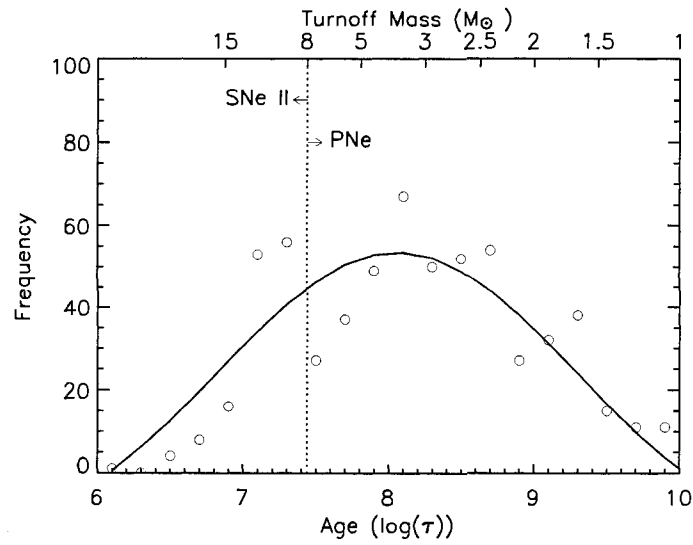
Figure 2.2 The distribution of open cluster ages compiled from the catalog of Dias et al. (2002) relative to the age/turnoff-mass relation given by Iben & Renzini (1983). Open cluster ages can be described by a normal distribution with a peak near $\log(\tau) \simeq 8$. The predicted upper turnoff mass limit, below which stars may evolve to produce planetary nebulae, is $M \simeq 8\ M_\odot$, above which Type II supernovae are expected.
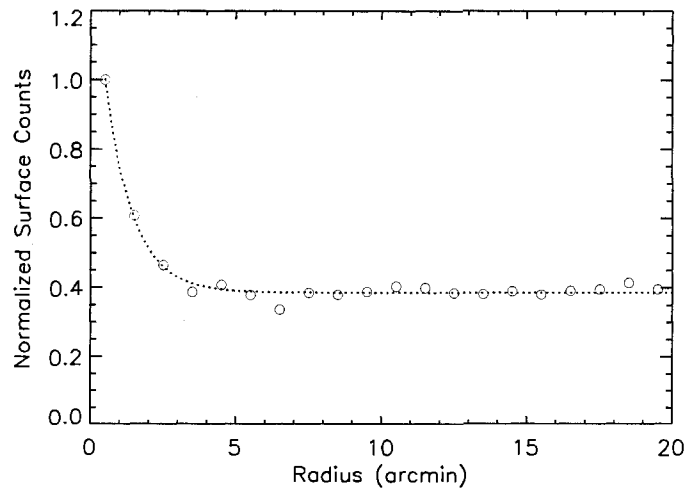
Figure 2.3 Star counts for the open cluster Berkeley 57 derived from data in the 2MASS survey.
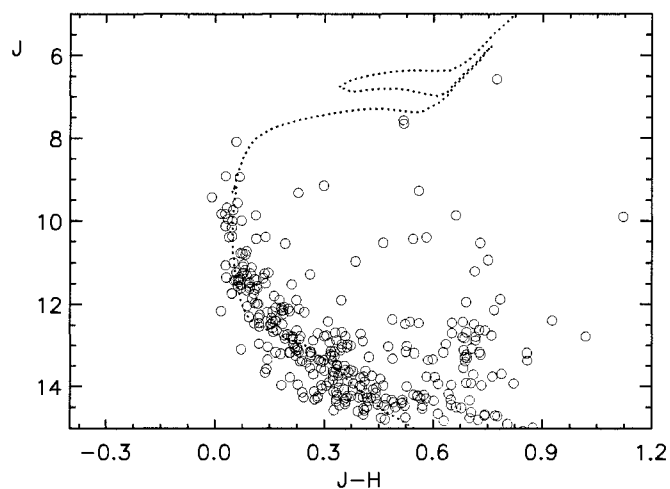
Figure 2.4 A color-magnitude diagram for M38 (NGC 1912) constructed from 2MASS data. A $\log(\tau) = 8.25 \pm 0.15$ (Z=0.008) isochrone has been fitted to the observations, yielding a distance of $d = 1050 \pm 150$ pc and a reddening of $E_{B-V} = 0.27 \pm 0.03$.
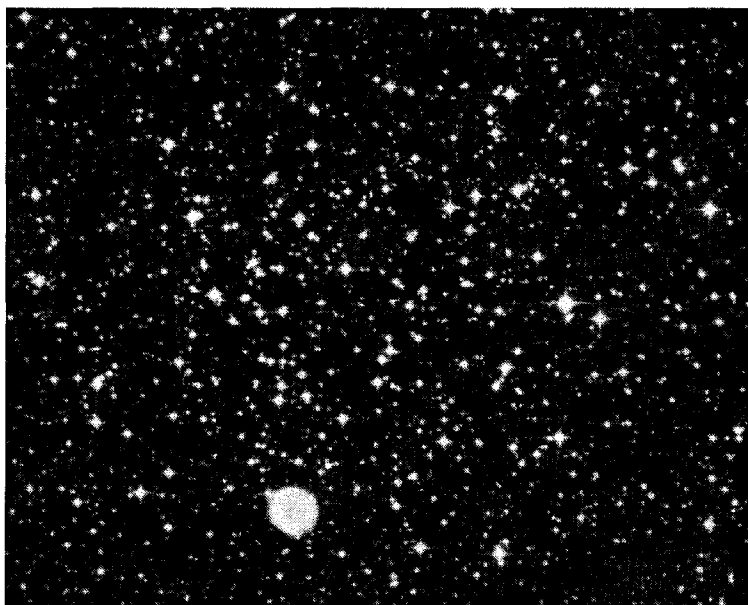
Figure 2.5 The field of view of M46 (NGC 2437), from a combination of images taken at the Abbey Ridge Observatory with POSS II.
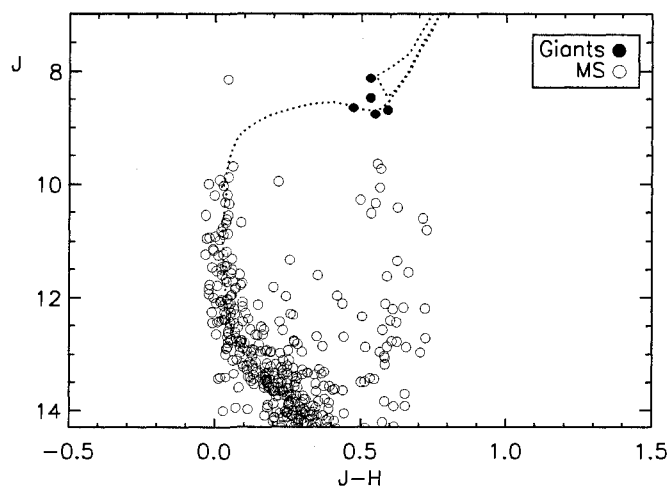
Figure 2.6 A color-magnitude diagram for M46 (NGC 2437) constructed from 2MASS data. A $\log(\tau) = 8.35$ isochrone has been fitted to the observations, yielding a distance of $d = 1700 \pm 250$ pc and a reddening of $E_{B-V} = 0.13 \pm 0.05$.

Figure 2.7 The field of view of NGC 2818, a pseudo color image constructed from POSS II data.
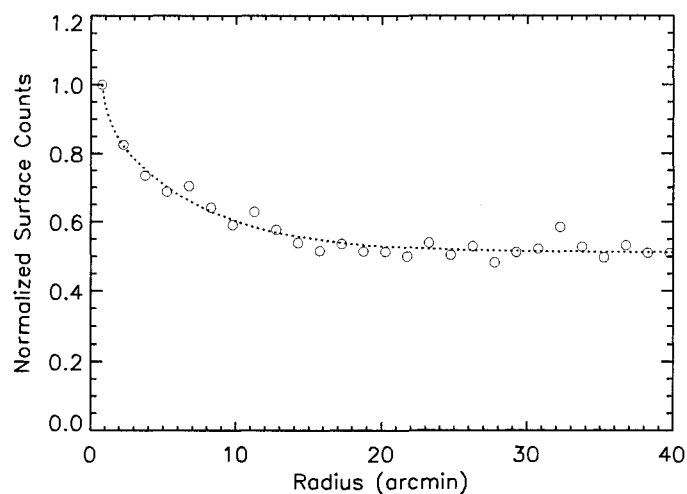
Figure 2.8 Star counts for the open cluster IC 2488 from 2MASS data.
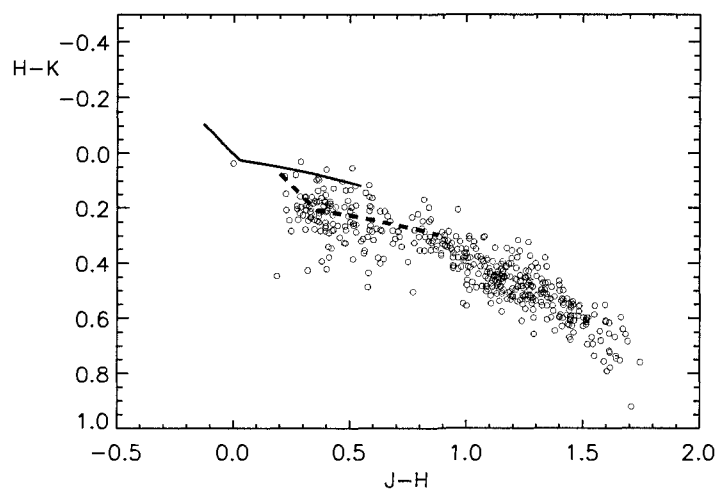
Figure 2.9 A *JHK* color-color diagram for Lyngå 5 constructed from 2MASS data. Likely cluster stars are reddened by $E_{J-H} = 0.33 \pm 0.03$, which is equivalent to $E_{B-V} = 1.18 \pm 0.11$. A reddening relation of slope $E_{J-H} = 1.72 \times E_{H-K}$ was adopted from Dutra et al. (2002); Bonatto et al. (2006).
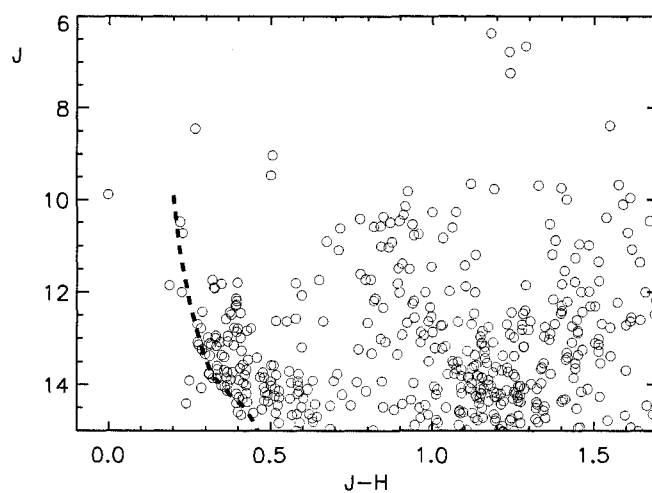
Figure 2.10 A *JH* color-magnitude diagram for the open cluster Lyngå 5 constructed from 2MASS data for stars within a 5′ field centered on the J2000 co-ordinates for the cluster cited here. A ZAMS fit yields a distance of $d = 1950 \pm 350$ pc for the reddening indicated in Fig. 9.

REFERENCES

Akhundova, G. V. & Seidov, Z. F. 1971, Soviet Ast., 14, 734

Andrews, A. D., & Lindsay, E. M. 1967, Irish Astronomical Journal, 8, 126

Barkhatova, K. A. 1950, AZh, 27, 180

Bensby, T., & Lundström, I. 2001, A&A, 374, 599

Bertelli, G., Bressan, A., Chiosi, C., Fagotto, F., & Nasi, E. 1994, A&AS, 106, 275

Bica, E., & Bonatto, C. 2005, A&A, 443, 465

Bonnarel, F., et al. 2000, A&AS, 143, 33

Bonatto, C., Bica, E., & Girardi, L. 2004, A&A, 415, 571

Bonatto, C., Bica, E., Ortolani, S., & Barbuy, B. 2006, A&A, 453, 121

Burki, G. 1978, A&A, 62, 159

Cahn, J. H., Kaler, J. B., & Stanghellini, L. 1992, A&AS, 94, 399

Cazetta, J. O., & Maciel, W. J. 2000, , 36, 3

Clariá, J. J., Piatti, A. E., Lapasset, E., & Mermilliod, J.-C. 2003, A&A, 399, 543

Cuffey, J. 1941, ApJ, 94, 55

Cuisinier, F., Maciel, W. J., Köppen, J., Acker, A., & Stenholm, B. 2000, A&A, 353, 543

Cutri, R. M., et al. 2003, The IRSA 2MASS All-Sky Point Source Catalog, NASA/IPAC Infrared Science Archive

Dambis, A. K. 1999, Astron. Letters, 25, 10

De Marco, O. 2006, ArXiv Astrophysics e-prints, arXiv:astro-ph/0605626

Dias, W. S., Alessi, B. S., Moitinho, A., & Lépine, J. R. D. 2002, A&A, 389, 871

Durand, S., Acker, A., & Zijlstra, A. 1998, A&AS, 132, 13

Dutra, C. M., Santiago, B. X., & Bica, E. 2002, A&A, 381, 219

Efremov, Yu. N. 2003, Astron. Rept., 47, 1000

Eggen, O. J. 1983, AJ, 88, 379

Feinstein, A., & Forte, J. C. 1974, PASP, 86, 284

Gurzadian, G. A. 1988, Ap&SS, 149, 343

Glushkova, E. V., & Rastorguev, A. S. 1991, Sov. Astron. Lett., 17, 13

Glushkova, E. V., Zabolotskikh, M. V., Rastorguev, A. S., Uglova, I. M., & Fedorova, A. A. 1997, Pis'ma Astron. Zh., 23, 90

Hasegawa, T., Malasan, H. L., Kawakita, H., Obayashi, H., Kurabayashi, T., Nakai, T., Hyakkai, M., & Arimoto, N. 2004, PASJ, 56, 295

Henize, K. G., & Fairall, A. P. 1983, in Planetary Nebulae, IAU Symp. 103, ed. D. R. Flower (D. Reidel Publ.: Dordrecht), p. 544

Iben, I., & Renzini, A. 1983, ARA&A, 21, 271

Janes, K. & Adler, D. 1982, ApJS, 49, 425

Jacoby, G. H. 1989, ApJ, 339, 39

Jacoby, G. H., Morse, J. A., Fullton, L. K., Kwitter, K. B., & Henry, R. B. C. 1997, AJ, 114, 2611

Jacoby, G. H., & van de Steene, G. 2004, A&A, 419, 563

Jennens, P. A., & Helfer, H. L. 1975, MNRAS, 172, 681

Kaler, J. B., Shaw, R. A., & Kwitter, K. B. 1990, ApJ, 359, 392

Kholopv, P. N. 1969, Soviet Ast., 12, 625

Koester, D., & Reimers, D. 1989, A&A, 223, 326

Kohoutek, L. 2001, VizieR Online Data Catalog, 4024, 0

Köppen, J., & Acker, A. 2000, in Massive Stellar Clusters, ASP Conf. Ser., 211, ed. A. Lançon & C. M. Boily (ASP: San Francisco), p. 151

Kwitter, K. B., Jacoby, G. H., & Lydon, T. J. 1988, AJ, 96, 997

Kwok, S. 2005, J. Korean Astron. Soc., 38, 271

Lada, C. J., & Lada, E. A. 2003, ARA&A, 41, 57

Larsen, S. S., & Richtler, T. 2006, A&A, 459, 103

Magrini, L. 2006, in Planetary Nebulae in our Galaxy and Beyond, IAU Symp. 234, ed. M. J. Barlow & R. H. Méndez (Cambridge University Press: Cambridge), p. 9

Mal'kov, Y. F. 1998, Astron. Reports, 42, 293

Mallik, D. C. V., Sagar, R., & Pati, A. K. 1995, A&AS, 114, 537

Meatheringham, S. J., Wood, P. R., & Faulkner, D. J. 1988, ApJ, 334, 862

Mermilliod, J. C., Mayor, M., & Burki, G. 1987, A&AS, 70, 389

Mermilliod, J.-C., Mayor, M., Andersen, J., Nordstrom, B., Lindgren, H., & Duquennoy, A. 1989, A&AS, 79, 11

Mermilliod, J.-C., Clariá, J. J., Andersen, J., Piatti, A. E., & Mayor, M. 2001, A&A, 375, 30

Meynet, G., Mermilliod, J.-C., & Maeder, A. 1993, A&AS, 98, 477

Moffat, A. F. J., & Fitzgerald, M. P. 1974, A&AS, 18, 19

Moitinho, A. 2001, A&A, 370, 436

Moitinho, A., Vázquez, R. A., Carraro, G., Baume, G., Giorgi, E. E., & Lyra, W. 2006, MNRAS, 368, L77

Nilakshi, N., Sagar, R., Pandey, A. K., & Mohan, V. 2002, A&A, 383, 153

Neckel, Th., & Klare, G. 1980, A&AS, 42, 251

O'Dell, C. R. 1963, PASP, 75, 370

Osterbrock, D. E., & Ferland, G. J. 2006, Astrophysics of Gaseous Nebulae and Active Galactic Nuclei (University Science Books: Sausalito)

Parker, Q. A., et al. 2006, MNRAS, 373, 79

Pauls, R., & Kohoutek, L. 1996, Astron. Nachr., 317, 413

Pedreros, M. 1987, AJ, 94, 92

Pedreros, M. 1989, AJ, 98, 2146

Pena, M., Ruiz, M. T., Bergeron, P., Torres-Peimbert, S., & Heathcote, S. 1997, A&A, 317, 911

Peton-Jonas, D. 1981, A&AS, 45, 193

Phillips, J. P. 2004, MNRAS, 353, 589

Schoenberner, D., & Bloecker, T. 1996, Ap&SS, 245, 201

Soker, N. 2006, ApJ, 645, L57

Svolopoulos, S. N. 1966, ZAp, 64, 67

Tifft, W. G., Conolly, L. P., & Webb, D. F. 1972, MNRAS, 158, 47

Turner, D. G. 1976a, AJ, 81, 97

Turner, D. G. 1976b, AJ, 81, 1125

Turner, D. G. 1979, PASP, 91, 642

Turner, D. G. 1985, in Cepheids: Theory and Observations, IAU Colloq. 82, ed. B. F. Madore (Cambridge Univ. Press: Cambridge), p. 209

Turner, D. G. 1986, AJ, 92, 111

Turner, D. G. 1996a, in The Origins, Evolution, and Destinies of Binary Stars in Clusters, ASP Conf. Ser., 90, ed. E. F. Milone & J.-C. Mermilliod (ASP: San Francisco), p. 443

Turner, D. G. 1996b, JRASC, 90, 82

Turner, D. G., & Burke, J. F. 2002, AJ, 124, 2931

Tylenda, R., Acker, A., Stenholm, B., & Koeppen, J. 1992, A&AS, 95, 337

Walker, A. R. 1985, MNRAS, 214, 45

Weidemann, V. 2000, A&A, 363, 647

Zhang, C. Y. 1995, ApJS, 98, 659

Zijlstra, A. A. 2007, Baltic Astron., 16, 79

Ziznovsky, J. 1975, Bull. Astron. Inst. Czech., 26, 248

ABSTRACT

The Exciting Star of the Berkeley 59/Cepheus OB4 Complex and

Other Chance Variable Star Discoveries

by Daniel J. Majaess, David G. Turner, David J. Lane, and Kathleen K. Moncrieff.

Abstract: A study is presented regarding the nature of several variable stars sampled during a campaign of photometric monitoring from the Abbey Ridge Observatory: 3 eclipsing binaries, 2 semiregulars, a luminous Be star, and a star of uncertain classification. For one of the eclipsing systems, BD+66°1673, spectroscopic observations reveal it to be an O5 V((f))n star and the probable ionizing star of the Berkeley 59/Cep OB4 complex. An analysis of spectroscopic observations and BV photometry for Berkeley 59 members in conjunction with published observations imply a cluster age of $\simeq$2 Myr, a distance of d=883±43 pc, and a reddening of $E_{B-V} = 1.38 \pm 0.02$. Two of the eclipsing systems are Algol-type, but one appears to be a cataclysmic variable associated with an X-ray source. ALS 10588, a B3 IVn star associated with the Cepheid SV Vul, is of uncertain classification, although consideration is given to it being a slowly pulsating B star. The environmental context of the variables is examined using spectroscopic parallax, 2MASS photometry, and proper motion data, the latter to evaluate the membership of the variable B2 Iabe star HDE 229059 in Berkeley 87, an open cluster that could offer a unique opportunity to constrain empirically the evolutionary lineage of young massive stars. Also presented are our null results for observations of a sample of northern stars listed as Cepheid candidates in the New Catalogue of Suspected Variable Stars.

CHAPTER 3

VARIABLE STAR DISCOVERIES

3.1 INTRODUCTION

The present study is the result of a survey of variable stars initiated at the Abbey Ridge Observatory (ARO). Most of the discoveries resulted from the variability of potential reference and check stars in the fields of Cepheid variables, the campaign's primary objective being to establish period changes for northern hemisphere Cepheids (Turner 1998, Turner et al. 1999). In two cases the interest lies in cluster stars discovered to be variable.

The program began in 1996 at the Burke-Gaffney Observatory (BGO) of Saint Mary's University, and was recently transferred to the ARO, which is located at a darker site. The stability of the ARO site and an upgrading of the photometric reduction routines facilitated the discoveries, some of which are described here. A preliminary survey was also made of stars in the New Catalogue of Suspected Variable Stars (NSV, Samus et al. 2004) thought to be potential Cepheid variables, with the goal of expanding the Galactic sample and eventually studying their period changes. Rate of period change, in conjunction with light amplitude, has been demonstrated to be an invaluable parameter for constraining a Cepheid's crossing mode and likely location within the instability strip (Turner et al. 2006a). Such constraints permit further deductions to be made concerning a Cepheid's intrinsic reddening and pulsation mode, and offer yet another diagnostic tool for establishing Cepheids as members of open clusters, such calibrators being the foundation for the extragalactic distance scale (Turner and Burke 2002).

The photometric signatures of some variable stars can be sufficiently ambiguous that spectroscopic follow-up was necessary to resolve the true nature of the light variations. Preliminary results

for the best-studied of the variables, summarized in Table 1, are presented here in order of increasing right ascension. The results for the NSV stars are given at the end.

3.2 OBSERVATIONS AND EQUIPMENT

The ARO is located in Stillwater Lake, a community $\simeq$ 23 km west of Halifax, Nova Scotia, Canada. The ARO allocated $\simeq$ 2 hours of observing time on each clear night in support of this research, with much of the remainder used to search for extragalactic supernovae and to participate in AAVSO observing campaigns and Special and Alert Notice targets. The site is quite dark, with typical Sky Quality Meter readings of 20.6 V mag. arcsec^{-2} on good nights. The observatory houses a 28-cm Celestron Schmidt-Cassegrain telescope equipped with an SBIG ST9-CCD camera and Bessel B and V filters. The facility is remotely accessible and completely automated, allowing unattended acquisition of astronomical and calibration images and providing a software pipeline that calibrates, combines, and performs differential aperture photometry. Much of the design and software development to realize the ARO's capability was completed in the form of the Abbey Ridge Auto-Pilot software (Lane 2007). Other software, in particular MaxIm DL/CCD (George 2007), provides many of the low-level image acquisition and processing functions.

Observations and image processing are guided by two data files provided by the observer. The first contains relevant information about each field to be imaged, including a unique identifier, center equatorial co-ordinates, and exposure times and number of exposures to be taken in each filter. If aperture photometry is to be performed automatically on the field, additional information is needed, including aperture photometry parameters, magnitude of the designated reference star, and equatorial co-ordinates for each star to be measured. The second file type contains a list of target fields (identifiers) to be observed on a given night.

All resulting photometric data represent means for multiple (15-25, or more) short-exposure

images, typically of 1 to 60 seconds duration, taken in immediate succession, combined using a noise-reduction algorithm developed by DJL. The algorithm first calibrates the individual images instrumentally, then registers them spatially using stars in the field. The mean and standard deviation are computed for each pixel position in the stack of images. Pixels on a given image that deviate more than a specified number of standard deviations from the mean of pixels at the same pixel positions on the other images are rejected, and a new mean is computed. The process is iterated up to five times until all deviant pixels are rejected, although no more than 30% of the pixels at a given pixel position are ever rejected. The resulting mean, without inclusion of rejected pixels, is used to form the combined image, which is plate-solved astrometrically using the PinPoint Astrometric Engine software (Denny 2007).

Differential aperture photometry is performed on each combined image using initial aperture and sky annulus parameters, and equatorial co-ordinates of the primary target star, reference star, and any number of check or other stars. The sky annulus radius and size are pre-selected for each field to be appropriate for all stars measured. The equatorial position of each star is converted to its corresponding X and Y pixel position using the plate solution embedded in the fts header. Aperture photometry is performed on the reference star 3 times iteratively to determine its precise X and Y pixel position and full-width half maximum (FWHM) seeing disk. A new aperture size is set to a pre-determined multiple of the measured FWHM, and the sky annulus position is adjusted so that it remains at the original radius from the star's center. The new aperture parameters and the same technique are used for the remaining stars measured. The instrumental magnitude derived for the reference star is used to convert instrumental magnitudes for the remaining stars into differential magnitudes.

The output for each measured star includes pertinent information, such as FWHM, sky annulus background, signal-to-noise ratio, and maximum pixel value, all of which are invaluable when assessing the data quality. In most instances the reference stars are selected from the comprehensive

Tycho-2 catalog (Hg et al. 2000), so there may be zero-point offsets, given that the reference stars are non-standards and the photometry is not explicitly normalized to the Johnson system. Also, differences in color between the reference and target stars are not normally taken into account.

The spectra used to classify the variables were obtained during two observing runs with the Dominion Astrophysical Observatory's 1.8m Plaskett telescope. During the first run in October 2006, the SITe-2 CCD detector was used to image spectra at a resolution of 120 Å mm^{-1} centered on 4740 Å. For the second run in October 2007, the SITe-5 CCD detector was used to image spectra at a resolution of 60 Å mm^{-1} centered on 4200 Å. The spectra were reduced and analyzed using the NOAO's routines in IRAF along with software packages by Christian Buil (Iris), Valrie Desnoux (Vspec), and Robert H. Nelson (RaVereC). Lastly, a search for periodicity in the photometry of periodic variables in the sample was carried out in the Peranso software environment (Vanmunster 2007) using the algorithms ANOVA (Schwarzenberg-Czerny 1996), FALC (Harris et al. 1989), and CLEANest (Foster 1995).

3.3 COMMENTS ON INDIVIDUAL STARS

3.3.1 BD+66°1673 (EA, O5 V((F))N)

BD+66°1673 lies on the northwestern edge of Berkeley 59, an open cluster embedded in an H II region (Figure 1) at the core of the Cep OB4 association. The star was classified previously from objective-prism spectra as O9-B0 (MacConnell 1968; Walker 1965), but is reclassified as O5 V((f))n from a spectrum at 60 Å mm^{-1} obtained at the DAO (Figure 2). BD+66°1673 now has the distinction of being the hottest star in Cep OB4. The star's implied high temperature drives mass loss via strong stellar winds that may be largely responsible for shaping and illuminating the surrounding H II region, along with playing a role in the formation of clearly-visible, cold, molecular pillars (Yang and Fukui 1992; Gahm et al. 2006).

BD+66°1673 was monitored as part of a search for variable stars in Berkeley 59, and was the first to exhibit convincing brightness variations. A period analysis of the photometry revealed a strong signal for $P = 5.33146 \pm 0.02000$ days. The phased light curve (Figure 3) is that of an Algol-type eclipsing binary system, with primary and secondary eclipse depths of $\simeq 0.13$ and $\simeq 0.06$ mag., although with eclipses skewed in phase indicating an eccentric orbit of $e \simeq 0.3$ and longitude of periastron $\omega \simeq 180°$. Our adopted ephemeris for light minimum in the system from regression fits for the light curve is:

HJDmin $= 2454400.5322 + 5.33146$ E.

For the inferred stellar mass and temperature of the primary, a preliminary model generated for the system using Binary Maker 3 (Bradstreet and Steelman 2004) constrains the companion to be an early-to-mid B-type star (B2-B3, say) in a system with an orbital inclination of $\simeq 75°$. A more detailed photometric study is needed to generate a full light curve to confirm the orbital eccentricity as well as to permit a more detailed analysis.

The distance to BD+66°1673 can be established from its likely membership in Berkeley 59 and Cep OB4, despite a spatial location outside the cluster nucleus. We obtained all-sky BV photometry of the cluster field on five nights, derived extinction coefficients using the techniques outlined by Henden and Kaitchuck (1998), and standardized the photometry to the Johnson system using stars in the nearby cluster NGC 225 (Hoag et al. 1961). Our data for cluster stars for which we have spectroscopic results are given in Table 2.

BV photometry does not permit one to assess the properties of the dust extinction in the field, and for that we must rely on the UBV photometry obtained by MacConnell (1968) for bright association members. A complete reanalysis is indicated, given that MacConnell (1968) derived different values for the ratio of total to selective extinction (RV) for different stars and regions of Cep OB4. Unusual reddening properties for the dust in the field were first suggested by Blanco and Williams (1959) in their study of Cep OB4. Such properties, if confirmed, would limit the accuracy of any derived

distance to the cluster and association stars. We therefore decided to reanalyze the RV estimate from the available photometric and spectroscopic data.

The new spectral classifications for Cep OB4 stars (Figure 2, Table 2) can be used with the UBV photometry of MacConnell (1968) to establish the reddening law for the dust in the field. The result for the four brightest stars is a reddening slope of X= 0.80 ± 0.01, identical to the reddening parameters inferred for dust obscuring nearby fields in Cygnus (Turner 1989). The observed UBV colors were dereddened with that reddening law and either zero-age main-sequence (ZAMS) luminosities from Turner (1976, 1979) or main-sequence luminosities for obvious non-ZAMS stars, with results presented in the variable-extinction diagram of Figure 4. Some stars have colors systematically too blue for their observed spectral types, a feature encountered for many early-type emission-line stars (Schild and Romanishin 1976). The reddening law in Cep OB4 is reasonably well defined by the data, and the slope of the relation depicted in Figure 4 is RV= 2.81 ± 0.09 from least squares and non-parametric straight line fits. The slope is consistent with the properties of nearby dust clouds (Turner 1996b).

The distance to Berkeley 59 and Cep OB4 follows from a ZAMS fit, which gives $V_0 - M_v = 9.73 \pm 0.11$, corresponding formally to d= 883 ± 43 pc. A main-sequence fit to our new photometry for stars in the core of Berkeley 59 (Table 2) is shown in Figure 5 along with data for association members. The results reveal another feature, namely an excess reddening for the B8 III star 2MASS 00021063+6724087: $E_{B-V} = 1.5$ relative to $E_{B-V} = 1.38 \pm 0.02$ for other, spatially-adjacent, cluster members. 2MASS 00021063+6724087 may be an example of a rotating star embedded in a dust torus (see Turner 1996a), and its location in Figure 5 is consistent with a star near the turn-on point for pre-main-sequence objects. The cluster radial velocity can be deduced by merging observations from Crampton and Fisher (1974) and Liu et al. (1989, 1991), which yields $V_R = -7 \pm 15$ km s^{-1} for BD+66°1674, and -8 ± 31 km s^{-1} for BD+66° 1675. Crampton and Fisher (1974) noted that scatter in the radial velocities for both objects suggested they are spectroscopic binaries. A

period search reveals putative periods of $P = 1.20$ days and $P = 5.30$ days for BD+66° 1674. The results are sufficiently interesting to justify additional radial velocity measures, which are essential to establish a unique solution.

The presence of a O5 V((f))n star in Berkeley 59 and the predominance of late B-type cluster members lying above the ZAMS indicates an extremely young cluster. An age of $\simeq 2 \times 10^6$ years for Berkeley 59 is estimated from BD+66° 1673 and the luminosities of stars lying near the cluster turn-on point in Figure 5 (see Guetter and Turner 1997), marking Berkeley 59 as one of the youngest and nearest clusters known. Certainly O5 V((f))n stars are rarely encountered in our Galaxy within a kiloparsec of the Sun. Much like Berkeley 87 discussed later, Berkeley 59 contains a sufficient number of exotic stars to make it an object of intense interest for future studies.

3.3.2 2MASS 00104558+6127556 (EA, A9 V)

The star 2MASS 00104558+6127556 was found to vary in light during monitoring of the Cepheid BD Cas. A dominant period of P= 2.7172 ± 0.0060 days produces a light curve (Figure 3) indicating an Algol-type eclipsing system with eclipse depths of $\simeq 0.43$ mag. for primary minimum and $\simeq 0.31$ mag. for secondary minimum. Our adopted ephemeris for light minimum in the system from regression fits for the light curve is:

HJDmin =2454404.8586 + 2.7172 E.

A spectrum (Figure 6) indicates a spectral type near A9 V, but with some features that may indicate contamination by a companion. For the inferred stellar mass and temperature of the primary, a preliminary model generated for the system using Binary Maker 3 (Bradstreet and Steelman 2004) constrains the companion to be a mid F-type star (F4-F5, say) in a system with an orbital inclination of $\simeq 88°$. Additional observations are needed to refine the period and to establish a complete light curve for a formal analysis.

3.3.3 2MASS 19064659+4401458 (XI?, G2 V)

2MASS 19064659+4401458 lies in the field of the nova-like cataclysmic variable MV Lyr, and was found to display a low level of variability while monitoring the suspected Cepheid NSV 11753 (see section 3.8). The star's variability was presumably discovered by Weber (1959, number 90 in his list), although it is misidentified in the original finder chart as a different star of constant brightness located a mere 1.4 arcminutes away (NSV 11753, J2000 19:06:54.19, +44:02:55.5). There is X-ray emission at a flux level of 2.21×10^{-2} counts s^{-1} from within an arcminute of the object (ROSAT ASSC source J190645.9+440139, Voges et al. 2000) that is distinct from an X-ray flux of 1.26×10^{-2} counts s^{-1} associated with MV Lyr itself (ROSAT ASSC source J190716.8+440109, Voges et al. 1999). The object's spectral type is G2 V (Figure 6), and its spectroscopic parallax (below) implies an X-ray luminosity of $L_X \simeq 10^3 0$ ergs s^{-1}, as estimated using the energy conversion factor of Huensch et al. (1996). The result is too low for a canonical low-mass X-ray binary (LX ? 1036 ergs s-1), but is similar to that of W UMa systems ($L_X \simeq 10^{29-30}$ ergs s^{-1}, Chen et al. 2006), chromospherically active stars (i.e., RS CVn variables), and compact binaries.

A preliminary period analysis resulted in a dominant signal corresponding to $P \simeq 7.0$ days, which is consistent with the initial estimate by Weber (1959) of 8 days, and agrees with more recent estimates by David Boyd and Christopher Lloyd (private communication). The phased light curve in Figure 3 displays a brief eclipse superposed on more rapid, irregular, quasi-sinusoidal variations. The possibility that 2MASS 19064659+4401458 is a close contact system is inconsistent with the inferred period, and chromospheric activity in the primary is precluded by the absence of Ca II H and K emission in its spectrum.

An alternative scenario would associate irregularities in the light curve with frictional heating in an accretion disk, implying that 2MASS 19064659+4401458 is a semi-detached binary system consisting of a G dwarf overfilling its Roche surface and orbiting a compact companion, presumably a white dwarf. During eclipses the irregular variations disappear, implying that they originate from

a hot spot in the accretion disk that is eclipsed by the G2 dwarf. It is hoped that the preliminary results presented here will motivate additional observers to join an ongoing campaign led by variable star observer David Boyd, with a group including Richard Huziak, Roger Pickard, Tomas Gomez, Gary Poyner, Tom Krajci, and Bart Staels, to constrain the period and further investigate the star. An understanding of the system via optical photometry, however, may be limited by the nature of the source driving the irregular variations. Time-series spectroscopy is also needed to assess the full nature of the system.

The object's distance is estimated from the canonical distance modulus relation reformulated for the infrared, namely with $A_J = 0.276 \times A_V$ and $E_{J-H} = 0.33 \times E_{B-V}$ (Bica and Bonatto 2005, Dutra et al. 2002). The 2MASS magnitudes for the star are $J = 11.275 \pm 0.020$, H= 10.776 ± 0.018, and K= 10.650 ± 0.016 (Cutri et al. 2003), and an absolute magnitude and intrinsic color can be established from the star's main-sequence spectral type as $M_J = 3.24 \pm 0.53$ and $(J - H)_0 = 0.28 \pm 0.06$, parameters deduced from a sample of $n \simeq 30$ G2 V stars in the Hipparcos database (Perryman et al. 1997) with cited parallax uncertainties 0.7 mas. The implied intrinsic color agrees with a value of $(J - H)_0 \simeq 0.38$ from Koornneef (1983), when converted to the 2MASS system with the appropriate transformation (Carpenter 2001). The resulting distance for $R_V = 3.1$ is $d = 310$ pc, while, if a nearly negligible field reddening is adopted, as advocated by a 2MASS color-color diagram of the region, it is $d \simeq 400$ pc.

3.3.4 BD+22° 3792 (SRB, M6 III)

The variability of BD+22° 3792, of spectral type M6 III (Shi and Hu 1999, see Figure 6), was discovered by the ASAS survey (Pojmanski et al. 2005). The semi-periodic nature of its photometric variations (Figure 7) and its spectral type are consistent with a Type B semi-regular variable. A Fourier analysis of our observations and those of ASAS-3 implies a possible period around 79 days. The star's spectral energy distribution displays far-infrared emission, indicating the presence of a

warm dusty envelope surrounding the star, likely stemming from mass loss.

BD+22° 3792 is 12' from the open cluster NGC 6823, but is not a member. The cluster's associated H II region is excited by numerous, young, reddened, OB stars, which are $\simeq (4-7) \times 10^6$ years old at a distance of $d = 2.1 \pm 0.1$ kpc (Guetter 1992). The star's distance can be estimated by spectroscopic parallax using photometry taken from Massey et al. (1995) and a set of intrinsic parameters, $M_V = -0.3 \pm 0.7$ and $(B-V)_0 = 1.36 \pm 0.09$, derived from a sample of $n = 7$ nearby M6 giants in the Hipparcos database (Perryman et al. 1997) with cited parallax uncertainties 0.9 mas. The intrinsic parameters for M6 giants in the literature are rather scattered (see Mikami 1986, and references therein), mainly because most are variable and exhibit intrinsic color excesses. The resulting distance to BD+22° 3792 is $\simeq 700$ pc for a reddening of $E_{B-V} \simeq 0.38$ from the Hipparcos data, while adoption of an intrinsic color of $(B-V)_0 = 1.58$ from Lee (1970) gives $d \simeq 950$ pc and $E_{B-V} \simeq 0.18$.

3.3.5 2MASS 19475544+2722562 (SRB, M4 III)

The star 2MASS 19475544+2722562 lies in the field of the Cepheid S Vul. A Fourier analysis suggests a rather short period of $\simeq 27$ days. The star's late spectral type of M4 III (Figure 6) suggests a likely designation as a Type B semiregular.

3.3.6 ALS 10588 = LS II+27 19 (SPB? ELL?, B3 IVn)

Alma Luminous Star 10588 (Reed 1998), or LS II+27 19 (Stock et al. 1960), is a close spatial neighbor of the Cepheid SV Vul, and a likely member of Vul OB1 (Turner 1980, 1984). The star's evolutionary status from its spectral type (B3 IVn, Figure 6) matches that of stars associated with SV Vul, namely main-sequence objects terminating at B3. Spectroscopic parallax places the star at a distance of 2040 ± 470 pc, consistent with the distance to Vul OB1 ($d = 2.1 - 2.5$ kpc, Turner 1986; Guetter 1992). ALS 10588 exhibits an IR excess with emission at 60 μm and 100 μm in the IRAS

survey (IRAS19498+2717), which might account for its larger space reddening of $E_{B-V} = 0.79 \pm 0.02$ relative to a value of $E_{B-V} = 0.50$ for SV Vul, provided that the former possesses an equatorial dust torus (see Turner 1996a).

The variability of ALS 10588 was revealed during monitoring of SV Vul, although it also appears to have been detected in a VI survey for new Cepheids by Metzger and Schechter (1998). A period analysis of the photometry revealed a dominant signal at $P = 1.8521 \pm 0.0005$ days, although a solution for twice that value ($P \simeq 3.704$ days) matches our observations and those of ASAS (Pojmanski et al. 2005) (Figure 8). The spectral type and period are consistent with the class of slowly pulsating B stars (SPBs), characterized by stars of spectral types B3-B8 oscillating with periods on the order of days (Waelkens and Rufener 1985). The observed V amplitude ($\simeq 0.25$ mag.), however, is unusually large for a SPB variable (De Cat et al. 2000). Similarly, if twice the period is adopted, the inferred ellipsoidal system has a light amplitude more than twice that observed in other B stars of the same class (Beech 1989). There is also an absence of spectroscopic contamination from the expected companion (Figure 6). A toroidal dust clump orbiting synchronously with the star would account for the IR excess as well as the star's excess reddening (Turner 1996a), and, if tied to the star's rotation, would imply a stellar rotational velocity of $\simeq 250$ km s^{-1}, consistent with the slightly diffuse nature of the star's spectrum. Yet there is no significant deviation from a repeatable light curve morphology over several seasons of observation. The star's status may ultimately need to be resolved by time-series spectroscopy to examine whether the resulting radial velocities are consistent with the trend noted for SPBs (De Cat and Aerts 2002), or the canonical features of binarity or extrinsic variability.

3.3.7 HDE 229059 (α Cyg variable, B2 Iabe)

HDE 229059 is a B2 Iabe supergiant that displays emission in the lower hydrogen Balmer lines (Figure 6) and has an infrared (IR) excess (Clarke et al. 2005). Such characteristics indicate active

mass loss and the presence of circumstellar dust. The General Catalogue of Variable Stars (Samus et al. 2004) designates stars with comparable spectral types and V amplitudes ($\simeq 0.1$ mag, Figure 7) to those of HDE 229059 as αCyg variables, with irregular light variations tied to overlapping modes of non-radial pulsation. Burki et al. (1978) suggest that all luminosity class Ia B-G supergiants probably vary in brightness (see also Bresolin et al. 2004, and references therein).

HDE 229059 lies in Berkeley 87, an open cluster that has received considerable attention because it is a strong source of γ and cosmic rays (Giovannelli 2002; Aharonian et al. 2006), which has motivated an area of research on how stellar winds interact with the interstellar medium, enabling young open clusters to become pseudo particle accelerators. Berkeley 87 also hosts an abundance of astronomical phenomona (compact H II regions, molecular clouds, masers, and radio sources) and exotic stellar constituents that includes V439 Cyg, Stephenson 3, and BC Cyg. V439 Cyg is an emission-line star that has exhibited dramatic spectroscopic changes over a short time-scale (Polcaro et al. 1990; Polcaro and Norci 1997; Norci et al. 1998; Polcaro and Norci 1998), Stephenson 3 is a rare type of Wolf-Rayet star (WO3) (Norci et al. 1998; Polcaro et al. 1997), and BC Cyg is an M3 Ia supergiant and type C semiregular variable (Turner et al. 2006b) that will eventually terminate in a Type II supernova explosion. The cluster therefore offers intriguing insights into the effects of initial mass and mass loss on the end states of evolution for O-type stars, and may allow us to place new constraints on the initial progenitor masses for WO stars and red supergiants. The situation of HDE 229059 in such an evolutionary scheme is not entirely clear, which is why further study is essential. As a start. we investigate the possibility of cluster membership for the stars using spectroscopic parallax, 2MASS photometry, and proper motion data.

The distance to HDE 229059 can be established by spectroscopic parallax using the photometry of Turner and Forbes (1982) and intrinsic parameters determined from a sample of blue supergiants: $M_V = -6.4 \pm 0.8$ and $(B - V)_0 = -0.19 \pm 0.03$ (Kudritzki et al. 1999; Blaha and Humphreys 1989; Garmany and Stencel 1992), values that compare favorably with unpublished results (Turner) of

$M_V = -6.3$ and $(B - V)_0 = -0.18$ for B2 Iab stars. The distance for $R_V = 3.0$ is $d = 970$ pc. For BC Cyg, with mean V and B-V from Turner et al. (2006b) and intrinsic parameters derived for the comparable M-type supergiant Alpha Orionis, the resulting distance is $d \simeq 1200$ pc.

2MASS photometry (Cutri et al. 2003) for the cluster field yields color-color and color-magnitude diagrams for Berkeley 87 presented in Figure 9. The reddening solution, $E_{J-H} = 0.42 \pm 0.04$ ($E_{B-V} \simeq 1.36$), is well-defined because of the presence of numerous young B-type stars in the cluster. Isochrones for the 2MASS system (Padova Database of Stellar Evolutionary Tracks and Isochrones, Bonatto et al. 2004) fit the data at a distance of $d = 1280 \pm 150$ pc. The reddening matches previous results, but the distance is larger than that found by Turner and Forbes (1982), although consistent with a later estimate of 1230 ± 40 pc (Turner et al. 2006b). Constraining the cluster's age from 2MASS data is complicated by the fact that BC Cyg lies near the saturation limit of the survey. The isochrone fit in Figure 9 is provided mainly to highlight the envisioned evolution, although high mass loss rates are indicated and the plotted isochrone is more closely linked with conservative mass evolution.

Proper motion data (Zacharias et al. 2004) exist for several bright stars whose membership in Berkeley 87 is supported by their locations in Figure 9, and can be compared with the similar values found for HDE 229059, BC Cyg, and Stephenson 3 (Table 3). The proper motions for such distant stars are small and may be dominated by measuring uncertainties. Consequently, we can only argue that a physical association between the above stars and the cluster cannot be excluded on the available evidence. Membership of the exotic variable stars of Berkeley 87 would be strengthened by radial velocity measures.

3.3.8 NSV VARIABLES

A number of stars from the New Catalogue of Suspected Variable Stars (NSV, Samus et al. 2004) were surveyed in a search for potential small-amplitude Cepheids. Reference stars of well-established

magnitude in each field were not available, so the observations were made differentially relative to other stars in the field, with unknown zero-point. The co-ordinates provided by the original sources are estimated to be uncertain by several arcminutes or more, which led us to make photometric sweeps of the immediate field to find objects that might correspond to the suspected variables. There are stars that are reasonably coincident with the co-ordinates for the NSV variables listed in Table 4, but none appear to be light variable. Listed in Table 4 are the co-ordinates from the NSV for the suspected variables, magnitudes from Samus et al. (2004), the standard deviation of the magnitude estimates for the stars selected in the present survey, and the number of observations made. None of the stars identified here in the fields of the suspected Cepheid variables displayed the canonical light variations expected, although other types of variability cannot be dismissed because of our limited observational sampling.

3.4 DISCUSSION

It is of interest to note how a program of regular observation of Cepheid variables has generated serendipitous discoveries of new variable stars because of the need to establish photometric standard stars and check stars in the fields of the CCD images. In many cases the variable stars prove to be interesting, possibly unique, objects in their own right. But additional photometric and spectroscopic observations may be essential for clarifying their overall properties.

ACKNOWLEDGEMENTS

Table 3.1. Monitored variable stars.

Star	RA & DEC (2000)	Type	P (days)	Sp. Type
BD+66° 1673	00:01:46.86 +67:30:25.1	EB	5.33146	O5 V((f))n
2MASS 00104558+6127556	00:10:45.58 +61:27:55.6	EB	2.7172	A9 V
2MASS 19064659+4401458	19:06:46.82 +44:01:46.5	XI?	7.0:	G2 V
BD+22° 3792	19:43:53.00 +23:11:36.0	SRB	79.4:	M6 III
2MASS 19475544+2722562	19:47:55.52 +27:22:57.8	SRB	27.3:	M4 III
ALS 10588	19:51:52.87 +27:25:00.1	SPB?	1.8521	B3 IVn
	⋯	ELL?	3.704	⋯
HDE 229059	20:21:15.45 +37:24:35.2	αCyg	⋯	B2 Iabe

Table 3.2. Proper motion data for Berkeley 87 stars.

Star	Identity	pmRA (mas/yr)	pmDE (mas/yr)
3	HDE 229059	-4.5 ± 0.6	-5.3 ± 0.7
4	⋯	-5.2 ± 0.7	-5.5 ± 1.0
13	⋯	-5.6 ± 0.7	-7.5 ± 0.7
15	V439 Cyg	$+1.1 \pm 5.4$	$+11.2 \pm 5.4$
25	⋯	-3.9 ± 0.7	-5.7 ± 1.1
26	⋯	-5.7 ± 1.3	-4.1 ± 2.4
29	Stephenson 3	-8.0 ± 5.4	-2.8 ± 5.4
32	⋯	-5.1 ± 2.0	-3.1 ± 0.7
78	BC Cyg	-4.5 ± 1.1	-7.7 ± 1.1

[a]Numbering from Turner and Forbes (1982)

Table 3.3. Photometry and spectroscopy of Berkeley 59 members.

Star	Coordinates (J2000)	V	B-V	Sp. Type
BD+66° 1673	00:01:46.91 +67:30:24.3	10.07±0.04	1.31±0.03	O5 V((f))n
BD+66° 1675	00:02:10.32 +67:24:32.5	9.08 ± 0.03	1.08 ± 0.02	O7V
BD+66° 1674	00:02:10.68 +67:25:44.5	9.60 ± 0.04	1.07 ± 0.02	B0IIIn
MacC 15	00:02:13.42 +67:25:05.5	11.30 ± 0.03	1.08 ± 0.02	B0.5 Vn
2MASS 00020012+6725109	00:02:00.17 +67:25:11.2	12.81 ± 0.03	1.20 ± 0.01	B3V
2MASS 00020762+6725418	00:02:07.67 +67:25:42.1	13.87 ± 0.03	1.19 ± 0.02	B8 III

Table 3.4.   Cepheid Candidates from the NSV Catalogue.

Star	RA & DEC (2000)	Mag.	s.d.	n
NSV 00924	02:48:19.91 +58:41:44.8	12.50	±0.003	3
NSV 11753	19:06:54.19 +44:02:55.5	13.50	±0.007	16
NSV 11931	19:21:11.73 +00:07:02.6	14.20	±0.014	7
NSV 14094	22:16:16.71 +49:13:13.8	12.10	±0.008	8
NSV 14237	22:35:04.02 +63:47:37.6	12.30	±0.006	8

[a]magnitudes from Samus et al. (2004).

Figure 3.1 The field of view of Berkeley 59, a pseudo color image constructed from POSS II data (Noel Carboni and Daniel Majaess).
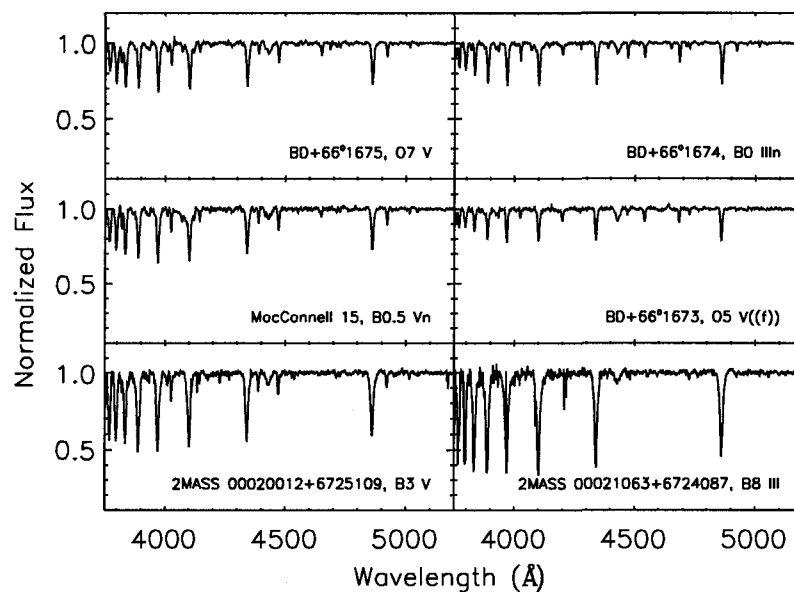
Figure 3.2 A mosaic of continuum-normalized CCD spectra for likely members of Berkeley 59 and Cep OB4.
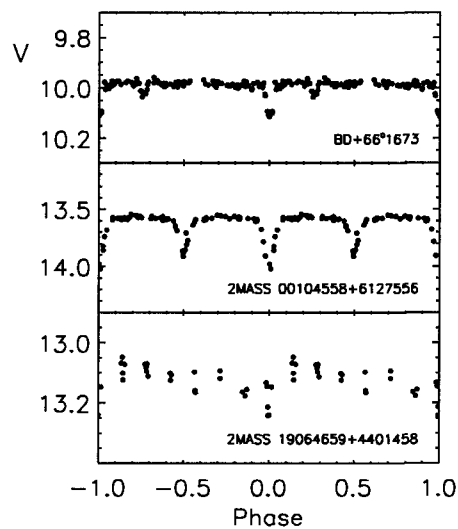
Figure 3.3 Light curves for the three eclipsing systems BD+66°1673, 2MASS 00104558+6127556, and 2MASS 19064659+4401458.
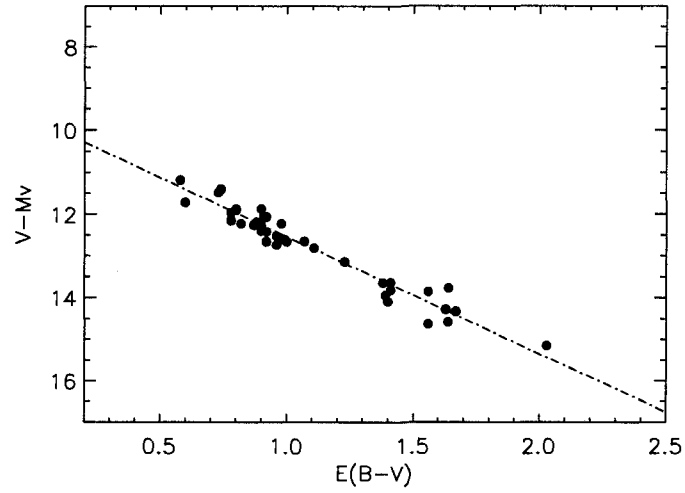
Figure 3.4 A variable-extinction diagram for likely main-sequence and zero-age main-sequence (ZAMS) members of Berkeley 59 and the Cep OB4 association. Least squares and non-parametric fits yield a ratio of the total to selective extinction of $R_V = 2.81 \pm 0.09$.
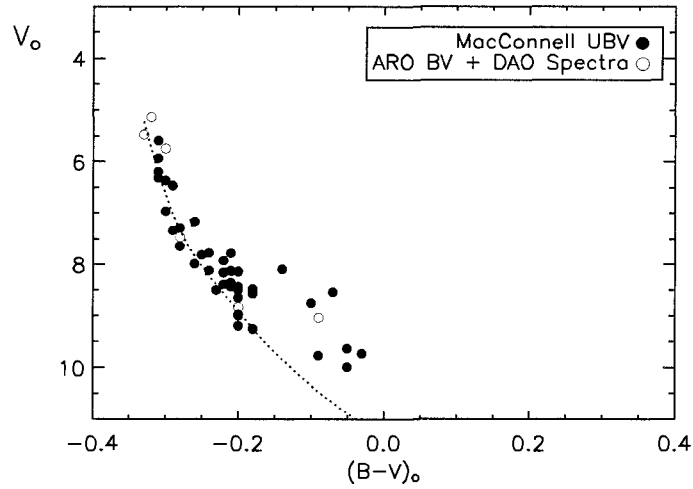
Figure 3.5 A reddening-free BV color-magnitude diagram for Berkeley 59 (open circles) and Cep OB4 (filled circles). A ZAMS fit to the observations yields a distance of $d = 883 \pm 43$ pc and a reddening of $E_{B-V} = 1.38 \pm 0.02$ in the core of the cluster.
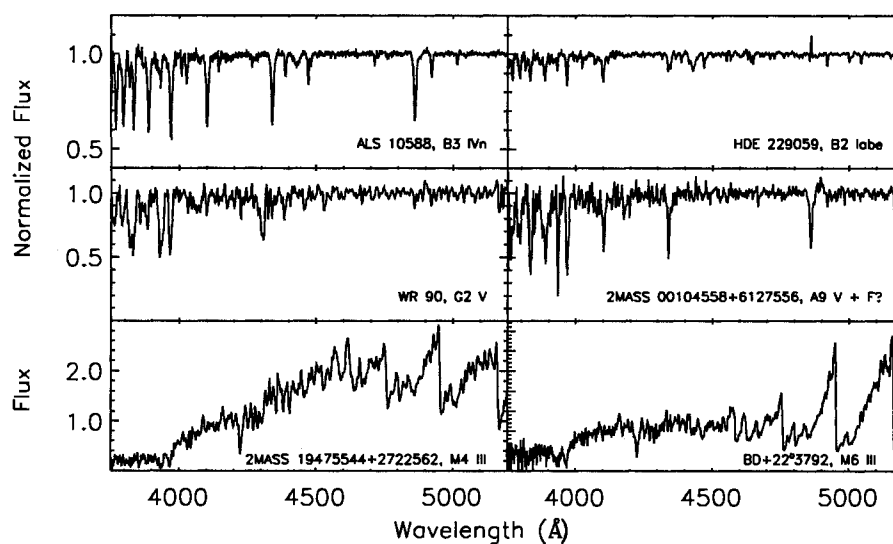
Figure 3.6 A mosaic of CCD spectra from the DAO 1.8-m Plaskett telescope for variables examined in this study.
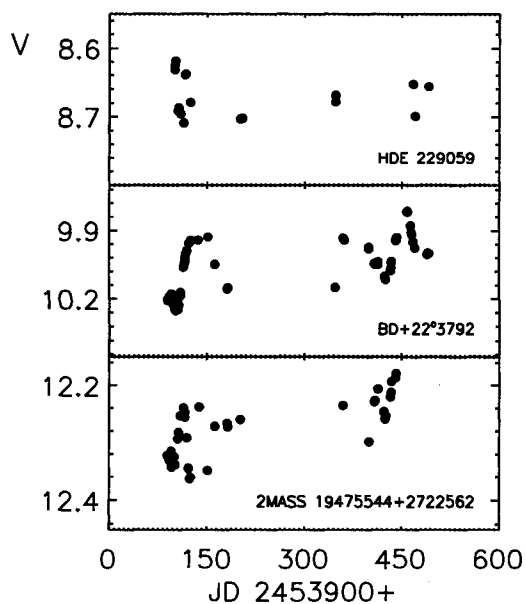
Figure 3.7 Light curves for variables examined in this study, constructed from differential photometry from the ARO. Zero-point offsets are expected (see text), although the standard deviation of observations for check stars in the same fields ranges from ±0.006 to ±0.008 mag.
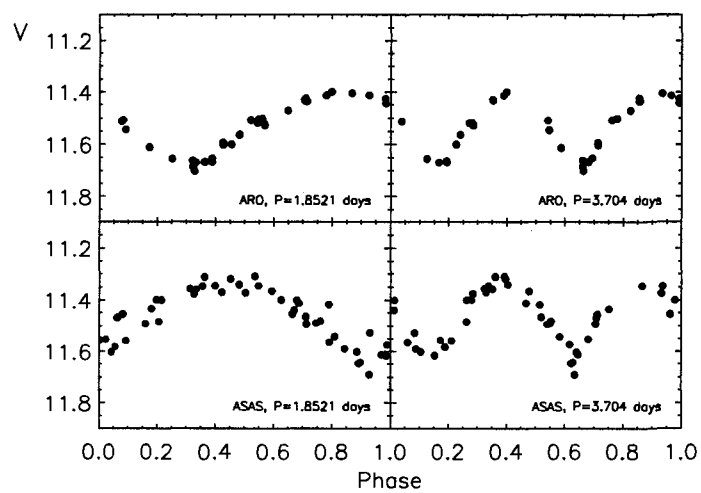
Figure 3.8 Light curves for ALS 10588 from ARO and ASAS data phased with possible periods of 1.8521 and 3.704 days.
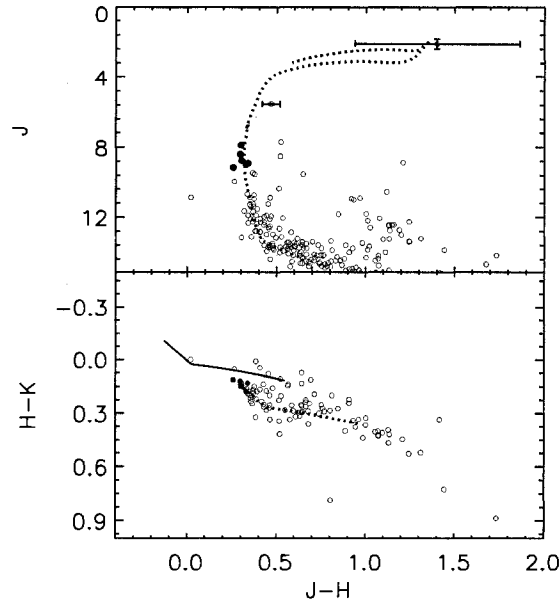
Figure 3.9 A color-color diagram (lower) and color-magnitude diagram (upper) for Berkeley 87 constructed from 2MASS data. The intrinsic color-color relation for the 2MASS system (Turner unpublished) is depicted as a solid line, as well as reddened by $E_{J-H} = 0.42 \pm 0.04$ ($E_{B-V} \simeq 1.36$) as a dotted line (lower). Filled circles correspond to stars likely to be cluster members. An isochrone fit (upper) is provided to highlight the assumed evolution (see text). The variable stars HDE 229059 ($J = 5.551$) and BC Cyg ($J = 2.117$) are provided with photometric error bars (BC Cyg is near saturation).

REFERENCES

Aharonian, F., et al. 2006, A&A, 454, 775

Beech, M. 1989, Ap&SS, 152, 329

Bica, E., & Bonatto, C. 2005, A&A, 443, 465

Blaha, C., & Humphreys, R. M. 1989, AJ, 98, 1598

Blanco, V. M., & Williams, A. D. 1959, ApJ, 130, 482

Bonatto, C., Bica, E., & Girardi, L. 2004, A&A, 415, 571

Bresolin, F., Pietrzyński, G., Gieren, W., Kudritzki, R.-P., Przybilla, N., & Fouqué, P. 2004, ApJ, 600, 182

Burki, G., Maeder, A., & Rufener, F. 1978, A&A, 65, 363

Carpenter, J. M. 2001, AJ, 121, 2851

Chen, W. P., Sanchawala, K., & Chiu, M. C. 2006, AJ, 131, 990

Clarke, A. J., Oudmaijer, R. D., & Lumsden, S. L. 2005, MNRAS, 363, 1111

Crampton, D., & Fisher, W. A. 1974, Publications of the Dominion Astrophysical Observatory Victoria, 14, 283

Cutri, R. M., et al. 2003, The IRSA 2MASS All-Sky Point Source Catalog, NASA/IPAC Infrared Science Archive.

De Cat, P., & Aerts, C. 2002, A&A, 393, 965

De Cat, P., Aerts, C., De Ridder, J., Kolenberg, K., Meeus, G., & Decin, L. 2000, A&A, 355, 1015

Dutra, C. M., Santiago, B. X., & Bica, E. 2002, A&A, 381, 219

Foster, G. 1995, AJ, 109, 1889

Gahm, G. F., Carlqvist, P., Johansson, L. E. B., & Nikolić, S. 2006, A&A, 454, 201

Garmany, C. D., & Stencel, R. E. 1992, A&AS, 94, 211

Giovannelli, F. 2002, Memorie della Societa Astronomica Italiana, 73, 920

Guetter, H. H. 1992, AJ, 103, 197

Guetter, H. H., & Turner, D. G. 1997, AJ, 113, 2116

Harris, A. W., et al. 1989, Icarus, 77, 171

Henden, A. A., & Kaitchuck, R. H. 1990, Richmond, Va. : Willmann-Bell, c1990.,

Hoag, A. A., Johnson, H. L., Iriarte, B., Mitchell, R. I., Hallam, K. L., & Sharpless, S. 1961, Publications of the U.S. Naval Observatory Second Series, 17, 343

Høg, E., et al. 2000, A & A, 355, L27

Huensch, M., Schmitt, J. H. M. M., Schroeder, K.-P., & Reimers, D. 1996, A&A, 310, 801

Koornneef, J. 1983, A & A, 128, 84

Kudritzki, R. P., Puls, J., Lennon, D. J., Venn, K. A., Reetz, J., Najarro, F., McCarthy, J. K., & Herrero, A. 1999, A&A, 350, 970

Lee, T. A. 1970, ApJ, 162, 217

Liu, T., Janes, K. A., & Bania, T. M. 1989, AJ, 98, 626

Liu, T., Janes, K. A., & Bania, T. M. 1991, AJ, 102, 1103

MacConnell, D. J. 1968, ApJS, 16, 275

Massey, P., Johnson, K. E., & Degioia-Eastwood, K. 1995, ApJ, 454, 151

Metzger, M. R., & Schechter, P. L. 1998, AJ, 116, 469

Mikami, T. 1986, Ap&SS, 119, 65

Norci, L., Meurs, E. J. A., Polcaro, V. F., Viotti, R., & Rossi, C. 1997, Ap&SS, 255, 197

Perryman, M. A. C., & ESA 1997, ESA Special Publication, 1200,

Pojmanski, G., Pilecki, B., & Szczygiel, D. 2005, Acta Astronomica, 55, 275

Polcaro, V. F., Rossi, C., Norci, L., & Giovannelli, F. 1990, Ap&SS, 169, 31

Polcaro, V. F., & Norci, L. 1997, Ap&SS, 251, 343

Polcaro, V. F., & Norci, L. 1998, A&A, 339, 75

Polcaro, V. F., Viotti, R., Rossi, C., & Norci, L. 1997, A&A, 325, 178

Reed, B. C. 1998, ApJS, 115, 271

Samus, N. N., & Durlevich, O. V. 2004, VizieR Online Data Catalog, 2250

Schild, R., & Romanishin, W. 1976, ApJ, 204, 493

Schwarzenberg-Czerny, A. 1996, ApJ, 460, L107

Shi, H. M., & Hu, J. Y. 1999, A&AS, 136, 313

Stock, J., Nassau, J. J., & Stephenson, C. B. 1960, Hamburger Sternw. Warner & Swasey Obs., 0

Turner, D. G. 1976, AJ, 81, 97

Turner, D. G. 1976, AJ, 81, 1125

Turner, D. G. 1979, PASP, 91, 642

Turner, D. G. 1980, ApJ, 235, 146

Turner, D. G., & Forbes, D. 1982, PASP, 94, 789

Turner, D. G. 1984, JRASC, 78, 229

Turner, D. G. 1986, A&A, 167, 157

Turner, D. G. 1989, AJ, 98, 2300

Turner, D. G. 1996, The Origins, Evolution, and Destinies of Binary Stars in Clusters, 90, 443

Turner, D. G. 1996, The Origins, Evolution, and Destinies of Binary Stars in Clusters, 90, 382

Turner, D. G. 1998, Journal of the American Association of Variable Star Observers (JAAVSO), 26, 101

Turner, D. G., Horsford, A. J., & MacMillan, J. D. 1999, Journal of the American Association of Variable Star Observers (JAAVSO), 27, 5

Turner, D. G., & Burke, J. F. 2002, AJ, 124, 2931

Turner, D. G., Rohanizadegan, M., Berdnikov, L. N., & Pastukhova, E. N. 2006, PASP, 118, 1533

Vanmunster, T. Peranso Light Curve and Period Analysis Software, http://www.peranso.com

Voges, W., et al. 2000, IAU Circular, 7432, 1

Waelkens, C., & Rufener, F. 1985, A&A, 152, 6

Walker, G. A. H. 1965, ApJ, 141, 660

Weber, R. 1959, Journal des Observateurs, 42, 106

Yang, J., & Fukui, Y. 1992, ApJ, 386, 618

Zacharias, N., Monet, D. G., Levine, S. E., Urban, S. E., Gaume, R., & Wycoff, G. L. 2004, Bulletin of the American Astronomical Society, 36, 1418

ABSTRACT

Assessing potential cluster Cepheids from a new distance and reddening parameterization and 2MASS photometry

by Daniel J. Majaess, David G. Turner, and David J. Lane.

Abstract: A framework is outlined to assess Cepheids as potential cluster members from readily available photometric observations. A relationship is derived to estimate colour excess and distance for individual Cepheids through a calibration involving recently published HST parallaxes and a cleaned sample of established cluster Cepheids. Photometric $V-J$ colour is found to be a viable parameter for approximating a Cepheid's reddening. The non-universal nature of the slope of the Cepheid PL relation for BV photometry is confirmed. By comparison, the slopes of the VJ and VI relations seem relatively unaffected by metallicity. A new Galactic Cepheid confirmed here, GSC 03729-01127 (F6-G1 Ib), is sufficiently coincident with the coronal regions of Tombaugh 5 to warrant follow-up radial velocity measures to assess membership. CCD photometry and O–C diagrams are presented for GSC 03729-01127 and the suspected cluster Cepheids AB Cam and BD Cas. Fourier analysis of the photometry for BD Cas and recent estimates of its metallicity constrain it to be a Population I overtone pulsator rather than a Type II s-Cepheid. AB Cam and BD Cas are not physically associated with the spatially-adjacent open clusters Tombaugh 5 and King 13, respectively, the latter being much older ($\log \tau \simeq 9$) than believed previously. Rates of period change are determined for the three Cepheids from archival and published data. GSC 03729-01127 and AB Cam exhibit period increases, implying fifth and third crossings of the instability strip, respectively, while BD Cas exhibits a period decrease, indicating a second crossing, with possible superposed trends unrelated to binarity. More importantly, the observed rates of period change confirm theoretical predictions. The challenges and prospects for future work in this area of research are discussed.

CHAPTER 4

CLUSTER CEPHEIDS & CEPHEID PARAMETERIZATIONS

4.1 INTRODUCTION

The *All Sky Automated Survey* (ASAS, Pojmanski, 2000), the *Northern Sky Variability Survey* (NSVS, Woźniak et al., 2004), and *The Amateur Sky Survey* (TASS, Droege et al., 2006) have detected many new Cepheid variables through their photometric signatures, resulting in a valuable expansion of the Galactic Cepheid sample (Samus et al., 2004) once confirmed by spectroscopic observation. In the case of GSC 03729-01127 (TASSIV 6349369), a suspected Cepheid studied here, the variable may be an open cluster member and a potentially valuable calibrator for the Cepheid period-luminosity (PL) relation. Cepheids continue to provide the foundation for the universal distance scale, and such variables could serve as an efficient means of quantifying the extinction to Galactic and extragalactic targets.

The results of the seminal Hubble Space Telescope (HST) Key Project yielded a Hubble constant of $H_0 = 72 \pm 8$ km s^{-1} Mpc^{-1} (Freedman et al., 2001), a value supported by cosmological constraints inferred from WMAP observations (Spergel et al., 2007). The HST results are tied to Large Magellanic Cloud (LMC) Cepheids, which advantageously provide a large sample of common distance. Distance estimates for the LMC exhibit an unsatisfactorily large scatter (Freedman et al., 2001; Benedict et al., 2002), however, resulting in an uncertain zero-point. Moreover there exists a difference in metallicity between LMC Cepheid variables relative to both Galactic Cepheids and those in galaxies used for calibrating secondary distance candles, the effects of which remain actively debated. Tammann et al. (2003), for example, suggest that the LMC Cepheid PL relation

appears to characterize short-period Cepheids as too bright relative to their Galactic counterparts, and long-period Cepheids as too faint. Conversely, van Leeuwen et al. (2007) and Benedict et al. (2007) suggest, on the basis of revised Hipparcos and newly-derived HST parallaxes, that the slopes of the PL relations (V, I) for Cepheids in the Galaxy and the LMC are consistent to within their cited uncertainties. Indeed, the results presented in section 4.3.2, complementing in part those of Fouqué et al. (2007), appear to confirm ideas put forth in each of the above studies, namely that the slope of the PL relation is not universal in certain passbands, and for VJ and VI constructed relations, any putative difference in slope arising from metallicity effects appears negligible in comparison with other concerns and uncertainties related to extragalactic observations. Nevertheless, a consensus has yet to emerge and a resolution to the above debate may be assisted by renewed efforts towards establishing Galactic Cepheids as cluster members, a connection that provides direct constraints on Cepheid luminosities, intrinsic colours, masses, metallicities, and pulsation modes.

Turner & Burke (2002) compiled an extensive list of suspected cluster Cepheids based upon preliminary analyses, but only a few cluster/Cepheid pairs have been studied with the necessary detail to determine the parameters of the associated clusters accurately, or to obtain the necessary radial velocity measures needed to establish membership in cases where reliable proper motions are unavailable. Efforts to discover new Galactic open clusters (Alessi et al., 2003; Moitinho et al., 2003; Kronberger et al., 2006) and Cepheid variables (Pojmanski, 2000; Woźniak et al., 2004; Droege et al., 2006) have resulted in a welcome increase to the number of suspected cluster Cepheids. This paper outlines a framework to assess the viability of such cases efficiently, with an intent to highlight cases requiring further attention and focus. Section 4.3 develops a relationship to estimate colour excesses and distances for individual Cepheids from several photometric parameters. Section 4.4 presents CCD photometry, spectroscopic results, and O–C analyses for the suspected cluster Cepheids BD Cas (Tsarevsky et al., 1966; Turner & Burke, 2002), AB Cam (van den Bergh, 1957; Tsarevsky et al., 1966), and a new Galactic Cepheid confirmed here, GSC 03729-01127. Distances, colour excesses,

and ages are also derived for the associated open clusters Tombaugh 5 and King 13 from 2MASS photometry (Cutri et al., 2003).

4.2   DATA ACQUISITION AND REDUCTIONS

Light curves for the Cepheids presented here were constructed from CCD photometry obtained with the 0.3-m Schmidt-Cassegrain telescope of the Abbey-Ridge Observatory (ARO), an automated facility located outside of Halifax, Nova Scotia. A description of the facility, its equipment and the data reduction procedures used for the observations are given elsewhere (Majaess et al., 2008). Low dispersion spectra at 120 Å mm^{-1} were obtained for the Cepheids with the Dominion Astrophysical Observatory's 1.8-m Plaskett telescope in October 2006 using the SITe-2 CCD detector. The spectra were reduced and analyzed using the NOAO's routines in IRAF, along with software packages by Christian Buil (IRIS), Valerie Desnoux (VSPEC) and Robert H. Nelson (RAVEREC).

Rates of period change for the Cepheids studied here were determined through O–C analyses using light curves constructed primarily from data derived from visual scanning of images in the Harvard College Observatory Photographic Plate Collection. Software tailored for the analysis of Cepheid light curves (see Turner & Berdnikov, 2004) was used to determine offsets in phase and magnitude space that minimize the χ^2 statistic when matching input light curves to a standard template.

4.3   CEPHEID-DISTANCE RELATION

The distance to a Cepheid can be established through adoption of intrinsic parameters from published PL ($\langle M_V \rangle$ versus $\log P$) and period-colour [$(B-V)_0$ versus $\log P$] relations, although such estimates typically idealize the result to an object located near the centre of the instability strip. Neglect of the intrinsic scatter inherent to such relationships can affect estimates of colour excess and distance

to individual Cepheids made from them, since the variable may lie anywhere within the strip (e.g., towards the red or blue edge). Large calibrating data sets are therefore required when constructing strict two-parameter Cepheid relations to ensure a reasonably even sampling of both sides of the strip and to avoid a least-squares solution biased towards predominantly red or blue edge objects, an important consideration that is often overlooked.

A distance relation applicable to Cepheid variables is formulated here, motivated by the work of Opolski (1983, 1988). Consider the canonical distance modulus equation:

$$5 \log d = V - A_V - M_V + 5 \,, \tag{4.1}$$

where $A_V = R_V \times E_{B-V}$ and $E_{B-V} = (B-V) - (B-V)_0$. The standard period-luminosity-colour (PLC) relation for Cepheids can be expressed as:

$$M_V = a \log P + b(B-V)_0 + c \,.$$

Equation (4.1) can therefore be rewritten as:

$$5 \log d = V - a \log P - b(B-V) + (b - R_V)E_{B-V} - c + 5 \,,$$

or:

$$5 \log d = V + \alpha \log P + \beta(B-V) + \delta E_{B-V} + \gamma \,. \tag{4.2}$$

A calibrating set (Table 1) consisting of established cluster Cepheids and Cepheids with parallaxes measured recently with the HST (Benedict et al., 2007) was used to determine the co-efficients in

equation (4.2) that minimize the χ^2 statistic, yielding an optimum solution given by:

$$5 \log d = V + 3.77 \log P - 2.40(B - V) - E_{B-V} + 7.03 \ .$$

The resulting relationship reproduces the distances to the calibrating set with a formal average uncertainty of $\pm 3\%$ (Fig. 4.1). The true scatter applying to use of the relationship for individual Cepheids may be larger, given that the calibrating set consists primarily of large-amplitude Cepheids lying near the centre of the instability strip.

The colour excess term can also be characterized in terms of observable parameters as:

$$E_{B-V} = \eta \log P + \lambda(V - J) + \phi \ , \tag{4.3}$$

where $(V-J)$ colour appears to be a viable surrogate for determining colour excess, although H- or K-band photometry could be substituted for J. A test of the colour excess relation using $(V-H)$ and $(V-K)$ produced slightly larger χ^2 statistics than when $(V-J)$ was used as the colour index, so the latter was adopted in the present study.

Suitable infrared and optical photometry for the calibrating Cepheids (Table 4.1) was obtained from Laney & Stobie (1992), Groenewegen (1999) and sources identified by Fouqué et al. (2007) (see discussion in their section 2.1), with J-band measures being standardized on the 2MASS system. The co-efficients of equation (4.3) that minimize the χ^2 statistic are:

$$E_{B-V} = -(0.270) \log P + (0.415)(V - J) - 0.255 \ . \tag{4.4}$$

The co-efficients of the same equation that minimize the χ^2 statistic for $(V-H)$ and $(V-K)$ are:

$$E_{B-V} = -(0.33) \log P + (0.37)(V - H) - 0.27 \ ,$$

and

$$E_{B-V} = -(0.30) \log P + (0.34)(V - K) - 0.27 \ .$$

Equation (4.4) reproduces the reddenings for the calibrating Cepheids with an average uncertainty of ± 0.03 mag. (Fig. 4.1), although the true scatter applying to use of the relationship for individual Cepheids will be larger. The relation makes use of V and J-band photometry (2MASS) that are widely available, and should provide a first order estimate in the absence of reddenings determined by means of BVI_c photometry (Laney & Caldwell, 2007; Laney & Stobie, 1994), spectroscopic analyses (Kovtyukh et al., 2008), or space reddenings (Laney & Caldwell, 2007; Turner et al., 2008). Alternatively, a reddening-free distance relation analagous to the Wesenheit function (Madore, 1982; van den Bergh, 1968) can be constructed by setting $\delta = 0$ [equation (4.3)], which results in a negligible increase in the χ^2 statistic relative to the optimum solution in equation (4.3). A reanalysis of the co-efficients then yields:

$$5 \log d = V + (4.42) \log P - (3.43)(B - V) + 7.15 \ .$$

$$5 \log d = V + (3.43) \log P - (2.58)(V - I) + 7.50 \ .$$

$$5 \log d = V + (3.30) \log P - (1.48)(V - J) + 7.63 \ .$$

Published results raise questions about the pulsation modes of the s-Cepheids EV Sct and QZ Nor (Coulson & Caldwell, 1985; Moffett & Barnes, 1986; Bono et al., 2001). With the relationship derived here, the memberships of EV Sct in the cluster NGC 6664 (Mermilliod et al., 1987) and QZ Nor in the cluster NGC 6087 (Coulson & Caldwell, 1985; Mermilliod et al., 1987), as established by radial velocity measures, imply that EV Sct and QZ Nor are overtone pulsators. Otherwise, equation (4.3) with the assumption of fundamental mode pulsation results in anomalous luminosities for the

Cepheids, namely values that differ from those resulting from implied cluster membership by several times the mean uncertainties. Such conclusions are sensitive, however, to the distances adopted for both clusters in Table 4.1.

4.3.1 DETERMINING $\langle J \rangle$

Reliable estimates for a Cepheid's colour excess from equation (4.4) require the availability of precise mean J-band magnitudes. Infrared light curves are readily available for the calibrating set (Table 4.1), but in most instances only single epoch 2MASS photometry exists. The derivation of mean magnitudes from single epoch observations is complicated by several issues. First, Cepheids undergo rapid period changes (Szabados, 1977, 1980, 1981; Berdnikov, 1994; Berdnikov et al., 1997; Glushkova et al., 2006; Turner et al., 2006), so a significant time lapse between single epoch observations and those of the reference optical light curve can result in correspondingly large phase offsets. On the other hand, most Cepheids with periods between 5 and 10 days exhibit relatively slow period changes, as confirmed observationally in section 4.4. Second, the mean magnitude deduced from single epoch observations is less certain because the morphological structure of the light curve can change between the optical and infrared (e.g., SV Vul); the former traces the temperature, and the latter the radius. Deriving colour excesses for stars lacking multiple observations is undoubtedly less precise, especially for large amplitude Cepheids and those exhibiting a significant, yet usually unknown, period change.

The mean J-magnitude $\langle J \rangle$ can be approximated by:

$$\langle J \rangle \simeq J_{\mathrm{JD}} - \left(\frac{|\, V(\phi_J) - V_{\mathrm{max}}\,|}{V_{\mathrm{a}}} - 0.5 \right) \times J_{\mathrm{a}} \,,$$

where J_{JD} is the magnitude for the single epoch observation, $V(\phi_J)$ is the visual magnitude at the same phase as J_{JD}, V_{max} is the V-band magnitude of the star at maximum brightness, and V_{a} and

J_a are the light amplitudes of the Cepheid in the visual and J-band, respectively. For the V to J amplitude relation outlined by Welch et al. (1984) and Soszyński et al. (2005) of $J_a \simeq 0.37 \times V_a$, the equation becomes:

$$\langle J \rangle \simeq J_{JD} - \left(\frac{\mid V(\phi_J) - V_{\max} \mid}{V_a} - 0.5 \right) \times 0.37 V_a \,. \tag{4.5}$$

A derivation of the mean magnitude for the cluster Cepheids DL Cas, CV Mon, QZ Nor, V340 Nor, and EV Sct, which are not saturated in the 2MASS survey and have been observed at a fairly recent epoch by ASAS, thereby minimizing the effects of period changes, yields an average difference of ±0.03 mag. relative to mean J-band magnitudes found in the literature. That may be an optimistic estimate given that the light curves for Cepheids in the above sample are primarily sinusoidal and of small amplitude. In spite of the cited uncertainties for single epoch 2MASS observations ($\Delta J \simeq \pm 0.03$ mag.) and the above considerations, equation (4.5) proves to be a satisfactory approximation for determining $\langle J \rangle$.

4.3.2 EXTRAGALACTIC COMPARISONS

The distance to the LMC and SMC can be established by adopting the reddening-free relations highlighted earlier and utilizing V and I photometry from OGLE (Udalski et al., 1999), V and J photometry from a combined set of OGLE and 2MASS data compiled by the authors (see Fig. 4.2),[1] and B and V photometry from OGLE. The first two methods yield distance moduli to the LMC of 18.39 ± 0.09 and 18.49 ± 0.19. The distance moduli to the SMC derived from VI and VJ photometry are 18.93 ± 0.14 and 19.02 ± 0.22.

The diagrams constructed from reddening-free VI and VJ relations remain generally unbiased towards redder colours, but there is an obvious bias for the BV distances that may be attributed to line blanketing effects arising from metallicity differences among Milky Way, LMC and SMC Cepheids. The effect is more pronounced for the SMC, an expected trend given that SMC Cepheids

---

[1]The OGLE + 2MASS dataset for the LMC and SMC are available online at the Vizier database.

exhibit a lower metallicity than those of the LMC (e.g., Mottini, 2006). The results confirm that the slope of the PL relation is not universal when based on *BV* photometry, while by comparison, the slopes for the *VJ* and *VI* relations seem relatively unaffected by metallicity. The derived distances are consistent with values found in the literature (see Laney & Stobie, 1994; Benedict et al., 2002)), although distances cited in other studies are preferred since a putative zero-point metallicity correction was not addressed here. The *VJ* result establishes the viabilitiy of 2MASS photometry in such analyses in spite of the survey's single epoch observations. Indeed, the uncertainty in the *VJ* result could be reduced by approximating the mean $\langle J \rangle$-band magnitude according to the prescription described earlier or that described by Soszyński et al. (2005). Lastly, it is noted that biases towards redder colours may also result from standardization problems (see Figure 14 of Zaritsky et al., 2002).

The giant elliptical galaxy NGC 5128 hosts large numbers of Cepheids, and Ferrarese et al. (2007) derived a distance of 3.1 ± 0.1 Mpc to the galaxy using the Wesenheit PL calibration (see Table 6 and section 5.3 in their paper). The distance to NGC 5128 established with the reddening-free *VI* relation formulated in section 4.3 is 3.1 ± 0.5 Mpc. Star C43 in Table 5 of Ferrarese et al. (2007) is presumably not a Type I Cepheid. Similarly, Phelps et al. (1998) derived a distance of 12.03 ± 0.9 Mpc to NGC 2090 from Cepheids, while the reddening-free *VI* relation given here yields a comparable distance of 11.8 ± 1.3 Mpc. A broader analysis including a larger sample of galaxies is needed to draw any meaningful conclusions, but to first order the results are in agreement.

4.4 POTENTIAL CLUSTER CEPHEIDS

4.4.1 GSC 03729-01127

The Cepheid-like variations of GSC 03729-01127 were first noted by Mike Sallman while inspecting TASS observations, a discovery that led to its identification with an earlier entry in the NSVS (object 1973907, Woźniak et al., 2004). Preliminary analysis of the TASS data produced a period

of $P \simeq 5.074$ days, a value closely approximated by our observations, which yield $P = 5.065 \pm 0.008$ days. A period analysis of the photometry was carried out in the PERANSO software environment (Vanmunster, 2007) using the algorithms ANOVA (Schwarzenberg-Czerny, 1996), FALC (Harris et al., 1989), and CLEANEST (Foster, 1995). The phased light curve (Fig. 4.3) has an amplitude of $\Delta V \simeq 0.72$ mag. ($\Delta B \simeq 1.09$ mag. in the blue), and displays a typical Cepheid signature with a rapid rise from minimum to maximum.

Spectroscopy confirms that the variable is indeed a Cepheid, displaying spectral variations from F6 Ib to G1 Ib over its cycle. All-sky BV photometry for GSC 03729-01127 was obtained on several nights, with extinction co-efficients derived using techniques outlined by Henden & Kaitchuck (1998) and Warner (2006). The photometry was standardized to the Johnson system using stars in the nearby open cluster NGC 225 (Hoag et al., 1961). The mean magnitude and colour are $\langle V \rangle \simeq 10.90$ and $\langle B - V \rangle \simeq 1.67$, which, with the formulation of section 4.3, result in an estimated distance of $d = 1230 \pm 120$ pc and a colour excess of $E_{B-V} = 1.05 \pm 0.05$. The Cepheid is assumed to be pulsating in the fundamental mode, as inferred from the morphological structure of its light curve (see Beaulieu, 1995; Beaulieu & Sasselov, 1998; Welch et al., 1995).

The Cepheid lies $21'.9$ from the core of Tombaugh 5 (Tombaugh, 1941), an open cluster estimated to be ~ 1.8 kpc distant (Reddish, 1954). Maciejewski & Niedzielski (2007) provide a more recent estimate of $d = 1.33 \pm 0.33$ kpc, which is smaller than $d = 1.75 \pm 0.15$ kpc derived by Lata et al. (2004) from multi-band photometry. The data of both groups imply a reddening of $E_{B-V} \simeq 0.8$. An analysis of 2MASS photometry for the field, fitted with a solar isochrone (Fig. 4.4) from the Padova Database of Stellar isochrones (Bonatto et al., 2004), implies a cluster age of $\log \tau = 8.35 \pm 0.15$, a distance of $d = 1.66 \pm 0.20$ kpc, and a reddening of $E_{J-H} = 0.22 \pm 0.02$ ($E_{B-V} \simeq 0.81$ according to the relations established in section 4.5).

Star counts were made for Tombaugh 5 from 2MASS data, relative to a cluster centre at 03:47:56, +59:04:59 (J2000) found from strip counts on the Palomar survey E-plate of the field. The data

(Fig. 4.5) imply a nuclear radius for the cluster of $r_n \simeq 8$ arcminutes, and a coronal radius of $R_c \simeq 23$ arcminutes, in the notation of Kholopov (1969). GSC 03729-01127 lies close to the cluster's tidal limit, which raises questions about its possible association with Tombaugh 5. The progenitor mass of GSC 03729-01127 can be estimated from its pulsation period as $\sim 4M_\odot$ (see Turner, 1996), consistent with the implied turnoff mass for Tombaugh 5 and a possible physical association.

Although the star count evidence is only marginally consistent with membership of GSC 03729-01127 in Tombaugh 5, the similarity of the distance estimates and evolutionary ages for Cepheid and cluster are sufficient to warrant follow-up radial velocity measures, which are needed before reaching any conclusions regarding membership. A list of likely cluster members has been tabulated for such a purpose (Table 4.2), with membership inferred from a correlation between a star's position in the 2MASS colour-colour and colour-magnitude diagrams.

The Cepheid's evolutionary history was examined through O–C analysis (Fig. 4.6, Table 4.3), based primarily upon photographic light curves obtained from examination of archival images in the Harvard College Observatory Photographic Plate Collection, supplemented by CCD observations from NSVS, TASS, ASAS, the ARO, and data from a continuing program of Cepheid monitoring at the Burke-Gaffney Observatory of Saint Mary's University (Turner et al., 1998, 1999, 2005). An adopted ephemeris of:

$$JD_{max} = 2453297.1935 + 5.06535E \,,$$

where E is the number of elapsed cycles, was found to fit the observations reasonably well over the last century, and was used to phase the data. GSC 03729-01127 appears to be undergoing a gradual period increase of $+0.272 \pm 0.088$ s yr^{-1}, confirming theoretical predictions on rates of period change for $P \simeq 5^d$ Cepheids as outlined by Turner et al. (2006). The rate of period change indicates that the Cepheid is evolving towards the red edge of the instability strip in the third or fifth crossing

(Turner et al., 2006). There is some ambiguity, given the Cepheid's small pulsation amplitude, but that is resolved from the reddening derived here. GSC 03729-01127 appears to lie on the cool (red) edge of the instability strip, in which case its rate of period increase and small pulsation amplitude imply that it is in the fifth crossing of the strip.

4.4.2   BD CAS

BD Cas is a small-amplitude, sinusoidal, $3^{\mathrm{d}}.65$ Cepheid ($\Delta V \simeq 0.33$, Fig. 4.3) discovered by Beljawsky (1931). Increased sampling and precision photometry indicate that the variations are not purely sinusoidal (Fig. 4.3), although the star could still qualify as an s-Cepheid. There is some uncertainty regarding the variable's pulsation mode and population type (Kienzle et al., 1999, see references and discussion therein). Kienzle et al. (1999) examined the structure of the Cepheid's radial velocity curve in Fourier space using CORAVEL measures and data from Gorynya et al. (1996) and noted that the values of A_1 and R_{21} are consistent with overtone pulsation, whereas ϕ_{21} is not. They argued that the analysis was hampered by large uncertainties because of undersampling, with further observations needed to constrain the pulsation mode unambiguously.

A Fourier analysis of the new ARO photometry yields an amplitude ratio of $R_{21} = 0.113 \pm 0.010$ and $\phi_{21} = 3.50 \pm 0.09$, which imply overtone pulsation by the criteria of Beaulieu & Sasselov (1998) and Zabolotskikh et al. (2005). The Cepheid's near-solar metallicity of [Fe/H]$= -0.07$ (Andrievsky et al., 2002) and Galactic location ($\ell, b = 118, -1$) are consistent with other Population I variables, which suggests that BD Cas is a classical Cepheid pulsating in the first overtone. The Cepheid's spectral type exhibits only small variations, from F6 II to F7 Ib. It should also be noted that a viable framework for discriminating a Cepheid's population type by means of Fourier analysis has yet to emerge (Fernie & Ehlers, 1999).

BD Cas lies $19'.6$ from the open cluster King 13 (King, 1949) and $\sim 16'$ from the suspected cluster Czernik 1 (Czernik, 1966). Marx & Lehmann (1979) examined King 13 using photographic

UBV photometry, and derived a distance of $d = 1730 \pm 200$ pc and a reddening of $E_{B-V} = 0.38$.

Subramaniam & Bhatt (2007) obtained a larger reddening of $E_{B-V} = 0.82 \pm 0.02$, a larger distance

of $d = 3100 \pm 300$ pc, and a cluster age of $\log \tau = 8.5$ from CCD photometry, while Maciejewski &

Niedzielski (2007) obtained an age of $\log \tau = 8.4$, a distance of $d = 3670 \pm 1300$ pc, and a reddening

of $E_{B-V} = 0.86 \pm 0.12$ by similar means. An analysis of 2MASS photometry for the field, fitted

with an isochrone from the Padova Database of Stellar isochrones (Bonatto et al., 2004), results in a

distance of $d = 2550 \pm 500$ pc and a reddening of $E_{J-H} = 0.15 \pm 0.02$ ($E_{B-V} \simeq 0.56$ according to the

relations derived in section 4.5). The colour-colour and colour-magnitude diagrams are dominated

by AF dwarfs (Fig. 4.4) and the reddening solution is well established. Moreover, the structure of

the main-sequence turnoff and the clustering of red giant members (Fig. 4.4) indicates an age near

$\log \tau = 9.0 \pm 0.15$. The distance estimate should be viewed cautiously because it is tied to stars

lying near the limiting magnitude of the 2MASS survey. The age and reddening estimates are tied

more directly to the colours of main sequence stars, and are consequently more reliable.

Star counts were made for King 13 from 2MASS data, relative to a cluster centre at 00:10:16.47,

+61:11:29.2 (J2000) found from strip counts on the Palomar survey E-plate of the field. The data

(Fig. 4.5) imply a nuclear radius for the cluster of $r_n \simeq 6$ arcminutes, and a coronal radius of

$R_c \simeq 20$ arcminutes. BD Cas therefore lies very close to the cluster's tidal limit. With the Cepheid

relationship formulated in section 4.3 and pertinent photometric parameters for BD Cas (Szabados,

1977), the Cepheid has an estimated distance of $d = 1520 \pm 150$ pc and a reddening of $E_{B-V} =$

0.99 ± 0.05, which places it well foreground to the cluster, but curiously with a larger reddening.

The large reddening for BD Cas is confirmed by an independent spectroscopic reddening estimate

of $E_{B-V} = 1.01$ (Kovtyukh et al., 2008). A possible physical association between the cluster

and Cepheid is further negated by the cluster's age, which implies a main-sequence turnoff mass

near 2 $M_\odot$. There are no other known Population I cluster Cepheids associated with a such a

correspondingly old cluster (Turner, 1996).

Lyngä (1995) has questioned the existence of the open cluster Czernik 1, which was suggested as an alternate parent cluster for BD Cas by Tsarevsky et al. (1966). Our analysis of 2MASS photometry and limited BV photometry for the cluster is inconclusive in that regard, so a possible connection with Czernik 1 remains unproven.

The star's evolutionary history was examined through O–C analysis (Fig. 4.6) using light curves constructed from data obtained from archival plates in the Harvard collection, data compiled by Szabados (1977, 1983), and more recent photoelectric and CCD photometry (Table 4.4). An ephemeris given by:

$$JD_{max} = 2441932.0320 + 3.65090E \,,$$

was found suitable for phasing the data. BD Cas is undergoing a period decrease amounting to -0.698 ± 0.048 s yr^{-1} (Fig. 4.6), which, in conjunction with its derived reddening and inferred overtone status, implies a second crossing of the instability strip (Turner et al., 2006) and a star lying towards the hot (blue) edge. The rate of period change was derived from a polynomial fit (see Fig. 4.6), but there are deviations in the O–C data derived from recent photoelectric and CCD photometry that may indicate non-evolutionary effects. The trends are unlikely to arise from binarity, since that would imply an unrealistically large mass for the companion. Yet binarity is not precluded, and is common among Cepheids (Szabados, 1995, 2003). The trends observed here and in the O–C diagrams of other Cepheids have yet to be explained satisfactorily, and remain an active and interesting area of research. Whether the superposed variations are small, as in the Cepheid RT Aur (Turner et al., 2007), or arise from random fluctuations in pulsation period (e.g., SV Vul, Turner & Berdnikov, 2004), the mechanism is yet to be established.

4.4.3 AB Cam

AB Cam is a large-amplitude, $5^d.79$ Cepheid ($\Delta V \simeq 0.94$, Fig. 4.3) discovered by Morgenroth (1934). The distance to AB Cam can be estimated from Johnson system photometry (Berdnikov et al., 2000) with the Cepheid relationship formulated in section 4.3. The implied distance is $d = 4470 \pm 450$ pc with a reddening of $E_{B-V} = 0.59 \pm 0.05$. The object's light-curve morphology (Fig. 4.3) is consistent with fundamental mode pulsation (Beaulieu & Sasselov, 1998; Beaulieu, 1995; Welch et al., 1995), which was assumed for estimating the distance. van den Bergh (1957) and Tsarevsky et al. (1966) examined the field of AB Cam in search of a host cluster with null results. Despite the Cepheid's apparent angular proximity to Tombaugh 5, the two are not physically related (see Fig. 4.5).

The star's evolutionary history was examined through O–C analysis (Fig. 4.6) using photographic light curves constructed with magnitude estimates from archival plates in the Harvard collection, supplemented by more recent photoelectric and CCD photometry (Table 4.5). An ephemeris given by:

$$JD_{max} = 2437400.6380 + 5.78745E \,,$$

proved suitable for phasing the data. AB Cam appears to be undergoing a very gradual increase of $+0.069 \pm 0.025$ s yr^{-1}. The rate is again consistent with observed rates of period change for $P \simeq 6^d$ Cepheids (Turner et al., 2006), and indicates, in conjunction with its large pulsation amplitude, a Cepheid in the third crossing of the instability strip lying towards the cool (red) edge. The object may be of added importance given that it falls near the lower bound for an undersampled locus of short-period third crossers in the rate of period change diagram (Turner et al., 2006).

4.5 OPTICAL TO INFRARED RELATIONS

Distance estimates for the open clusters studied in the preceeding section were established using the following expression:

$$5 \log d = [J - M_J] - E_{J-H} \times R_j + 5 .$$

The infrared colour excess E_{J-H} and the distance modulus J–M_J can be derived by simultaneously fitting an intrinsic relation (Turner, unpublished) and isochrone (Bonatto et al., 2004) to the stars in a colour-colour and colour-magnitude diagram (see Fig. 4.4). A ratio of total to selective extinction of $R_J = 2.60$ was adopted (Bica & Bonatto, 2005; Dutra et al., 2002), and the following relationship between reddening in the infrared to that in the optical was used to permit direct comparison of cluster reddenings derived from 2MASS photometry with more frequently cited optical results found in the literature:

$$E_{J-H} = (0.27 \pm 0.03) \times E_{B-V} . \tag{4.6}$$

Equation (4.6) was established from the calibrating set of open clusters in Table 4.1, and compares satisfactorily with relationships cited by Laney & Stobie (1993), Bica & Bonatto (2005) and Dutra et al. (2002). The co-efficient derived here is smaller, however, and may be indicative of our visual fitting biases rather than a global relationship. We refer the reader to Laney & Stobie (1993) for a more rigorous discussion of the correlation.

4.6 DISCUSSION

The relationships highlighted in section 3 yield reliable parameters when investigating short period Cepheids ($P \leq 11^d$). Parameters determined for longer period Cepheids from such relations are less certain, primarily because of an absence of mid-to-long period calibrators needed to identify a unique

set of co-efficients consistent over a broad period baseline. At present ℓ Car is the only established long-period calibrator (parallax) used in deriving the co-efficients. A further drawback of the analysis rests in the adopted parameters for the calibrating clusters, which exhibit an unsatisfactory amount of scatter in the literature and more recent analyses (e.g., An et al., 2007; Hoyle et al., 2003). Refining distance estimates to the calibrating set of clusters by means of deep CCD photometry, analagous to the impressive results from the CFHT Open Cluster Survey (Kalirai et al., 2001a,b), is a priority in moving forward. The framework is also tied to the HST sample of Cepheids with parallaxes and field reddenings established by Benedict et al. (2007). It is noted that the parallax measures for RT Aur and Y Sge differ significantly between HST and Hipparcos (van Leeuwen et al., 2007, see their table 1).

The framework outlined here should permit an efficient investigation of suspected cluster Cepheids (Turner & Burke, 2002), including objects uncovered by cross correlations between newly discovered Cepheids in the ASAS and TASS with open cluster databases (i.e., WebDA). A potential goal is an expansion of the sample of cluster Cepheids, with particular emphasis on long period cluster Cepheids. Of equal importance, however, is the task of purging line-of-sight coincidences from current lists promulgating the literature, something that is particularly acute given that high-precision data are needed to address the question of the universality of the PL relation.

Four longer term objectives exist. First is to use the new relations to determine Galactic parameters and map interstellar extinction. Second, is to establish mean photometry for an entire calibrating set. Third, with regard to the universality of the PL relation and establishing long-period Cepheid calibrators, realistically it will be the highly anticipated results from the GAIA mission (Crifo & The French Gaia Team, 2006), a next generation follow-up to the Hipparcos mission, that will provide the large and unbiased sample of Cepheid parallaxes needed to advance our knowledge of the field. In conjunction with a cleaned sample of cluster Cepheids, it should lead to a proper refinement of the relations outlined in section 4.3, and, consequently, the realization of the outlined objectives.
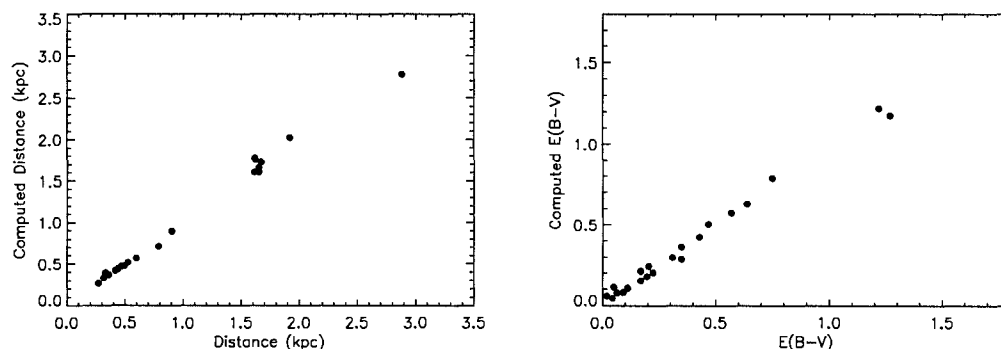
Figure 4.1 A comparison of the output from the Cepheid relations developed in section 4.3 with literature values.

Fourth is the longer term prospect of conducting extragalactic surveys using JWST (Gardner et al., 2006) to determine the distances and extinction to, and within [equation (4.4)], higher redshift galaxies. The aperture size and infrared sensitivity of the telescope will permit deeper sampling of extragalactic Cepheids, especially since the variables are substantially brighter in the infrared than the optical and the diminishment in flux from reddening is comparitively less.

ACKNOWLEDGEMENTS

Table 4.1 Calibrating Data Set.

Cepheid	Period (days)	Cluster	Distance (pc)	E_{B-V}	Source
EV Sct	4.39	NGC 6664	1612	0.64	(1)
CF Cas	4.88	NGC 7790	2884	0.57	(2,3)
CV Mon	5.38	van den Bergh 1	1650	0.75	(4)
QZ Nor	5.47	NGC 6067	1621	0.35	(5)
V Cen	5.49	NGC 5662	790	0.31	(6)
V367 Sct	6.29	NGC 6649	1650	1.27	(7,8)
U Sgr	6.75	IC 4725	599	0.43	(9,10)
DL Cas	8.00	NGC 129	1670	0.47	(11)
S Nor	9.75	NGC 6087	902	0.17	(12)
TW Nor	10.79	Lyngå 6	1923	1.22	(13,14,10)
V340 Nor	11.29	NGC 6067	1621	0.35	(15)
RT Aur	3.73	...	417	0.051	(16)
T Vul	4.44	...	526	0.064	(16)
FF Aql	4.47	...	356	0.224	(16)
δ Cep	5.37	...	273	0.092	(16)
Y Sge	5.77	...	469	0.205	(16)
X Sgr	7.01	...	333	0.197	(16)
W Sgr	7.59	...	439	0.111	(16)
β Dor	9.84	...	318	0.044	(16)
ζ Gem	10.15	...	360	0.018	(16)
ℓ Car	35.55	...	498	0.17	(16)

Data sources: (1) Turner (1976), (2) Pedreros et al. (1984), (3) Takala (1988), (4) Turner et al. (1998), (5) Walker (1985b), (6) Clariá et al. (1991), (7) Madore & van den Bergh (1975), (8) Turner (1981), (9) Pel (1985), (10) Turner & Burke (2002), (11) Turner et al. (1992), (12) Turner (1986), (13) Madore (1975), (14) Walker (1985a), (15) Walker (1985b), (16) Benedict et al. (2007).

Table 4.2 Likely Evolved B-type Members of Tombaugh 5.

2MASS Designation	J
03473515+5907588	10.307
03482167+5903410	11.607
03481681+5901295	11.321
03471767+5904333	11.542
03473265+5901398	11.589
03481650+5905219	12.018

Table 4.3 O–C Data for GSC 03729-01127.

JD$_{max}$	Cycles	O–C (days)	Data Points	Weight	Source
2411726.028	−8207	+0.162	13	1.0	(1)
2412480.634	−8058	+0.031	13	1.0	(1)
2413959.564	−7766	−0.121	25	1.0	(1)
2416127.206	−7338	−0.450	11	1.0	(1)
2416816.473	−7202	−0.070	22	1.0	(1)
2418492.862	−6871	−0.312	19	1.0	(1)
2420417.567	−6491	−0.440	24	1.0	(1)
2422894.642	−6002	−0.321	8	1.0	(1)
2425720.892	−5444	−0.536	8	1.0	(1)
2426855.472	−5220	−0.595	28	1.0	(1)
2427225.308	−5147	−0.529	11	1.0	(1)
2428841.526	−4828	−0.157	27	1.0	(1)
2430563.605	−4488	−0.298	15	1.0	(1)
2432463.383	−4113	−0.026	14	1.0	(1)
2440537.114	−2519	−0.463	13	1.0	(1)
2442710.182	−2090	−0.430	27	1.0	(1)
2444584.756	−1720	−0.036	24	1.0	(1)
2446534.863	−1335	−0.089	34	1.0	(1)
2451478.579	−359	−0.154	69	3.0	(2)
2453284.296	−3	−0.049	94	3.0	(3)
2453808.799	+101	+0.005	18	3.0	(4)
2454087.385	+156	−0.003	49	3.0	(5)

Data sources: (1) Harvard Collection, (2) NSVS, Woźniak et al. (2004), (3) TASS, Droege et al. (2006), (4) Burke-Gaffney Observatory, (5) Abbey Ridge Observatory.

Table 4.4 New O–C Data for BD Cas.

JD$_{max}$	Cycles	O–C (days)	Data Points	Weight	Source
2412584.617	−8038	−1.964	9	1.0	(1)
2412952.110	−7937	−1.497	7	1.0	(1)
2413325.649	−7835	−1.647	7	1.0	(1)
2415070.128	−7357	−1.687	8	1.0	(1)
2415558.129	−7223	−1.818	12	1.0	(1)
2415922.588	−7124	−1.844	11	1.0	(1)
2416287.608	−7024	−1.493	11	1.0	(1)
2416670.007	−6919	−1.851	20	1.0	(1)
2417044.552	−6816	−1.705	20	1.0	(1)
2417778.542	−6615	−1.232	40	1.0	(1)
2419650.202	−6103	−0.912	35	1.0	(1)
2421893.150	−5488	−1.128	30	1.0	(1)
2423454.303	−5061	−0.808	17	1.0	(1)
2424225.733	−4849	−0.442	7	1.0	(1)
2425372.119	−4535	−0.825	22	1.0	(1)
2425744.076	−4433	−0.350	8	1.0	(1)
2426109.087	−4333	−0.654	10	1.0	(1)
2427007.120	−4088	−0.675	13	1.0	(1)
2429772.037	−3330	+0.083	49	1.0	(1)
2431560.580	−2840	+0.003	43	1.0	(1)
2433312.640	−2360	−0.183	21	1.0	(1)
2440495.195	−393	−0.144	19	1.0	(1)
2441932.979	+0	−0.277	21	2.0	(2)
2442829.249	+245	−0.294	66	1.0	(1)
2445089.520	+865	−0.541	...	1.5	(3)
2446379.817	+1218	−0.509	100	1.0	(1)
2447482.216	+1520	−0.431	14	2.0	(4)
2448218.562	+1721	−0.438	98	2.0	(5)
2448797.229	+1880	−0.442	28	2.0	(5)
2453086.229	+3055	−0.500	55	3.0	(6)
2453858.027	+3266	−0.506	17	3.0	(7)
2454047.561	+3318	−0.529	56	3.0	(8)

Data sources: (1) Harvard Collection, (2) Szabados (1977, 1983), (3) Busquets (1986), (4) Schmidt (1991), (5) Hipparcos, Perryman et al. (1997), (6) TASS, Droege et al. (2006), (7) Burke-Gaffney Observatory, (8) Abbey Ridge Observatory.

Table 4.5 O–C Data for AB Cam.

JD_{max}	Cycles	O–C (days)	Data Points	Weight	Source
2412196.403	−4355	+0.110	16	1.0	(1)
2414158.338	−4016	+0.099	22	1.0	(1)
2416444.214	−3621	−0.068	28	1.0	(1)
2418487.415	−3268	+0.163	15	1.0	(1)
2420454.905	−2928	−0.079	24	1.0	(1)
2423429.801	−2414	+0.068	13	1.0	(1)
2425391.706	−2075	+0.027	16	1.0	(1)
2426856.054	−1822	+0.149	26	1.0	(1)
2427185.941	−1765	+0.152	20	1.0	(1)
2428817.943	−1483	+0.093	26	1.0	(1)
2431769.375	−973	−0.074	92	1.0	(1)
2436902.916	−86	−0.002	28	3.0	(2)
2440531.679	+541	+0.030	13	1.0	(1)
2442713.505	+918	−0.012	26	1.0	(1)
2443610.625	+1073	+0.053	14	3.0	(3)
2444577.019	+1240	−0.057	24	1.0	(1)
2446527.506	+1577	+0.059	34	1.0	(1)
2448107.531	+1850	+0.111	13	3.0	(4)
2448657.297	+1945	+0.069	9	3.0	(5)
2450324.052	+2233	+0.038	13	3.0	(6)
2452905.354	+2679	+0.137	18	2.0	(7)
2453432.000	+2770	+0.126	26	2.0	(7)
2453651.965	+2808	+0.167	19	2.0	(7)
2453802.368	+2834	+0.096	12	3.0	(8)
2454051.208	+2877	+0.076	45	3.0	(9)

Data sources: (1) Harvard Collection, (2) Bahner et al. (1962), (3) Haupt (1980), (4) Berdnikov (1992), (5) Schmidt & Seth (1996), (6) Berdnikov et al. (1998), (7) TASS, Droege et al. (2006), (8) Burke-Gaffney Observatory, (9) Abbey Ridge Observatory.
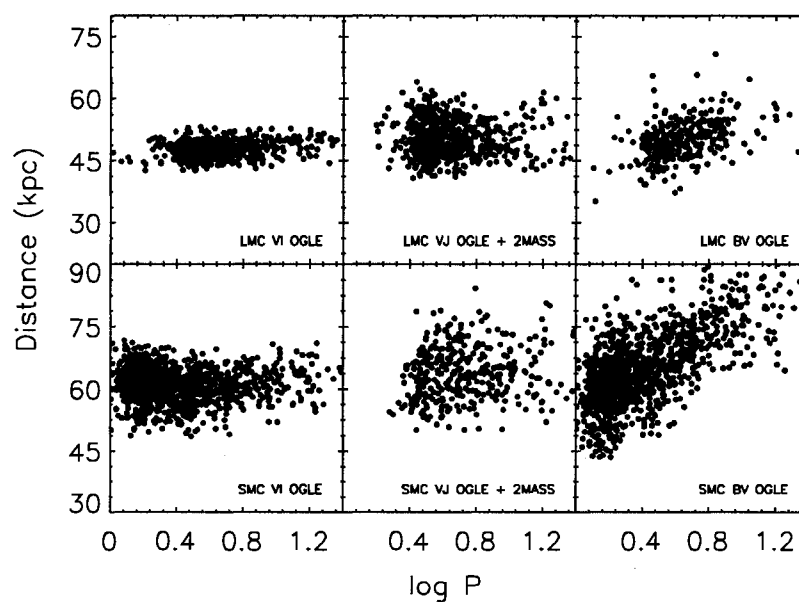
Figure 4.2 Cepheid distance diagrams (CDD) constructed for the Magellanic Clouds. See text for details.
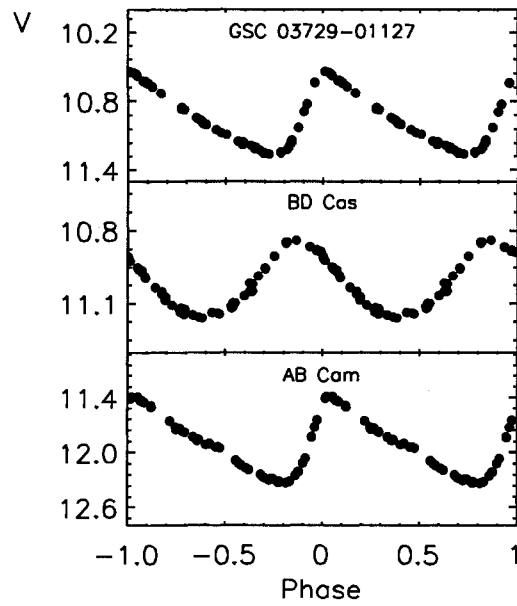
Figure 4.3 The light-curves for the Cepheids GSC 03729-01127, BD Cas, and AB Cam, constructed from differential photometry obtained at the Abbey Ridge Observatory. Standard deviations across check stars in the Cepheid fields typically range from ±0.006 to ±0.008 mag.
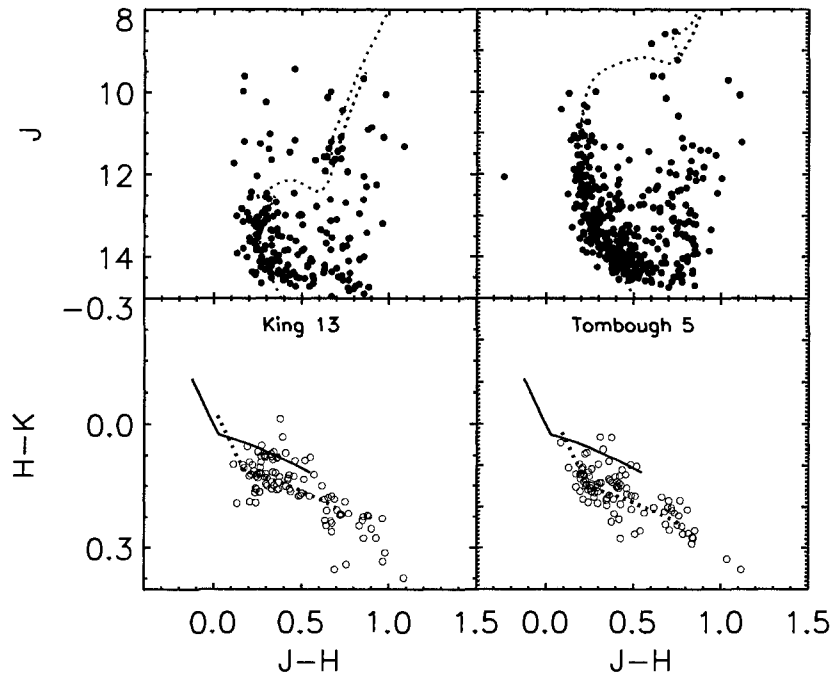
Figure 4.4 Colour-colour and colour-magnitude diagrams for King 13 (left) and Tombaugh 5 (right) constructed from 2MASS data. Clearly visible sequences of AF-type stars (King 13) and late B-type stars (Tombaugh 5) produce reddenings of $E_{J-H} = 0.14 \pm 0.02$ ($E_{B-V} \simeq 0.52$) and $E_{J-H} = 0.22 \pm 0.02$ ($E_{B-V} \simeq 0.81$), respectively. King 13 and Tombaugh 5 have inferred ages of $\log \tau = 9.0 \pm 0.2$ and $\log \tau = 8.35 \pm 0.15$, and distances of $d = 2.55 \pm 0.50$ kpc (see text) and $d = 1.66 \pm 0.20$ kpc, respectively. A reddening relationship of $E_{J-H} = 1.72 \times E_{H-K}$ was adopted from Bica & Bonatto (2005) and Dutra et al. (2002).
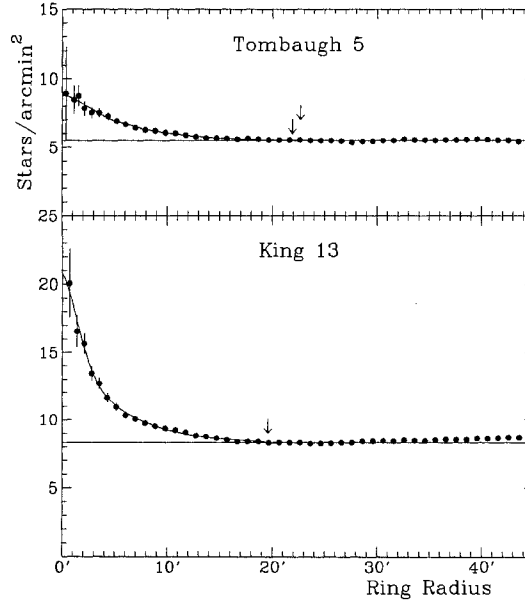
Figure 4.5 Star counts for the open clusters Tombaugh 5 and King 13, compiled from 2MASS observations. Arrows indicate the locations of GSC 03729-01127 and AB Cam (inner and outer points, upper figure) and BD Cas (lower figure) relative to their respective cluster centres.
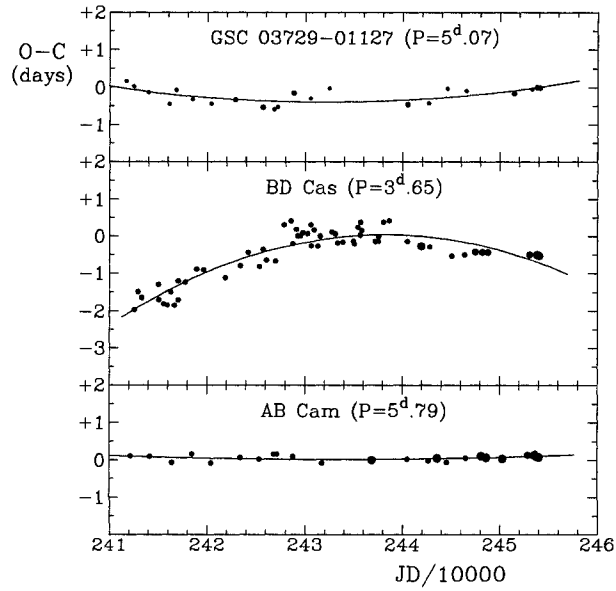
Figure 4.6 The O-C diagrams for GSC 03729-01127, BD Cas, and AB Cam (from top to bottom), including observations compiled by Szabados (1977, 1983). The size of each data point is proportional to the weight assigned in the analysis, and the parabola in each case represents a regression fit.

REFERENCES

Alessi B. S., Moitinho A., Dias, W. S., 2003, A&A, 410, 565

An D., Terndrup D. M., Pinsonneault, M. H., 2007, ApJ, 671, 1640

Andrievsky S. M., et al., 2002, A&A, 381, 32

Bahner,K., Hiltner W. A., Kraft R. P., 1962, ApJS, 6, 319

Beaulieu J. P., 1995, in Stobie R. S., Whitelock P. A., eds., IAU Coll. 155, ASP Conf. Series Vol. 83, Astrophysical Applications of Stellar Pulsation: the Interaction between Observation and Theory, Astron. Soc. Pac., San Francisco, p. 260

Beaulieu J. P., Sasselov D. D., 1998, in Bedding T. R., Booth A. J., Davis J., eds., IAU Symp. 189, Fundamental Stellar Pulsation: The Interaction between Observation and Theory, Kluwer, Dordrecht, p. 126

Beljawsky S., 1931, AN, 243, 115

Benedict G. F., et al. 2002, AJ, 123, 473

Benedict G. F., et al., 2007, AJ, 133, 1810

Berdnikov L. N., 1992, A&AT., 2, 157

Berdnikov L. N., 1994, Astr. Lett., 20, 232

Berdnikov L. N., Ignatova V. V., Pastukhova E. N., Turner D. G., 1997, Astr. Lett., 23, 177

Berdnikov L. N., Ignatova V. V., Vozyakova O. V., 1998, A&AT, 17, 87

Berdnikov L. N., Dambis A. K., Vozyakova O. V., 2000, A&AS, 143, 211

Bica E., Bonatto C., 2005, A&A, 443, 465

Bonatto C., Bica E., Girardi L., 2004, A&A, 415, 571

Bono G., Gieren W. P., Marconi M., Fouqué, P., 2001, ApJ, 552, L141

Busquets J., 1986, GEOS Circ. Cepheids, No. Cep 1, 7, p. 1

Clariá J. J., Lapasset E., Bosio M. A., 1991, MNRAS, 249, 193

Coulson I. M., Caldwell J. A. R., 1985, MNRAS, 216, 671

Crifo, F., & The French Gaia Team 2006, SF2A-2006: Semaine de l'Astrophysique Française, 459

Cutri R. M., Skrutskie M. F., van Dyk S., et al., 2003, The IRSA 2MASS All-Sky Point Source Catalog of Point Sources, NASA/IPAC Infrared Science Archive

Czernik M., 1966, Acta Astr., 16, 93

Droege T. F., Richmond M. W., Sallman M. P., Creager R. P., 2006, PASP, 118, 1666

Dutra C. M., Santiago B. X., Bica, E., 2002, A&A, 381, 219

Ferrarese L., Mould J. R., Stetson P. B., Tonry J. L., Blakeslee J. P., Ajhar E. A., 2007, ApJ, 654, 186

Fernie J. D., Ehlers P., 1999, AJ, 117, 1563

Foster G., 1995, AJ, 109, 1889

Fouqué P., et al., 2007, A&A, 476, 73

Freedman W. L., et al., 2001, ApJ, 553, 47

Gardner, J. P., et al. 2006, SpSciRev, 123, 485

Glushkova E. V., Berdnikov L. N., Turner D. G., 2006, Mem. Soc. Astr. It., 77, 127

Gorynya N. A., Rastorguev A. S., Samus N. N., 1996, Pis'ma AZh, 22, 38

Groenewegen, M. A. T., 1999, A&AS, 139, 245

Harris H. C., 1980, PhD thesis, Univ. Washington

Harris A. W., et al., 1989, Icarus, 77, 171

Henden A. A., Kaitchuck R. H., 1998, Astronomical Photometry: A Text and Handbook for the Advanced Amateur and Professional Astronomer, Willmann-Bell, Richmond

Hoag A. A., Johnson H. L., Iriarte B., Mitchell R. I., Hallam K. L., Sharpless S., 1961, Pub. U.S. Naval Obs., 17, 343

Hoyle F., Shanks T., Tanvir N. R., 2003, MNRAS, 345, 269

Kalirai J. S., et al., 2001, AJ, 122, 257

Kalirai J. S., Ventura P., Richer H. B., Fahlman G. G., Durrell P. R., D'Antona F., Marconi G., 2001, AJ, 122, 3239

Kholopov P. N., 1969, SvA, 12, 625

Kienzle F., Moskalik P., Bersier D., Pont F., 1999, A&A, 341, 818

King I., 1949, Harvard College Obs. Bull., 919, 41

Kovtyukh V. V., Soubiran C., Luck R. E., Turner D. G., Belik S. I., Andrievsky S. M., Chekhonadskikh F. A., 2008, MNRAS, submitted

Kronberger M., et al., 2006, A&A, 447, 921

Laney C. D., Stobie R. S., 1992, A&AS, 93, 93

Laney C. D., Stobie R. S., 1993, MNRAS, 263, 921

Laney C. D., Stobie R. S., 1994, MNRAS, 266, 441

Laney C. D., Caldwell J. A. R., 2007, MNRAS, 377, 147

Lata S., Mohan V., Pandey A. K., Sagar R., 2004, Bull. Astr. Soc. India, 32, 59

Lyngä, G., 1995, VizieR Online Data Catalog, 7092, 0

Maciejewski G., Niedzielski A., 2007, A&A, 467, 1065

Madore B. F., 1975, A&A, 38, 471

Madore, B. F., van den Bergh, S., 1975, ApJ, 197, 55

Madore B. F., 1982, ApJ, 253, 575

Majaess D. J., Turner D. G., Lane D. J., Moncrieff K. E., 2008, JAAVSO, 36, in press

Marx S., Lehmann H., 1979, AN, 300, 295

Mermilliod J.-C., Mayor M., Burki G., 1987, A&AS, 70, 389

Moffett T. J., Barnes T. G., III, 1986, MNRAS, 219, 45P

Moitinho A., Alessi B. S., Dias W. S., 2003, EAS Pub. Series, 10, 141

Morgenroth O., 1934, AN, 251, 17

Mottini M., 2006, Ph.D. Thesis

Opolski A., 1983, IAU Inf. Bull. Var. Stars, 2425, 1

Opolski A., 1988, Acta Astr., 38, 375

Pedreros M., Madore B. F., Freedman W. L., 1984, ApJ, 286, 563

Pel J. W., 1985, in Madore B. F., ed., IAU Colloq. 82, Cepheids: Theory and Observations, Cambridge Univ. Press, Cambridge, p. 1

Perryman M. A. C., et al., 1997, The Hipparcos and Tycho Catalogues, ESA SP-1200, ESA Publ. Div., Noordwijk

Phelps R. L., et al., 1998, ApJ, 500, 763

Pojmanski G., 2000, Acta Astr., 50, 177

Reddish V. C., 1954, MNRAS, 114, 583

Samus N. N., Durlevich O. V., et al., 2004, Combined General Catalogue of Variable Stars, VizieR Online Data Catalog, II/250

Schwarzenberg-Czerny A., 1996, ApJ, 460, L107

Schmidt E. G., 1991, AJ, 102, 1766

Schmidt E. G., Seth A., 1996, AJ, 112, 2769

Sebo K. M., et al., 2002, ApJS, 142, 71

Soszyński I., Gieren W., Pietrzyński G., 2005, PASP, 117, 823

Spergel D. N., et al., 2007, ApJS, 170, 377

Subramaniam A., Bhatt B. C., 2007, MNRAS, 377, 829

Szabados L., 1977, Comm. Konkoly Obs. Hungary, 70, 1

Szabados L., 1980, Comm. Konkoly Obs. Hungary, 76, 1

Szabados L., 1981, Comm. Konkoly Obs. Hungary, 77, 1

Szabados L., 1983, Ap&SS, 96, 185

Szabados L., 1995, in Stobie R. S., Whitelock P. A., eds., IAU Coll. 155, ASP Conf. Series Vol. 83, Astrophysical Applications of Stellar Pulsation: the Interaction between Observation and Theory, Astron. Soc. Pacific, San Francisco, p. 357

Szabados L., 2003, IAU Inf. Bull. Var. Stars, 5394, 1

Takala J. M., 1988, MSc thesis, Saint Mary's Univ.

Tammann G. A., Sandage A., Reindl B., 2003, A&A, 404, 423

Tombaugh C. W., 1941, PASP, 53, 219

Tsarevsky G. S., Ureche V., Efremov Y. N., 1966, Astr. Tsirk., 367, 1

Turner D. G., 1976, AJ, 81, 1125

Turner D. G., 1981, AJ, 86, 231

Turner D. G., 1986, AJ, 92, 111

Turner D. G., 1996, JRASC, 90, 82

Turner D. G., 1998, JAAVSO, 26, 101

Turner D. G., 2003, JAAVSO, 31, 160

Turner D. G., Berdnikov L. N., 2004, A&A, 423, 335

Turner D. G., Burke J. F., 2002, AJ, 124, 2931

Turner, D. G., Forbes, D., Pedreros M., 1992, AJ, 104, 1132

Turner D. G., Pedreros M. H., Walker A. R., 1998, AJ, 115, 1958

Turner D. G., Horsford A. J., MacMillan J. D., 1999, JAAVSO, 27, 5

Turner D. G., Savoy J., Derrah J., Abdel-Sabour Abdel-Latif M., Berdnikov L. N., 2005, PASP, 117, 207

Turner D. G., Abdel-Sabour Abdel-Latif M., Berdnikov L. N., 2006, PASP, 118, 410

Turner D. G., Bryukhanov I. S., Balyuk I. I., et al., 2007, PASP, 119, 1247

Turner D. G., MacLellan R. F., Henden A. A., Berdnikov L. N., 2008, MNRAS, in preparation

Udalski A., et al., 1999, Acta Astr., 49, 223

van den Bergh S., 1957, ApJ, 126, 323

van den Bergh S., 1968, JRASC, 62, 145

van Leeuwen F., Feast M. W., Whitelock P. A., Laney C. D., 2007, MNRAS, 379, 723

Vanmunster T., 2007, PERANSO Light Curve and Period Analysis Software, http://www.peranso.com

Walker A. R., 1985a, MNRAS, 213, 889

Walker A. R., 1985b, MNRAS, 214, 45

Walker A. R., 1987, MNRAS, 229, 31

Warner B. D., 2006, A Practical Guide to Lightcurve Photometry and Analysis, Springer, Berlin

Welch D. L., Wieland F., McAlary C. W., McGonegal R., Madore B. F., McLaren R. A., Neugebauer G., 1984, ApJS, 54, 547

Welch D. L., et al., 1995, in Stobie R. S., Whitelock P. A., eds., IAU Coll. 155, ASP Conf. Series Vol. 83, Astrophysical Applications of Stellar Pulsation: the Interaction between Observation and Theory, Astron. Soc. Pac., San Francisco, p. 232

Woźniak P. R., et al., 2004, AJ, 127, 2436

Zabolotskikh M. V., Sachkov M. E., Berdnikov L. N., Rastorguev A. S., Egorov I. E., 2005, The Three-Dimensional Universe with Gaia, 576, 723

Zaritsky D., Harris J., Thompson I. B., Grebel E. K., Massey P., 2002, AJ, 123, 855

ABSTRACT

Asteroid 349 Dembowska, a Minor Study of its Shape and Parameters.

by Daniel J. Majaess, Joel T. Tanner, Jonathan Savoy, and Beth Sampson.

Abstract: Photometry of asteroid 349 Dembowska was obtained at a high-latitude aspect, yielding a synodic rotational period of $P_R = 4.7029 \pm 0.0054$ h. Lightcurve inversion, performed with the new observations combined with archival photometry, yields an asymmetric elongated ellipsoid as the dominant shape solution. The absolute magnitude and phase coefficient for 349 Dembowska were redetermined using archival photometry to be $M_v = 6.14 \pm 0.07$ and $\beta_v = 0.022 \pm 0.004$ mag/degree. We estimate Dembowska's diameter (143 km) by adopting a simple formulism to interpret the object's thermal emission and we demonstrate that the spectral energy distribution from the *Two Micron All Sky Survey* and the *Sloan Digital Sky Survey* can be used to reveal the known signature of olivine and pyroxene absorption near 1μm.

CHAPTER 5

349 DEMBOWSKA

5.1 INTRODUCTION

Located just prior to the prominent 7 : 3 resonance with Jupiter, 349 Dembowska is among the larger asteroids in the main belt with an estimated diameter of ~ 140 km (Tedesco, 1989) and is classified as an R-Type asteroid from the presence of strong absorption bands of olivine and pyroxene with little or no metals (Gaffey et al., 1993). In this study, observations taken during an epoch of high-latitude viewing were used to deduce the asteroid's rotational period and phased lightcurve parameters. Our photometry was supplemented by archival observations in order to model the asteroid's shape and determine its intrinsic brightness. We also examine the asteroid's spectral energy distribution using data from the Sloan Digital Sky Survey (SDSS), the Two Micron All Sky Survey (2MASS), and the Infrared Astronomical Satellite (IRAS), enabling us to investigate the object's spectral composition and size.

5.2 LIGHT CURVE

349 Dembowska has been well monitored during its passage through ecliptic longitudes of $60° - 70°$ and $230° - 240°$ (Abell & Gaffey, 2000, see references therein). The lightcurve exhibits bimodal structure with two maxima and minima separated by nearly 0.4 magnitude. However, during ecliptic longitudes of $150° - 160°$ and $330° - 360°$, the brightness profile transitions to display only one peak per orbital period and a significant decrease in amplitude is noted. The evolution in the lightcurve morphology may be consistent with a transformation from a near equatorial viewing perspective to

one of high latitude. The need for precision photometry at high latitude inspired this study.

The asteroid was observed on four nights in March 2003 from the Burke-Gaffney Observatory at Saint Mary's University in downtown Halifax, Nova Scotia, Canada. The observatory houses a 0.4m Cassegrain reflector and is equipped with an SBIG ST-8 CCD camera. All images were obtained unfiltered, which allowed a high signal-to-noise ratio during this particular epoch (ecliptic longitude $\sim 155°$). Pre-processing and differential photometry were performed using MAXIMDL and MIRAMETRICS MIRA PRO. The asteroid's motion necessitated different reference stars on each night. Consequently, the data needed to be standardized in magnitude space before a period search could ensue.

A period search was then initiated after removal of spurious data obtained through clouds or during twilight. The period analysis was carried out using PERANSO (Vanmunster, 2007), which incorporates the FALC algorithm (Harris et al., 1989). A synodic period of 4.7029 ± 0.0054 h was found. Figure 1 shows the data phased to that period. Our result is consistent with, although less precise than, that of Zappala et al. (1979) who obtained a period of 4.70117 ± 0.00007 h. The lightcurve has an amplitude of ~ 0.1 magnitude, and displays one maximum and minimum per orbital period. There is an obvious plateau that bridges the extrema; this imposed valuable constraints during modeling.

5.3 SHAPE

The asteroid's surface profile was modeled using MPO LCINVERT, a GUI package based on the photometric inversion techniques of Kaasalainen et al. (2001). For the inversion process our own observations were supplemented by a number of other studies (Table 1) summarized in digitized form in the Asteroid Photometric Catalog (Lagerkvist et al., 2001). A period search was carried out in LCInvert using the entire data set. The result was a sidereal period of 4.701207 ± 0.000058 h,

which was adopted for the inversion. The uncertainty is merely the dispersion among the top five solutions with the lowest χ^2 statistic.

A single shape (Fig. 2) consistently emerged among the solutions and can be described as an asymmetric elongated ellipsoid (the canonical potato shape), which generally agrees with the structure of 349 Dembowska as suggested by Torppa et al. (2003). The model fits compare satisfactorily to the observations (Fig 3). However, we were unable to identify a unique pole orientation confidently. Additional observations, especially absolute photometry, should help resolve the ambiguities. Lastly, we note that Abell & Gaffey (2000) have suggested that 349 Dembowska could exhibit albedo variation.

5.4 DIAMETER

Veeder & Walker (1995) cite several measurements of the asteroid's diameter and geometric albedo that were derived from IRAS data by adopting a standard thermal model. A weighted mean and weighted standard deviation of their results yields a diameter of 139 ± 9 km and geometric albedo of 0.36 ± 0.05. Alternatively, we decided to assess how parameters determined from a simpler formalism would compare. For a blackbody, the emitted surface flux, $f(s, \nu)$, at a specific frequency is related to the Planck function, $I(\nu, T)$ by: $f(s, \nu) = \pi I(\nu, T)$. For a spherical geometry, the total flux measured at a distance d from a source of radius R is given by: $f(s) = \pi I(\nu, T)(R/d)^2$. A temperature of ~ 210 K and diameter of ~ 143 km produced the best fit to the IRAS photometry (Fig. 4). During the fitting process, however, the flux densities produced by the above equation were not convolved with the IRAS filter transmission functions. Testing indicates that the resulting uncertainties are of order $\sim 1 - 10\%$, nonetheless, the diameter is in general agreement with the value derived from the more robust standard thermal model.

5.5 SPECTRAL ENERGY DISTRIBUTION

A profile of the asteroid's spectral energy distribution (SED) was created by using photometry from IRAS (Veeder & Walker, 1995), 2MASS (Sykes et al., 2001), and SDSS (Krisciunas et al., 1998). The available observations enabled a broad sampling of the spectrum from the far-infrared to the ultraviolet. To homogenize the set, the data were reduced to unity Sun-Earth distance. The SED (Fig. 5) highlights both the reflected and reradiated regimes along with a prominent absorption feature near $1\mu m$, denoting the likely presence of olivine and pyroxene (Hiroi & Sasaki, 2001; Gaffey & McCord, 1978). The presence of such minerals may explain the asteroid's high albedo and could place important constraints on the body's formation history since olivine and pyroxene may be found in the mantle of differentiated objects. Lastly, we note the usefulness of the all-sky surveys in determining the spectral composition of minor bodies, which may be of added importance when studying lesser-known objects.

5.6 ABSOLUTE MAGNITUDE AND PHASE COEFFICIENT

When an asteroid is not observed at opposition, the flux received is diminished because of fractional illumination and shadowing (for fluxes reduced to unit distance). The effect can be described by a phase function diagram (Fig. 6) from which the absolute magnitude (M_v) and phase coefficient (β_v) of the asteroid are determined. In the case of 349 Dembowska, the parameters were derived from the combined data sets of Zappala et al. (1979), Weidenschilling et al. (1987), and di Martino et al. (1987). A linear least squares fit to data with phase angles between $10°$ and $20°$, thus avoiding the oppositional surge, found $M_v = 6.14 \pm 0.07$ and $\beta_v = 0.022 \pm 0.004$ mag/degree. That is consistent with the results of Zappala et al. (1979), confirming that 349 Dembowska is among the brighter asteroids in the main belt.

Table 5.1. Photometric Studies Used in the Inversion

Study	Date	# Datapoints	Weight
Zappala et al. (1979)	March 11th, 1965	45	1
Zappala et al. (1979)	April 1st, 1965	56	1
Zappala et al. (1979)	April 24th, 1965	50	2
Zappala et al. (1979)	May 6th, 1965	57	1
Zappala et al. (1979)	May 9th, 1965	43	1
Zappala et al. (1979)	May 21st, 1965	61	1
Zappala et al. (1979)	June 3rd, 1965	48	1
Zappala et al. (1979)	June 18th, 1965	59	1
Haupt (1980)	December 31st, 1977	70	2
Weidenschilling et al. (1987)	April 9th, 1984	30	1
Authors	March 10th, 2004	18	1
Authors	March 16th, 2004	93	1
Authors	March 24th, 2004	130	2
Authors	March 28th, 2004	163	2

Table 5.2. Survey Observations

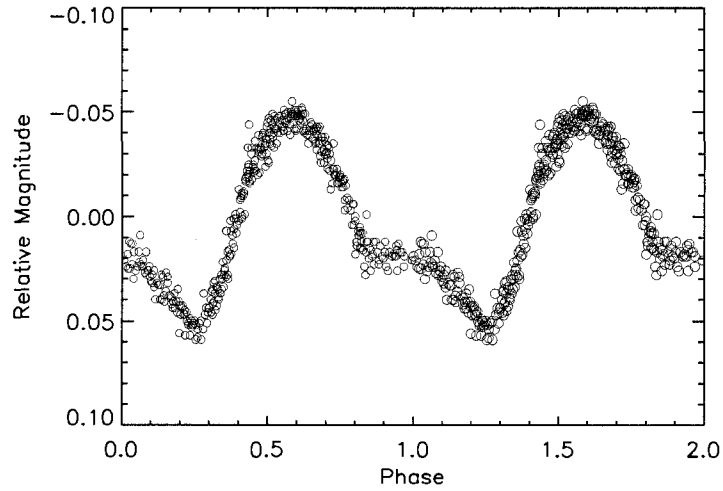| Survey	Date of Observation
IRAS	February 17th & March 2nd 1983
2MASS	November 30th 1997
SDSS	September 29th 1997

ACKNOWLEDGEMENTS

Figure 5.1 The light-curve of 349 Dembowska phased with a rotational period of $P_R = 4.7029 \pm 0.0054$ hours. The observations were taken during an epoch of high-latitude viewing (ecliptic longitude $\ell \simeq 155°$).
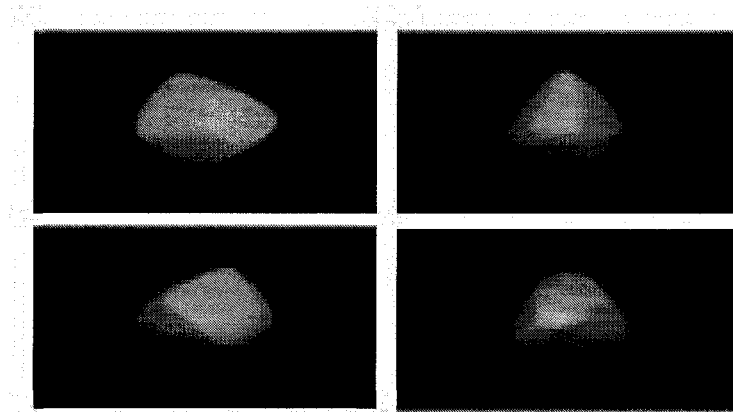

Figure 5.2 The possible surface geometry of 349 Dembowska as modelled using the software package LCINVERT. All perspectives are viewed with the rotation axis oriented vertically, while incrementing the rotation by a quarter phase from left to right, and top to bottom.
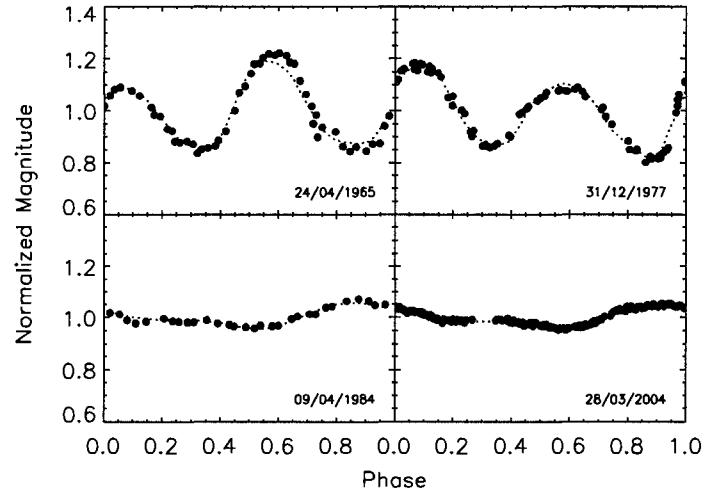
Figure 5.3 A sample of photometric observations (filled circles) compared to synthetic light-curves (dotted line) computed using the asteroid's modelled shape (figure [5.2]). Our photometry of the low amplitude phase is presented in the lower right panel.

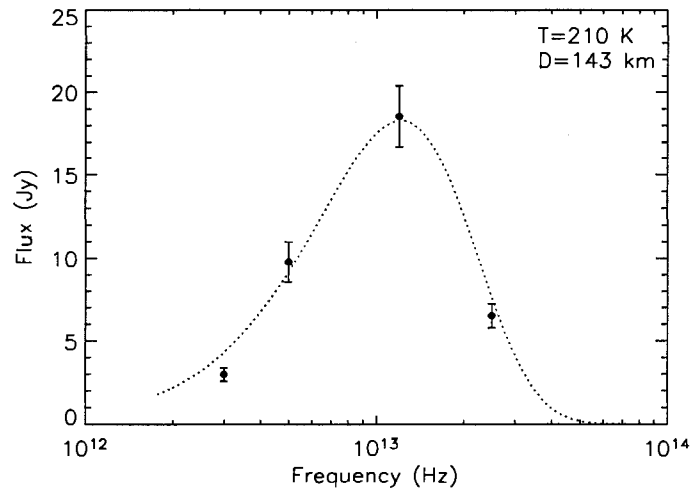Figure 5.4 A contour plot (left) reveals that a temperature of $T \simeq 210$ K and a diameter of $D \simeq 143$ km produce the minimum χ^2 statistic when fitting a modified Planck function to the asteroid's thermal emission (right, IRAS photometry).
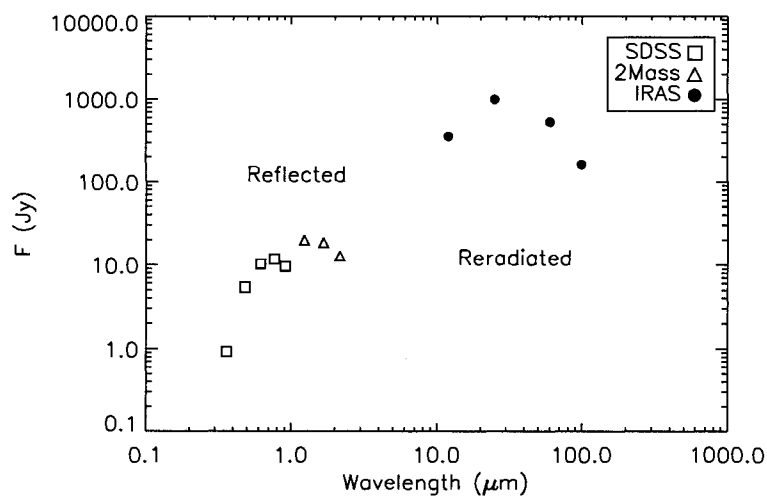
Figure 5.5 The spectral energy distribution for 349 Dembowska established from SDSS, 2MASS, and IRAS data. Both the regimes of reflected and reradiated energy are distinctly visible, along with a likely absorption feature near 1 μm (olivine & pyroxene).

Figure 5.6 The phase function for 349 Dembowska compiled from archival photometry. A linear least squares fit to data with phase angles between 10° and 20° gives an absolute magnitude of $M_v = 6.14 \pm 0.07$ and a phase coefficient of $\beta_v = 0.022 \pm 0.004$ mag/degree.

REFERENCES

Abell, P. A., & Gaffey, M. J. 2000, Lunar and Planetary Institute Conference Abstracts, 31, 1291
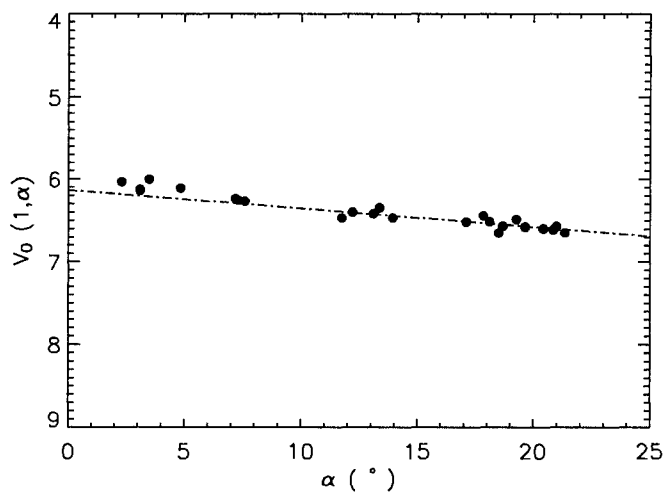
di Martino, M., Zappala, V., de Sanctis, G., & Cacciatori, S. 1987, Icarus, 69, 338

Gaffey, M. J., Burbine, T. H., & Binzel, R. P. 1993, Meteoritics, 28, 161

Gaffey, M. J., & McCord, T. B. 1978, Space Science Reviews, 21, 555

Harris, A. W., et al. 1989, Icarus, 77, 171

Haupt, H. 1980, Oesterreichische Akademie Wissenschaften Mathematisch naturwissenschaftliche Klasse Sitzungsberichte Abteilung, 189, 429

Hiroi, T., & Sasaki, S. 2001, Meteoritics and Planetary Science, 36, 1587

Høg, E., et al. 2000, A & A, 355, L27

Kaasalainen, M., & Torppa, J. 2001, Icarus, 153, 24

Kaasalainen, M., Torppa, J., & Muinonen, K. 2001, Icarus, 153, 37

Krisciunas, K., Margon, B., & Szkody, P. 1998, PASP, 110, 1342

Lagerkvist, C.-I., Piironen, J., Erikson, A. 2001, Asteroid Photometric Catalogue, Fifth Update. Uppsala Astron. Obs.

Sykes, M. V., Cutri, R. M., Fowler, J. W., Tholen, D. J., & Skrutskie, M. F. 2001, Bulletin of the American Astronomical Society, 33, 1120

Tedesco, E. F. 1979, Science, 203, 905

Tedesco, E. F. 1989, Asteroids II, 1090

Torppa, J., Kaasalainen, M., Michalowski, T., Kwiatkowski, T., Kryszczyńska, A., Denchev, P., & Kowalski, R. 2003, Icarus, 164, 346

Vanmunster, T. Peranso Light Curve and Period Analysis Software, http://www.peranso.com

Veeder, G. J., & Walker, R. G. 1995, VizieR Online Data Catalog, 7091, 0

Weidenschilling, S. J., Chapman, C. R., Davis, D. R., Greenberg, R., Levy, D. H., & Vail, S. 1987, Icarus, 70, 191

Zappala, V., van Houten-Groeneveld, I., & van Houten, C. J. 1979, A&AS, 35, 213

ABSTRACT

New Constraints on the Asteroid 298 Baptistina, the Alleged Family

Member of the K/T Impactor

by D. J. Majaess, D. Higgins, L. A. Molnar, M. J. Haegert, D. J. Lane, D. G. Turner, I. Nielsen.

Abstract: In their study Bottke et al. (2007) suggest that a member of the Baptistina asteroid family was the probable source of the K/T impactor which ended the reign of the Dinosaurs 65 Myr ago. Knowledge of the physical and material properties pertaining to the Baptistina asteroid family are, however, not well constrained. In an effort to begin addressing the situation, data from an international collaboration of observatories were synthesized to determine the rotational period of the family's largest member, asteroid 298 Baptistina ($P_R = 16.23 \pm 0.02$ hrs). Discussed here are aspects of the terrestrial impact delivery system, implications arising from the new constraints, and prospects for future work.

CHAPTER 6

NEW CONSTRAINTS ON 298 BAPTISTINA

6.1 INTRODUCTION

Terrestrial impactors (asteroids and comets) have been suggested to play a major role in modulating the existence of life on Earth, as the dating of craters linked to kilometer-sized impactors at Popigai and Chesapeake Bay, Chicxulub (Hildebrand, 1993), and Morokweng and Mjolnir strongly correlate in age with three of the last major global extinctions. One of the challenges, undoubtedly, is to explain how such impactors transition from otherwise benign orbits in the solar system to become near-Earth objects (NEOs). Historically, it has been suggested that the cause of such extinctions may be linked to an influx of comets by means of a perturbation of the Oort Cloud, a spherical zone of loosely-bound comets thought to encompass the periphery of the solar system. A litany of possible causes have been put forth as catalysts for such a perturbation, most notably density gradients (stars and the interstellar medium) encountered as the Sun oscillates vertically through the plane of the Milky Way during its revolution about the Galaxy, or interactions with a suspected *sub*stellar companion to the Sun (Nemesis). Certain ideas are advocated because they inherently assume a periodicity to mass extinction events, although unproven, rather than stochastic punctuations (showers).

A different impact delivery system revisited below is based primarily on orbital resonances, and favours a reservoir of projectiles from the asteroid belt located between Mars and Jupiter, in addition to comets from the Kuiper Belt and Oort Cloud, the former extending beyond Neptune from 35 A.U. to 50+ A.U.
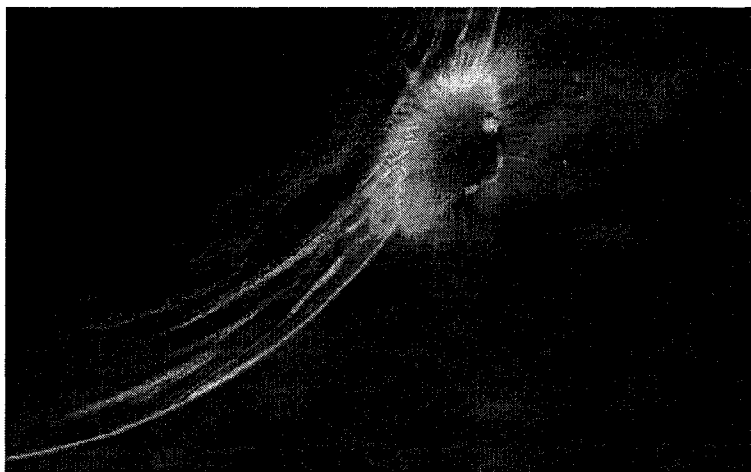
Figure 6.1 Artwork by Inga Nielsen.

6.1.1 RESONANCES

Large bodies can be delivered from both Belts into Earth-crossing orbits by means of resonances (secular and mean motion). Formally, a resonance occurs where the orbital periods of two bodies are commensurate (ratios of integers). For example, an asteroid that is near a 2:1 resonance with Mars will orbit the Sun once for each two orbits Mars completes. Most importantly, asteroids near resonances may experience periodic perturbations from a planet that could lead to an increasing eccentricity and a subsequent close encounter, resulting in the asteroid being gravitationally scattered. Observations confirm that areas in the Main Belt associated with strong resonances with the orbit of Jupiter are indeed devoid of asteroids (see Kirkwood Gaps), securing the resonance phenomenon as a feasible mechanism for transporting objects from the Belt. Inevitably, a fraction of the asteroids depleted by orbital resonances become NEOs.

A distribution analogous to the Kirkwood Gaps is also noted in computational models of the Kuiper Belt (Majaess, 2004), where Neptune plays a major role in scattering comets. Moreover, simulations confirm that comets from the region could then enter other planet-crossing orbits, although the relevant impact probabilities are difficult to constrain because firm statistics on the Kuiper

Belt's comet population lie beyond present limits of solid observational data. The James Webb Space Telescope, scheduled for launch in $\simeq$ 2014, and the ongoing Canada France Ecliptic Plane Survey (CFEPS) should place firmer constraints on the KB demographic. Indeed, many Canadian astronomers and institutions are active partners in JWST (i.e. John Hutchings, NRC-HIA, René Doyon, Université de Montréal) and CFEPS (i.e. JJ Kavelaars and Lynne Jones, NRC-HIA, Brett Gladman, UBC).

6.1.2 THE YARKOVSKY EFFECT

The Yarkovsky Effect (YE) is another component of the delivery system that can work to enhance the transport of asteroids (or comets) into resonances, essentially increasing the possibility that bodies not near resonances may eventually arrive at such locations. In its simplest form, the canonical YE arises from a temperature differential between the sunlit and dark sides of an object exposed to the Sun. Thermal energy from the object is therefore reradiated asymmetrically, causing the body to experience a thrust that may result in an outwards or inwards orbital migration, depending upon its sense of rotation and the direction of the resulting rocket force (see Rubincam (1998) for details).

The YE also allows constraints to be placed on the ages of asteroid families (Vokrouhlický et al., 2006), although such a framework is still in its scientific infancy. The force causes smaller asteroids to undergo a greater orbital migration in comparison with larger bodies, producing a characteristic fingerprint in semi-major axis space (see figure 1, Bottke et al., 2007). Computer simulations can then determine at what time after the fragmentation of a parent body the present day distribution (fingerprint) of an asteroid family is reproduced satisfactorily. Such analyses depend on knowledge of several different parameters, which in the case of the Baptistina asteroid family (BAF) are not well established (see below). Lastly, the YE has been invoked to describe the motion of asteroid 6489 Golevka (Chesley et al., 2003), with additional efforts to confirm the effect observationally still forthcoming.
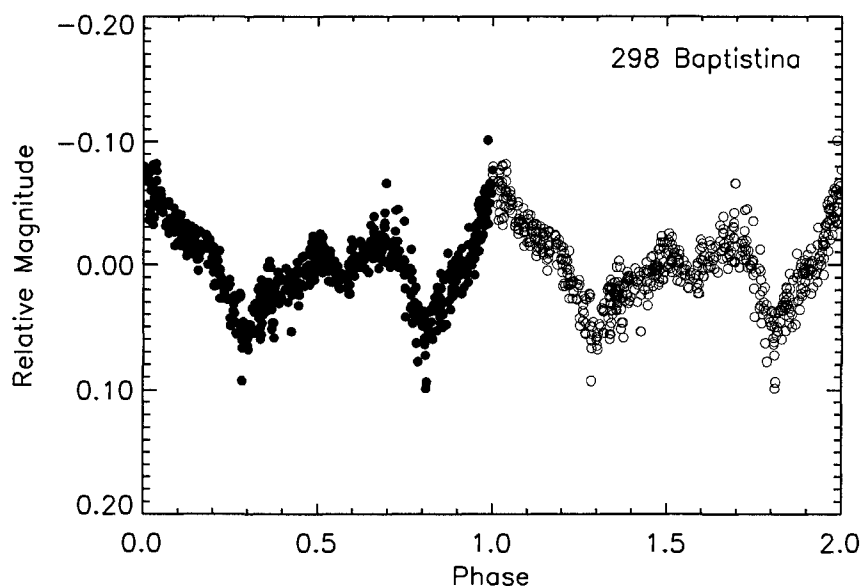
Figure 6.2 The light curve for 298 Baptistina phased with a period of $P_R = 16.23 \pm 0.02$ hours.

6.1.3 SUMMARY

In sum, a three-component terrestrial impact delivery system could begin in the Belt with the fragmentation of a parent body near a resonance by means of a collision that spawns hundreds of smaller asteroids, thereby augmenting the statisticaly probability and likelihood of a terrestrial impactor. After fragmentation, a particular asteroid could then enter a nearby resonance or drift there by means of the YE, where it may be scattered by a planet into an Earth-crossing orbit.

6.2 THE ALLEGED BAPTISTINA/KT IMPACTOR CONNECTION

In harmony with the delivery model revisited above, Bottke et al. (2007) postulate that the Baptistina asteroid family formed from the catastrophic breakup of its progenitor approximately 160 Myr ago, following which some debris entered a nearby resonance that eventually led to the ejection of what would inevitably become the K/T impactor (Figure 1). Their proposal is supported by the

following lines of evidence[1]: (i) the asteroid family is located near a resonance capable of delivering

passing asteroids into planet-crossing orbits. (ii) The purported destruction of the parent body 160

Myr ago, an age inferred from sorting the asteroids into orbital parameter space according to the

YE, created a prodigious supply of BAF members that inevitably populated the NEO demographic,

consistent with an alleged increase in the terrestrial impact rate during the same era. It should

be noted, however, that the terrestrial record of impacts suffers from poor statistics owing to the

subsequent erosion of craters with time, complicating any statistical interpretation. (iii) The K/T

impactor and BAF share a similar composition. Although the C-type composition of BAF members

is also not unique; such asteroids are found throughout the Belt.

Unavoidably, the final conclusions are based on statistical grounds, namely the probability that

the impactor was a fragment from the creation of the BAF rather than a random C-type asteroid

(or background population). Bottke et al. (2007) suggest that there is a 90% chance that the K/T

impactor was a BAF member, or 1 ± 1 BAF members of size d$\geq$ 10 km impacted Earth in the past

160 Myr. Readers should be aware that contributions from the background population are difficult

to assess (as noted by the authors), and, furthermore, the terrestrial impact rate originating from

d$\geq$ 10 km BAF members supposedly peaked $\simeq$ 120 Myr ago (see figure 4, Bottke et al., 2007), nearly

twice the age of the K/T extinction event (65 Myr ago). In addition, accurate modeling of the YE

requires knowledge of both physical and material properties that are conducive to BAF members,

sensitive parameters that are poorly constrained and require further research by the community at

large. Indeed, the rotational period derived here for BAF member 298 Baptistina ($P_R = 16.23 \pm 0.02$

hrs, see below) is a factor of three greater than the value used in the simulations, although Bottke

et al. (2007) adopted a value that may be consistent with smaller-sized BAF members ($P_R \simeq 6 \pm 2$

hours, Pravec & Harris, 2000; Pravec et al., 2002). The difference in rotational periods noted

above is sufficient to warrant additional investigations to confirm the mean rotational period and

---

[1] The reader is also referred to the comprehensive supplemental texts that accompany the Bottke et al. (2007) paper.

material properties conducive to kilometer-sized BAF members. Such work needs to be pursued in conjunction with increasing the number of known family members and reaffirming the family's taxonomy. Efforts to secure such parameters will invariably lead to stronger constraints on the properties of family members and might permit a more confident evaluation of whether the source of the K/T impactor was indeed a $\simeq$ 10 km sized BAF member. Lastly, and most importantly, irrespective of the conclusion regarding the putative source of the K/T impactor, the approach outlined by Bottke, Vokrouhlický, and Nesvorný provides the quantitative framework and a pertinent example needed to effectively characterize the terrestrial impact delivery system.

6.3 OBSERVATIONS

Asteroid 298 Baptistina was discovered over a century ago, in September 1890, by the French astronomer Auguste Charlois. The origin of the asteroid's designation (Baptistina) is unknown, an uncertainty that is also representative of the asteroid's rotational period, morphology, size, etc. A need to establish such parameters inspired the present study, especially in light of the asteroid's reputed status. Asteroid 298 Baptistina was therefore observed throughhought March and April 2008 from the Abbey Ridge Observatory (Halifax, Canada), the Hunter Hill Observatory (Canberra, Australia), and the Calvin-Rehoboth Observatory (New Mexico, USA). Image pre-processing and differential photometry were performed using MPO CANOPUS (Warner, 2006) and MAXIMDL (George, 2007). The asteroid's large proper motion required the selection of different reference stars on each night (Warner, 2006; Henden & Kaitchuck, 1998), consequently the FALC algorithm was employed to search both magnitude and temporal space for a period solution (Harris et al., 1989). The period analysis was carried out in the MPO CANOPUS (Warner, 2006) and PERANSO (Vanmunster, 2007) software environments.

A rotational period of $P_R = 16.23 \pm 0.02$ hours was determined for 298 Baptistina from the

analysis, and the resulting phased light curve is presented in Figure 2. The light curve exhibits a peak to peak amplitude of $\simeq 0.15$ magnitude and displays complex characteristics that are likely indicative of irregular surface features. Continued photometric observations are envisioned to refine the rotational period, and in conjunction with archival observations by Wisniewski et al. (1997) and Ditteon & Hawkins (2007), to model the asteroid's shape and spin axis by light curve inversion (Molnar & Haegert, 2008; Kaasalainen & Torppa, 2001). The data will also permit a detailed study of the asteroid's absolute magnitude and oppositional surge, fundamental for any subsequent research. Thermal imaging and spectroscopic follow-up would also be of value, permitting a precise determination of the asteroid's diameter and confirmation of its taxonomical class.

ACKNOWLEDGEMENTS

REFERENCES

Bottke, W. F., Vokrouhlický, D., & Nesvorný, D. 2007, Nature, 449, 48

Chesley, S. R., et al. 2003, Science, 302, 1739

Ditteon, R., & Hawkins, S. 2007, Minor Planet Bulletin, 34, 59

George D. B., 2007, MAXIMDL Advanced CCD Imaging Software, http://www.cyanogen.com

Harris A. W., et al., 1989, Icarus, 77, 171

Henden A. A., Kaitchuck R. H., 1998, Astronomical Photometry: A Text and Handbook for the Advanced Amateur and Professional Astronomer, Willmann-Bell, Richmond

Hildebrand, A. R. 1993, JRASC, 87, 77

Kaasalainen, M., & Torppa, J. 2001, Icarus, 153, 24

Majaess D. J. 2004, Undergraduate Thesis, Saint Mary's University.

Molnar, L. A., & Haegert, M. J. 2008, AAS/Division of Dynamical Astronomy Meeting, 39, #02.03

Pravec, P., Harris, A. W., & Michalowski, T. 2002, Asteroids III, 113

Pravec, P., & Harris, A. W. 2000, Icarus, 148, 12

Rubincam, D. P. 1998, Journal of Geophysical Research, 103, 1725

Vanmunster T., 2007, PERANSO Light Curve and Period Analysis Software, http://www.peranso.com

Vokrouhlický, D., Brož, M., Bottke, W. F., Nesvorný, D., & Morbidelli, A. 2006, Icarus, 182, 118

Warner B. D., 2006, A Practical Guide to Lightcurve Photometry and Analysis, by B.D. Warner. 2006 XIII, 297 p. 0-387-29365-5. Berlin: Springer, 2006

Wisniewski, W. Z., Michalowski, T. M., Harris, A. W., & McMillan, R. S. 1997, Icarus, 126, 395

CHAPTER 7

VITA

Name: Daniel Josef Majaess
Place of Birth: Halifax, Nova Scotia, Canada
Education: Bachelor of Science, Saint Mary's University.
Related Experience: Visiting Astronomer Dominion Astrophysical Observatory and Harvard College Observatory Photographic Plate Stacks.
Publications:

Berdnikov, L. N., Pastukhova, E. N., Turner, D. G., and Majaess, D. J. "A Search for Evolutionary Changes in the Periods of Cepheids using Archival Data from the Harvard Observatory Plate Collection. IV. NSV 9159," Pis'ma v Astronomicheskii Zhurnal, submitted, 2008.

Majaess, D. J., Higgins, D., Molnar, L. A., Haegert, M. J., Lane, D. J., Turner, D. G., Nielsen, I. 2008, "New Constraints on the Asteroid 298 Baptistina, the Alleged Family Member of the K/T Impactor", Journal of the Royal Astronomical Society of Canada, submitted, 2008.

Majaess, D. J., Turner, D. G., and Lane, D. J. 2008, "Assessing Potential Cluster Cepheids from a New Distance and Reddening Parameterization and 2MASS Photometry", Monthly Notices of the Royal Astronomical Society, in press, astro-ph arXiv:0808.2937

Majaess, D. J., Tanner, J., Savoy, J., Sampson, B. 2008, "349 Dembowska: A Minor Study of its Shape and Parameters", The Minor Planet Bulletin, Vol. 35, No. 2, p. 88-91

Majaess, D. J., Turner, D. G., Lane, D. J., and Moncrieff, K. A. 2008, "The Exciting Star of the Berkeley 59/Cepheus OB4 Complex and Other Chance Variable Star Discoveries", Journal of the American Association of Variable Star Observers, 36, Preprint 74, in press, astro-ph arXiv:0801.3749

Majaess, D. J., Turner, D. G., and Lane, D. J. 2007, "In Search of Possible Associations between Planetary Nebulae and Open Clusters", Publications of the Astronomical Society of the Pacific, 119, 1349-1360

Turner, D. G., Panko, E. A., Sergienko, O., Lane, D. J., and Majaess, D. J. 2008, "New Insights into the Nature of the Eclipsing System V609 Aquilae", The Observatory, 128, 2-14

Turner, D. G., Bryukhanov, I. S., Balyuk, I. I., Gain, A. M., Grabovsky, R. A., Grigorenko, V. D., Klochko, I. V., Kosa-Kiss, A., Kosinsky, A. S., Kushmar, I. J., Mamedov, V. T., Narkevich, N. A., Pogosyants, A. J., Semenyuta, A. S., Sergey, I. M., Schukin, V. V., Strigelsky, J. B., Tamello, V. G., Lane, D. J., and Majaess, D. J. 2007, "The Period Changes of the Cepheid RT Aurigae", Publications of the Astronomical Society of the Pacific, 119, 1247-1255